Photonic applications of biomaterials with special reference to biopolymers and microbes

Thesis submitted to
Cochin University of Science and Technology
in partial fulfillment of the requirements for the award of the degree of

Doctor of Philosophy

By

Nithyaja.B

INTERNATIONAL SCHOOL OF PHOTONICS
COCHIN UNIVERSITY OF SCIENCE AND TECHNOLOGY
COCHIN – 682 022, KERALA, INDIA

January 2012

Photonic applications of biomaterials with special reference to biopolymers and microbes
"Thesis in the field of Photonics, an important branch of Physics."

Author:

Nithyaja B
Research Fellow,International School of Photonics,
Cochin University of Science and Technology
Cochin-22,Kerala,India
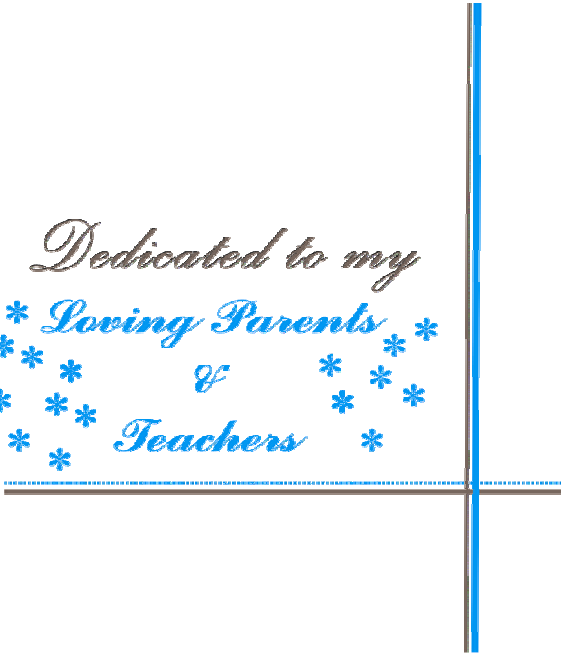*email:nithyaja_b@yahoo.com,nithyajab@yahoo.com*

Research Advisor:

Dr. V P N Nampoori
Emeritus Professor, International School of Photonics
Cochin University of Science and Technology
Cochin-22, Kerala, India
email: nampoori@gmail.com

International School of Photonics
Cochin University of Science and Technology
Cochin – 682 022, Kerala, India
URL//www.photonicscusat.edu

January 2012

Dedicated to my
* Loving Parents *
&
Teachers *

Cochin University of Science and Technology
International School of Photonics
Cochin -682022, Kerala, India.

Dr. V P N Nampoori
Emeritus Professor

Certificate

      Certified that the research work presented in this thesis entitled "**Photonic applications of biomaterials with special reference to biopolymers and microbes"** is an authentic record of the bonafide research work done by **Mrs**. **Nithyaja. B** under my guidance at the International School of Photonics, Cochin University of Science and Technology, Cochin, India and has not been included in any other thesis submitted previously for the award of any degree.

Cochin-22   **Dr. V P N Nampoori**

02- 01- 2012   *(Supervising guide)*

Phone: +91 484 2575848   Fax: 0091-484-2576714.
Email: nampoori@cusat.ac.in
           nampoori@gmail.com

Declaration

I hereby declare that the work presented in the thesis entitled **"Photonic applications of biomaterials with special reference to biopolymers and microbes"** is entirely original and was carried out by me independently under the supervision of **Dr. V P N Nampoori** (Emeritus Professor, International School of Photonics, Cochin University of Science and Technology) and has not been included in any other thesis submitted previously for the award of any other degree.

Kochi-22
02-01-2012

Nithyaja.B

Preface

The continued development of photonics technology is crucially dependent on the availability of suitable optical materials. Biomaterials are emerging as an important class of materials for producing novel or otherwise improved photonic devices. From the rich world of organic materials, biomaterials are of particular interest as they often have unusual properties that are not easily replicated in conventional organic or inorganic materials in the laboratory. Furthermore, natural biomaterials are a renewable resource and are inherently biodegradable. The most important and famous biomaterial known to man is DNA (Deoxyribonucleic Acid), the polymeric molecule that carries the genetic code in all living organisms. It is clear that the unique structure of DNA results in many optical and electronic properties that are extremely interesting for photonic applications. DNA can be used as a photonic material for making optical waveguide, both on its own and also as a host material accepting appropriate chromophores.

Another application of biomaterials is for the synthesis of nano materials. Synthesis of nanoparticle is an emerging field due to its potential application in catalysis, optical, magnetic and electronic devices. Among biological molecules deoxyribonucleic acid (DNA) and protein bovine serum albumin (BSA) have been used extensively as biotemplates to grow inorganic quantum confined structure and to organize non biological building blocks into extended hybrid materials. Biological macromolecules are capable of controlling nucleation and growth to a remarkable degree through bio- mineralization. DNA template has also been described as a smart glue for assembling nano particles. In general, synthesis of nano particles based on DNA template has been done by incubating metal ion coated DNA in a reduction agent solution. The ion DNA complexes control the release of metal ions, thereby slowing down their reduction and

effectively inhibiting metal ions from growing into big clusters. Nano-structures of metals such as silver, gold, palladium, platinum, copper, and nickel have been successfully synthesized by using DNA network templates.

The nonlinear optical properties of the metal nanoparicles depend on the host material which supports them. A large number of investigations has been carried out to study nonlinear optical properties of metal nano particles dispersed in different optically transparent solid matrices and liquids. However, only limited research has been done on the nonlinear optical property of the metal nanoparticles in bio polymer template.

Research on synthesis of semiconductor nanoparticles having a controlled size distribution has attracted significant interest because of their luminescent properties, quantum size effects and other important size dependent physical and chemical properties. Semiconductor nano crystals are tiny light-emitting particles on the nanometer scale. Researchers have studied the characteristics of these particles extensively and have developed them for broad applications in solar energy conversion, optoelectronic devices, molecular and cellular imaging, and ultra sensitive detection. A major feature of semiconductor nano particles is the quantum confinement effect, which leads to spatial enclosure of the electronic charge carriers within the nanocrystal. For instance, the band gap emission can be tunable over wide wavelengths by adjusting an appropriate size of the particle. The particles prepared from such viewpoint should be useful as a fluorescence agent for optical and biotechnological applications.

Laser Induced Fluorescence has proven to be a versatile tool for a myriad of applications. It is a powerful technique for studying molecular interactions in analytical chemistry, biochemistry, cell biology, physiology, nephrology, cardiology, photochemistry, and environmental science. As the theoretical underpinnings of fluorescence became more understood, a more powerful set of

applications emerged that yield detailed information about complex molecules and their reaction pathways. Measuring of fluorescence quantum efficiency is one of the experimental techniques to characterize biological samples.

A detailed investigation will be presented in the present thesis related to direct applications of biopolymers into some selected area of photonics and how the growth kinetics of an aerial bacterial colony on solid agar media was studied using laser induced fluorescence technique.

In **chapter 1**, an overview of various biomaterials and their application to photonics are presented. A wide range of photonics applications using biomaterials include efficient harvesting of solar energy, low-threshold lasing, high-density data storage, optical switching, filtering and template for nano structures. The chapter discusses these applications of biomaterials briefly. The most extensively investigated photonics applications in biology is Laser induced fluorescence technique. The importance of fluorescence studies in different biological and related fields and are also mentioned in this chapter.

Chaper 2 describes the effect of DNA on nonlinear optical properties of Rhodmine 6G-PVA solution through open aperture Z-scan. Saturable absorption (SA) at 532nm was observed for dye solution without DNA. A strong influence on SA behavior of dye solution was observed by adding DNA. As the concentration of DNA is increased, we observed RSA within SA. Theoretical analysis has been performed using a model based on nonlinear absorption coefficient and saturation intensity.

In **chapter 3** we present results of investigation on the influence of DNA on amplified spontaneous emission of Rhodamine 6G –PVA solution and thin film. The presence of DNA reduces the threshold value of lasing and full width half maximum of fluorescence spectra. Thin solid film of DNA has been fabricated by treating with polyvinyl alcohol (PVA) and used as host for the

laser dye Rhodamine 6G. The edge emitted spectrum clearly indicated the existence of laser modes and amplified spontaneous emission (ASE).

Studies on nanoparticle synthesis using DNA is the subject matter of **chapter 4.** Highly stable silver nanoparticles in aqueous solution at room temperature is synthesized by standard reduction method using DNA as stabilizing agent. The linear and nonlinear optical properties of silver nanoparticles at different concentration of DNA is studied. Absorption spectra shows the Ag plasmon resonance lies around 410 nm and silver nano-particles formed in higher concentration is less. The nonlinear absorption coefficient β and imaginary part of third order susceptibility depends on the concentration of DNA at low pump power. It is observed that at high pump power, the nonlinear absorption coefficient (β) and imaginary part of third order susceptibility does not depend on the concentration of the DNA. The imaginary parts of third order nonlinear optical susceptibility measured by Z-scan technique revealed that silver nano particle synthesized in aqueous solution of DNA have good nonlinear optical response and could be chosen as ideal candidate with potential applications for nonlinear optics. The nonlinear absorption of silver nanoparticles at high intensity is attributed to the influence of DNA on nanoparticles. We also studied photo luminescence of silver nanoparticles at different concentration of DNA. It is observed that the emission of silver nanoparticles is getting enhanced as concentration of DNA increases.

In **chapter 5** describes the work related to the synthesis of silver nano particles using bovine serum albumin (BSA) biopolymer. Highly stable silver nano particles in aqueous solution at room temperature is synthesized by standard reduction method using BSA as a stabilizing agent. Prepared solution shows strong absorption peak originating from the surface plasmon absorption of nanosized silver particles in aqueous solution of BSA. The photo

iv

luminescence spectra show emission peak at 538 nm at excitation wavelength 250 nm. The nonlinear optical properties were investigated by a single beam Z-scan setup. The nanosol show an excellent nonlinear optical property. Silver nanoparticle in BSA template is a potential candidate for optoelctronic device applications.

Chapter 6 discusses band gap tunability of CdS nanoparticles in biotemplates DNA and BSA. DNA is more efficient in controlling the size of the nanoparticles. Since nanoparticles are capped with biomaterials, they were very useful for biolabeling. We have studied excitation wavelength dependence on fluorescence emission of CdS nanoparticles stabilized with DNA and BSA. Excitation wavelength changed from 260 nm to 480 nm.

Chapter 7 discusses laser induced fluorescence technique, which has been used for studying growth dynamics of an aerial gram positive bacterial colony on nutrient agar medium. This technique has been shown to be a useful technique for obtaining information about the different growth phase of the bacterial colony. Quenching effect of dye by bacterial colony can be effectively used to analyze growth kinetics of bacterial colony. Quenching effect of fluorescence indicates that cultured bacteria were gram positive. The rate of quenching of fluorescence of dye from bacterial colony was proportional to rate of increase in area of the bacterial colony which in turn indicates that the rate of quenching of the fluorescence was proportional to rate of growth of bacteria.

General conclusions drawn from the studies and further areas in which the work can be extended are discussed in **chapter 8.**

LIST OF PUBLICATIONS

A. Journal Publications:

1. **B. Nithyaja**, V. K. Jisha, R. Tintu, A.V. Saramma and V. P. N. Nampoori; "kinetics of bacterial colony growth by laser induced fluorescence" , Laser Phys. **19**, 468 (2009)

2. **Nithyaja Balan**, Misha Hari, Vadakkedathu Parameswaran Narayana Namppori; "Selective mode excitation in the dye –doped DNA polyvinyl alcohol thin film", Appl. Opt. **48** 3521(2009)

3. **B. Nithyaja,** H. Misha, P. Radhakrishnan and V P N Nampoori; " Effect of DNA on nonlinear optical properties of Rhodamine6G-PVA solution", J. Appl. Phys. **109**, 023110 (2011)

4. **Nithyaja B,** Yogeshwar Nath M , Amit Kumar S,Misha H and Nampoori V P N; "Linear and nonlinear optical properties of silver nanoparticles stabilized by bovine serum albumin" J. Nonlinear Optical Physics and Materials **20** (2011)

5. **B. Nithyaja**, H. Misha and V.P.N. Nampoori; "Synthesis of silver nanoparticles in DNA template and its influence on nonlinear optical properties", Journal of Applied physics (Communicated)

6. **Nithyaja B**, Misha H, Nampoori V P N; "Fluorescence enhancement of silver nanoparticles using DNA as a stabilizing agent", Proc. SPIE **8173**, 81731K (2010)

7. K.Vishnu ,**B. Nithyaja** ,C. Pradeep , R. Sujith ,P. Mohanan and V.P.N. Nampoori; "Studies on the effect of mobile phone radiation on DNA using laser induced fluorescence technique**",** Laser Phys. **21**, 1(2011)**)**

8. Rose Leena Thomas, Vasuja, Misha HariI, **B. Nithyaja** S. Mathew, I. Rejeena, Sheenu Thomas , V. P. N. Nampoori and P. Radhakrishnan;

"Optical Limiting in TeO_2–ZnO glass from Z-scan technique" , J. Nonlinear Optical Physics & Materials **20**, 3 (2011)

B) Conference Papers:

1. **B. Nithyaja**, V. K. Jayasree, Lyjo K Joseph and VPN Nampoori; "Studies on the Time Dependence of Nonlinear Optical Properties of Deoxyribonucleic Acid (DNA) using Z-Scan Technique. (NLS-07).

2. **B. Nithyaja**, B. Bavishna and V. P. N. Nampoori; "Effect of deoxyribonucleic acid (DNA) on amplified spontaneous emission in dye-doped poly vinyl alcohol solution". (NLS 2009)

3. **B. Nithyaja**, V. K. Jisha, R. Tintu, A.V.Saramma and V. P. N. Nampoori; "Laser-bacterial interaction by using laser induced fluorescence technique" (Photonics 08)

4. Vishnu K, **Nithyaja B**, S. Mathew and Nampoori V P N; "Bandgap tunability of CdS nanoparticles using biotemplates" (Photonics 2010)

5. **Nithyaja B ,** Misha H, Nampoori V P N; **"**Fluorescence enhancement of silver nanoparticles using DNA as a stabilising agent"(photonics 2010)

6. **Nithyaja B**, Yogeshwar Nath M , Amit Kumar S, Misha H and Nampoori V P N; "Nonlinear optical properties of silver nanoparticles stabilized by bovine serum albumin"(ICMST 2010)

7. Misha Hari, Santhi A. J, G. S. Avadhani, **Nithyaja B**, Deep Pung, Bishwajeet S, P. Radhakrishnan, V P N Nampoori; "Enhanced thermal diffusivity of R6G dye on addition of Ag/TiO2 nanocomposite" (Photonics 2010)

8. Misha Hari, Santhi Ani Joseph, **Nithyaja Balan**, Mathew S, , Ravi Kumar, Giridhar Mishra, R. R. Yadhav,P. Radhakrishnan,V. P. N. Nampoori; "Linear and nonlinear optical characterization of gold nanoparticles in polyvinyl alcohol"(ICMST 2010)

Acknowledgement ....

Contents

Chapter 3

Amplified spontaneous emission of radiation from Dye –PVA-DNA system..49-74

Chapter 4

Synthesis and optical characterization of silver nanoparticles in DNA template..75-93

Chapter 5

Linear and nonlinear optical properties of silver nanoparticles stabilized by bovine serum albumin......94-105

Chapter 6

Studies on CdS nanoparticles prepared in DNA and BSA based biotemplates..106-124

Chapter 7

Studies on bacterial colony growth dynamics by laser induced fluorescence..125-137

Chapter 8
Conclusions and future prospects...................................138-142

LIST OF TABLES

LIST OF FIGURES

xviii

Chapter **1**

Biomaterials and their application to Photonics-An overview

Abstract

This chapter is an overview of the spectrum of biomaterials and their application to Photonics. The chapter discusses a wide range of biomaterials based photonics applications like efficient harvesting of solar energy, low-threshold lasing, high-density data storage, optical switching, filtering and template for nano structures. The most extensively investigated photonics application in biology is Laser induced fluorescence technique. The importance of fluorescence studies in different biological and related fields are also mentioned in this chapter.

1.1 INTRODUCTION

Biophotonics deals with interactions between light and biological matter, which is an integration of three major technologies namely photonics, nanotechnology and biotechnology. Fusion of these technologies offers a new dimension in the medical field for both diagnostics and therapy. The use of photonics for optical diagnostics, as well as for light-activated and light-guided therapy give great hope for the early detection of diseases like cancer and for new modalities of light guided and light-activated therapies[1-10]. Optical bioimaging can be used to investigate structures and functions of cells and tissues as well as to profile diseases at cellular, tissue, and *in vivo* specimen levels [11-15]. Also, biology offers feedback to the advancement of Photonics, since naturally occurring biopolymers (or artificially constructed facsimiles) are showing promise in the development of new photonic media for technological applications. Availability and future development of new multifunctional materials, that can dramatically improve speed and encryption, as well as provide terabit data storage and large-area high-resolution display, are of vital importance for implementation of the full scope of new-generation information technology [1].

The four types of biomaterials that hold promise for photonic applications are (i) bioderived materials, naturally occurring or their chemical modifications, (ii) bioinspired materials, synthesized based on guiding principles of biological systems, (iii) biotemplates for self-assembling of photonic active structures, and (iv) bacteria bioreactors for producing photonic polymers [1]. The wide range of photonics applications using these biomaterials include efficient harvesting of solar energy, low-threshold lasing, high-density data storage, optical switching, and filtering. This chapter discusses these applications of biomaterials.

1.1.1 Bioderived materials

One of the important bioderived materials useful for photonics is green fluorescent protein (GFP). Green fluorescent protein in its wild and mutant forms have attracted a great deal of interest as biological fluorescent markers for *in vivo* imaging and fluorescence energy transfer imaging (FRET) to study protein–protein and DNA–protein interactions [1,16]. Fig. 1.1 shows confocal image of the worm Caenorhabditis elegas where six luminous spots can be distinguished on the worm representing the fluorescence yielded from GFP molecule. A number of other photonic applications have been proposed by utilizing a number of properties exhibited by GFP molecules. GFP can be used as a photosensitizer due to the existence of two absorption bands at 395 nm and 475 nm covering a broad range of UV and visible regions [17]. The two absorption bands are attributed to the presence of two resonant forms, a neutral and an anionic, of the same chromophore, *p*-hydroxybenzylidene- imidazolidone and can be interconverted in the excited state by proton transfer. The relative stabilities of these two forms can be manipulated by the appropriate choice of the close environment surrounding the chromophore [18]. Single molecules of GFP mutants, immobilized in aereated aqueous polymer gels exhibit an unusual repeated cycle of fluorescence emission (on/off blinking) on a time scale of several seconds when excited with light of 488 nm wavelength [19]. This phenomenon can be applied in molecular photonic switches or optical storage elements, addressable on the single molecule level. GFP also exhibits efficient two-photon excitation when excited at 800 nm. Two-photon excitation has successfully been used to produce up-conversion lasing in GFP. This is the first report of two-photon pumped lasing in a biological system [1, 20]. In addition, GFP is extremely compact and thermally stable molecule. Since its 3-D structure insulates the chromophore from the external environment, GFP fluorescence is insensitive to oxygen quenching and is stable in a variety of harsh environments

(temperatures up to 70°C, pH 6–12; detergents, proteolysis). Furthermore, renaturation can be achieved to restore the optical properties of GFP by reversing the conditions of any denaturation [21-22]. Another photonic application of GFP include making a molecular photodiode. GFP exhibits a very efficient photoinduced electron transfer such as those found for photoelectric conversion in retina and long-range electron transfer in photosynthetic organisms. Moreover, these electron transfers are unidirectional and hence can be realised as optical circulators [23].
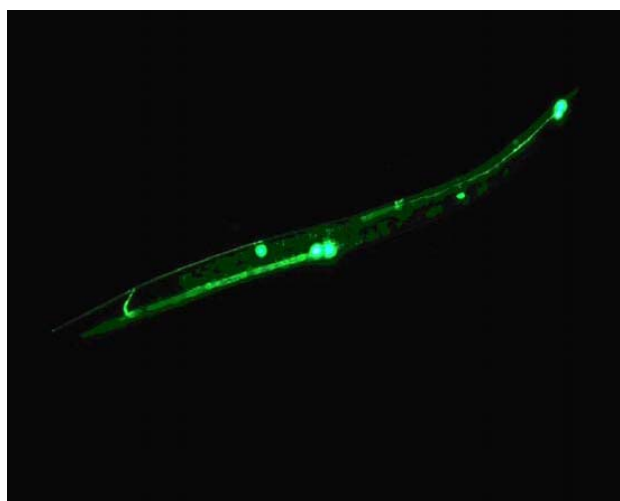
Figure 1.1 *Confocal image of the worm Caenorhabditis elegas.Six luminous spots can be distinguished on the worm, representing the fluorescence yielded from the Green Fluorescent Protein (GFP) molecules***[24]**

Another example for bioderived material for photonics is bacteriorhodopsin. The main focus has been to utilize its excited-state properties and associated photochemistry for high-density holographic data storage. A large number of photonic applications for this naturally occurring protein has been proposed, because of its robustness, ease of processing into optical quality films, suitable photophysics and photochemistry of the excited state, and flexibility for chemical and genetic modifications. The photonics applications include random access thin-film memories, photon counters and photovoltaic

converters, spatial light modulators, reversible holographic media, artificial retinas, two-photon volumetric memories and pattern recognition systems [1]. Recently, the DNA has been proposed as photonic media for optical waveguide and host for laser dyes. In the present thesis most of the experiments are performed using DNA as biomaterial. Photonic applications of DNA are discussed in section 1.2.

1.1.2 Bioobjects and biocolloids

In nature there exists many unique forms of bioobjects, which show highly precise shapes and monodisperse size in 1, 2, and 3 dimensions (plates, rods, icosahedral etc.). Examples of these bioobjects are viruses, sponges, sea urchin needles, platelets from abalone shell, and so on. Above all, the surface chemistry of these bioobjects is heterogeneous and precise. For example, virus particles are comprised of a capsid consisting of arranged protein subunits that form a hollow particle which encloses the genome. The genomic material in the core of a virus particle can be replaced by other functional interiors to produce novel photonic functions. Also using appropriate protein chemistry, surfaces of virus particles are being exploited for various applications. One promising prospect is the use of these monodispersed bioobjects as building blocks for photonic crystals. The virus particles of sizes 100–300 nm and varied shapes enable one to assemble them in both fcc and non-fcc packing to produce a wide range of self-assembled photonic crystals. These bioobjects form biocolloids by dispersing in suitable solvent, which will self-assemble into a close-packed structure exhibiting photonic crystal behaviour. It is also reported that viruses can be packed not only in an fcc structure, but also in other lattices such as orthorhombic and monoclinic systems. SEM image of close packing of irido viruses in a periodic structure is show in Fig. 1.2. Parker et al. [25] produced a spine from the sea mouse aphrodita which is an example of close-packed bioobjects. The electron micrograph of a section of the spine reveals a close-packed array of hollow cylinders, with the long axis of the cylinders along the

spine and each cylinder having six nearest neighbours. The dielectric constant of a photonic crystal can be enhanced by incorporating other materials such as high-refractive-index nanoparticles within the capsid of a virus to manipulate its refractive index [1].
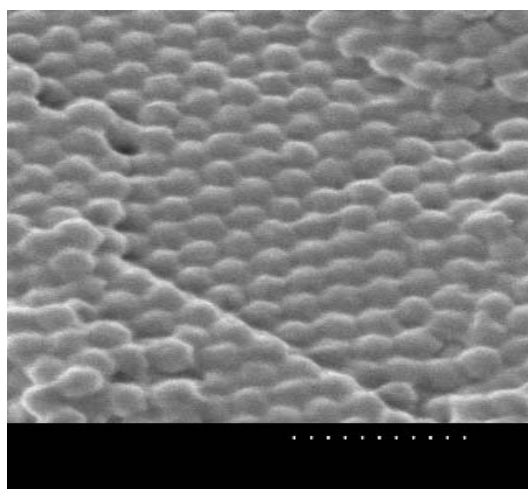
Figure: 1.2. *SEM micrograph of close packing of irido viruses in a periodic structure[1].*

1.1.3. Bioinspired materials

Bioinspired materials are synthetic materials produced by mimicking natural processes of synthesis of biological materials. An example of this category is a light-harvesting photonic material, which consists of a chlorophyll assembly to perform photosynthesis. The photosynthetic system consists of a large array of chlorophyll molecules that surround a reaction centre. This chlorophyll array acts as an efficient light-harvesting antenna to capture photons from the sun and transfer the absorbed energy to the reaction centre. The reaction centre utilizes this energy to produce charge separation, eventually forming ATP and NADPH. Frechet et al. have demonstrated two-photon excited efficient light harvesting in novel dendrite systems. Here the antennas are

efficient two-photon absorbers that absorb near-IR photons at 800 nm and transfer the excitation energy quantitatively to the core molecule [1]. The chemical structure of light-harvesting antenna-based dendritic system is shown in Fig. 1.3.

Ar=3,5-di-*tert*-butylphenyl
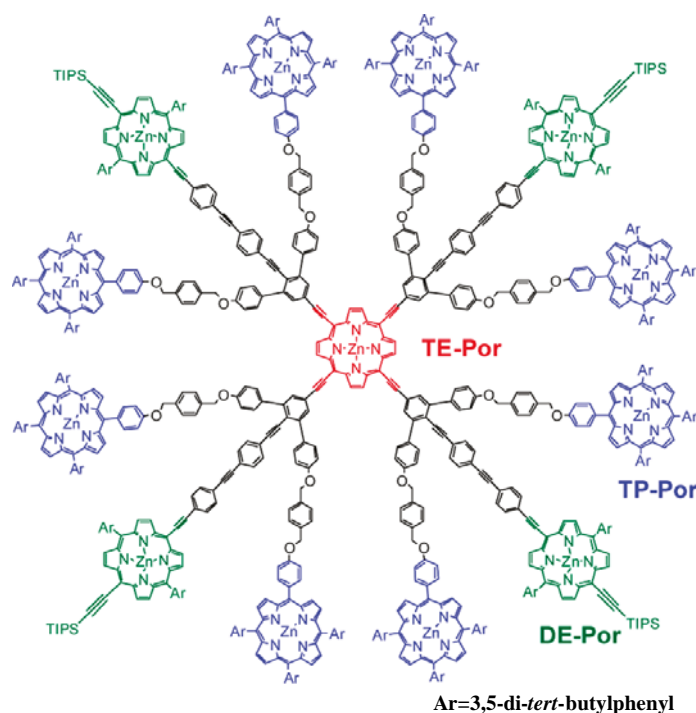
Figure:1.3.   Light-harvesting antenna-based dendritic structure (chemical structure). Antenna has three different Zn porphyrins: eight tetraphenyl Zn porphyrin units (TP-Por), four Zn porphyrin units with two meso-ethynyl and two meso-phenyl groups (DE-Por), and a Zn porphyrin unit with four meso-ethynyl groups   (TE-Por)[26]

1.1.4 Biotemplates

Biotemplates refer to natural microstructures with appropriate morphologies and surface interactions to serve as templates for creating multiscale and multicomponent photonics materials. The biotemplates can be naturally occurring biomaterials or a chemically modified, bioderived material. Some specific examples for bio templates are DNA, bovine serum albumin

(BSA) and virus. A great deal of research shows the capacity of DNA as a template to grow inorganic quantum confined structures details of which will be discussed in section 1.2.2. Viruses with well-defined morphology, flexible microstructures, and surfaces can be modified easily and can be used as a suitable template for producing novel photonic materials [1]. Bovine serum albumin (also known as BSA) is a serum albumin protein which has numerous biochemical applications can be used as good stabilising agent in nanoparticle synthesis [27]. One of the challenges in nano technology is developing methodologies with biological molecules as templates for nanomaterial synthesis.

1.1.5 Bioreactors

Bioreactors refer to the naturally occurring biosynthetic machinery that can be manipulated to produce a family of helical polymers having a wide range of optical properties. An example is a bacterial reactor that can be used to synthesize customized polymeric structures for photonic applications. The biosynthetic behavior of bacteria can be harnessed to prepare unique polymers which are useful in developing photonic devices. An example is the production of a family of polyhydroxyalkanoic acid (PHA) polymers synthesized by the bacteria Pseudomonas oleovorans. This organism has the capacity to synthesize various PHAs containing C6 to C14 hydroxyalkanoic acid dependent on the 3-hydroxyl alkanoate monomer present [1].

1.2. DNA AS A PHOTONIC MATERIAL

The most important and famous biomaterial known to man is DNA (Deoxyribonucleic Acid), that carries the genetic code in all living organisms. During the last two decade, DNA "the molecule of life" has been attracting attention of researchers in diverse areas of science and technology. Many experimental reports have been published in the last two decades which show

DNA research has emerged as an expanding field attractive enough to obtain more attention from scientists and engineers. Applications of DNA include variety of fields like electronic, optics, biochemistry, environmental protection etc. The DNA-based biopolymer is abundant, inexpensive, replenishable, and composed of green materials. A variety of agricultural and fish industry waste products can be used as raw materials, and because the biopolymer is not fossil fuel-based, it will not deplete natural resources or harm the environment.

DNA photonic devices can be either in solid or liquid form. The wet category contains primarily optofluidic devices, where the DNA molecules are present in either as aqueous or organic-solvent solution and are transported in a fluid under the influence of electric fields or fluid flow. The solid-state devices are based on thin films of DNA. DNA films are produced by treating aqueous solution of DNA with a cationic surfactant (such as cetyl trimethyl ammonium chloride-CTMA) producing a DNA– lipid complex that is insoluble in water but soluble in alcohols. This technique allows casting or spin coating of DNA thin-films, which do not dissolve other organic layers on contact and can thus be integrated into organic devices [28-31]. The characteristics of DNA - CTMA films can be controlled by adjusting the DNA molecular weight and the concentration of the reagents. Therefore, the electrical resistivity of DNA can be tuned via control of the molecular weight. This property of DNA is very useful for optimizing device operation. The electrical resistivity measures three to five orders of magnitude lower than that of polymer materials. Furthermore, the DNA – CTMA complex is thermally stable up to 200 – 250 °C and it maintains its double helical structure to temperature in excess of 100 °C, which gives some flexibility in device fabrication [28, 32-38].

DNA based biopolymer also shows low optical loss. Optical losses ranging from 0.1 to 1.2 dB/cm have been observed over a broad wavelength range of 600 -1700 nm [28, 29]. In the case of DNA - based films, value of third

harmonic generation (THG) susceptibility is one order of magnitude larger than that of silica. This difference is due to the presence of highly polarizable conjugated π electrons in DNA. In addition, combining DNA – CTMA films with polymers that have large nonlinear optical coefficients can result in improved poling efficiency when creating nonlinear optical devices [32-35, 37, 39].

Studies have shown that DNA – CTMA films also show low dielectric - loss values, ranging from 0.11 dB at 10 GHz to 0.5 dB at 30 GHz, and a loss tangent of less than 0.1 at microwave frequencies [40, 41]. The performance of organic field effect transistors (OFETs) has improved a lot by incorporating DNA – CTMA films as the gate insulator. These characteristics make the biopolymer very attractive for designing electro optic devices [35].

It is shown that, by incorporating DNA as an electron-blocking layer (EBL) in BioLEDs, luminance and luminance efficiency became significantly higher compared to conventional organic LEDs. For example, the luminance efficiency for a green emitting DNA BioLED reaches as high as 8 cd/A compared to 2 cd/A for a conventional OLED structure without the DNA layer. The EBL blocks electron flow which enhance the probability of radiative electron-hole recombination, leading to increased luminous efficiency and luminance of the device. Enhanced efficiency using DNA – CTMA nanometre thick films as EBL material has been demonstrated in both green- and blue-emitting devices [42-44].

Kobayashi et al. described the red electroluminescence of a device constructed with a water-soluble DNA-polyaniline complex containing $Ru(bpy)_3^{2+}$ the device performance is improved by adding DNA [45]. DNA can contribute in enhancing light emission by adding appropriate lumophores or chromophores to DNA molecules. The high fluorescence enhancement upon

binding of ethidium bromide (EB) to poly nucleotides has been the subject of intensive studies and many different mechanisms have been proposed for this enhancement. Although the mechanisms are not yet completely understood for enhanced light emission, it is speculated that, many fluorescent dyes can readily be intercalated into helices of DNA. These dye molecules can be situated inside the double helix structure or at some grooves beside the main chains. Because of the intercalation or groove binding of dyes in the DNA strand make molecules get isolated from each other thereby reducing the fluorescence quenching caused by aggregation. Dye molecules intercalated between base pairs in the DNA structure, are essentially shielded from non radiative relaxation centres in the host material, thus opening the door to efficient photon emission. Another possible explanation is related to the tight spatial fit between intercalated molecules and the base-pair structure, which may prevent the conformational relaxation of excited lumophores and thereby enhance the process of radiative relaxation [42, 45-49]. This intercalation makes DNA films to act as a far better host for lumophores than conventional polymer hosts. The DNA-based biopolymers could be doped at a much higher level without aggregation than other polymer host materials, such as polymethyl methacrylate (PMMA). For example, DNA-CTMA thin films doped with the luminescent dye sulforhodamine (SRh) have been reported to exhibit photoluminescence intensity more than an order of magnitude higher than that of SRh in PMMA, which is a popular polymer host. Other lumophores have also been reported to luminesce very efficiently in DNA thin-films. Large amplifications of fluorescence light were attained in the case of Eu+++ or Tb+++ with increasing amount of DNA [42, 45-49].

Recently it is reported that DNA molecules can be used as a data storage medium. DNA memory, utilizing DNA molecules and DNA reactions for data processing, has been proposed as a high capacity and high density memory. The

base sequence of DNA determines the address in DNA memory, and the addressing to a DNA memory is based on several DNA reactions, such as hybridization and denaturation. DNA on substrate is virtually divided into multiple small areas. The individual areas can be identified with unique positional addresses. DNA reactions are generally induced by temperature shift. In the photonic DNA memory, the temperature shift is controlled by light irradiation. The irradiation achieves accurate control of DNA reactions in each local space [50, 51]. The biopolymeric material of DNA complexed with the cationic surfactant CTMA and doped with the photochromic disperse red 1 dye is being used in fast dynamic holography applications due to its short recovery times, good optical stability, and complete reversibility[52].

Another application for DNA being explored is in the field of nano biotechnology. Establishing a strong tie between biotechnology and nanotechnology resulted a new field called nano biotechnology. DNA can be used as a template to grow inorganic quantum confined structures like quantum dots, quantum wires, metallic nanoparticles etc. The biotemplate approach is a top down approach for building a nanostructured photonic material. DNA template can be described as"smart glue" for assembling nanoscale building blocks. After stretching and positioning, the DNA molecules are generally treated with a metal ion solution to bind metal ions to DNA. These metal ions can be reduced to form metal clusters. As the metal seeds on the DNA templates serve as catalysts for further reduction, the clusters keep growing until the reaction is finished. With such an approach, various metallic nanowires have been prepared by the deposition of silver, palladium, platinum, nickel, copper, and cobalt metal ions on DNA. Coffer and co-workers were the first to utilize DNA as a template for CdS nanoparticles [53-59].

DNA can be used as a guiding template for the polymerization of conducting polymers also. For example polypyrrole and polyaniline are

synthesized on the DNA template by the interaction of cationic monomers to the backbone of DNA immobilized on a Si surface. This approach has potential for fabrication of high-density conducting polymer nanowires with a predetermined position and orientation on a Si surface [60].

Applications of DNA as electronic, optical, and biomaterials, as catalyst, and in environmental protection, separation, rely on few fundamental properties of DNA that relate to the famous double helical structure [Fig. 1.4]. A DNA molecule consists of two polynucleotide strands coiled around each other in a helical fashion, (Watson and Crick model) with a diameter of approximately 2 nm. The 'monomer' unit of DNA is made up of a base which is covalently bonded to a sugar molecule, which is again covalently bonded to a phosphate group that makes up the backbone of the DNA polymer. There are four different base molecules that make up DNA: adenine (A), thymine (T), guanine (G), and cytosine (C) [Fig. 1.5]. Each base has a conjugated ring structure [28, 60].
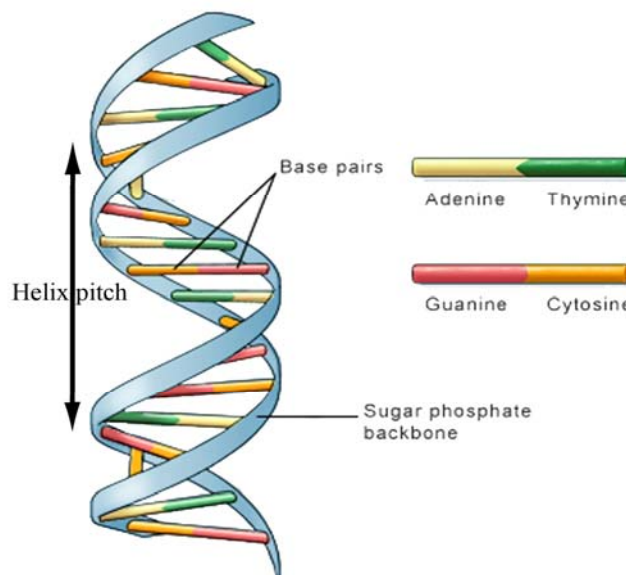
Figure:1.4 Double helix structure of DNA
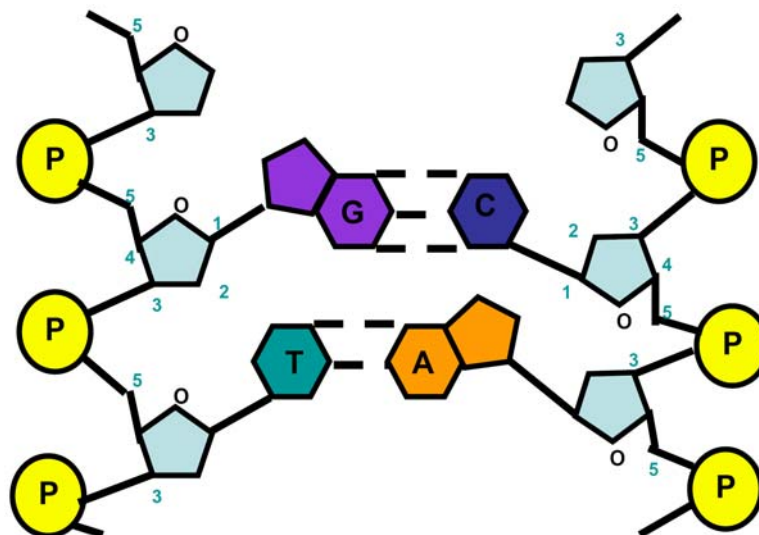
Figure: 1.5. *Back bone of double helix structure of DNA*

Moreover, the double helix chains of DNA are negatively charged by the phosphate groups that are regularly arranged in the two backbones [Fig.1.6]. Highly charged double helical structure, which shows local stiffness in a range of about 50 nm but long-range flexibility in water. Therefore, DNA is an ideal template to fabricate highly ordered nanostructures by binding cationic agents such as metal ions, cationic surfactants and poly cationic agents. In dilute solutions DNA forms wormlike coils. However, the DNA molecules in dilute solution can be easily stretched to linear templates that can lead to ordered nanostructures. The mechanism of DNA condensation has been mainly considered to be a nucleation – growth process, in which the highly ordered toroidal structure starts from a spontaneous nucleation loop of a single DNA molecule as a proto-toroid, followed by the collection of additional DNA leading to growth. Such ordered structures formed by the DNA condensation have implications for their usability in fabrication of nanostructures. When DNA reacts with cationic surfactants such as hexadecyl trimethyl ammonium chloride, a precipitate is formed, producing a complex that is soluble in common organic solvents, and thus can be easily cast to thin films. The conformation of the DNA–surfactant complex is controllable and often locally ordered.

Figure: 1.6. *Helical anionic polynucleotic backbone [60]*

Another important feature of DNA is its selective affinity for small molecules. The most common DNA structure is the B - DNA type in which the stacked bases are regularly spaced 0.34 nm along the helix axis, and the helical structure possesses a wide major groove and a narrow minor groove of approximately the same depth [Fig.1.7]. This makes small molecules to intercalate into the spaces between the stacked bases, or bind in the grooves between the two backbones. Both of the interaction patterns are highly selective toward the structure of the small molecules. By this special affinity, DNA can be used as an environmental material to selectively remove toxic pollutants, or as a template to arrange functional molecules. Also, DNA is perfectly biocompatible, as it can be found in almost all living organisms. This offers DNA excellent prospects for serving as biomaterials [28, 60].
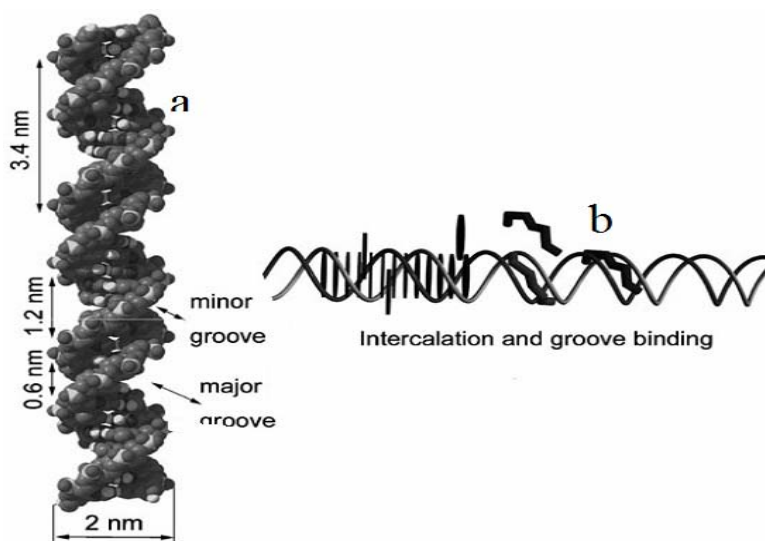
Figure: 1.7 **a).** *Different grooves present in DNA*
b). *Intercalation and groove binding of DNA* **[60]**

1.3. LASER INDUCED FLUORESCENCE(LIF)

Laser-induced fluorescence (LIF) is a spectroscopic method used for studying structure of molecules, detection of selective species and flow visualization and measurements. In this case laser provides a very selective means for populating excited states, which gives more accurate and sensitive measurements. The excited species will de excite and emit at longer wavelength after some time, usually in the order of few nanoseconds to microseconds. This emitted light known as fluorescence is measured. As the theoretical underpinnings of fluorescence became more understood, a more powerful set of applications emerged that yield detailed information about complex molecules and their reaction pathways. For example the quantum efficiency of fluorophores can change as a function of variations in the local environment of the fluorophore molecule like viscosity, temperature, refractive index, pH, calcium and oxygen concentration, electric field etc. Measuring fluorescence quantum efficiency is one of the experimental techniques to characterize biological samples. The signal-to-noise ratio of the fluorescence signal is very high, providing a good sensitivity to the process. It is also possible to distinguish between more species, since the lasing wavelength can be tuned to a particular excitation of a given species which is not shared by other species. In analytical chemistry and biology, resonance fluorescence is used extensively for efficient detection and identification of single molecules [61-65].

Some of the applications of LIF in biology are ….

1. Studies in energy transfer particularly in the field of proteins and membranes

2. Rate study of the decay processes of excited state species.

3. Effect on fluorescence of molecules due to the environment, e.g. solvent PH

4. Change in fluorescence due to structural changes in the molecules.

5. Biochemists are involved in studies relating to the metabolism e.g.catecholamines, tryptophan metabolites.

6. Determination of proteins orientation.

7. Determination of binding site of proteins.

8. Membrane studies.

9. Presence of glucose and metabolites can determine in blood.

1.4. CONCLUSIONS

A general introduction to Biophotonics is given in this chapter. The use of photonics in biology include laser induced fluorescence technique, early detection of diseases, light-activated therapies etc. The various types of biomaterials being investigated for photonics are presented in this chapter. Biomaterials are emerging as an important class of materials for a variety of photonics applications. Among biomaterials, DNA shows promising applications in the area of photonics. The unique double helix nano structure of DNA plays an important role in intercalating dye molecules and in enhanced optical properties. Biotemplates refer to natural microstructures with appropriate morphologies and surface interactions to serve as templates for creating multiscale and multicomponent photonic materials. The use of biopolymer as a template to grow quantum confined structures is also discussed in this chapter. Critical analysis of the applications of DNA as biomaterials has revealed that the mechanism of DNA based photonic devices have not yet been completely understood. Only limited works are available in the literature on the use of DNA in realizing new laser media. Subsequent chapters describe the studies carried out in these directions.

REFERENCES

1. P. N. Prasad, *"Introduction to Biophotonics"* ,Wiley-Interscience, (2003)

2. M. A. Calin, S. V. Parasca; *"Photodynamic therapy in oncology"*, J. Opt. Adv. Mater.**8**, 1173(2006)

3. Byoung-chan Bae, Kun Na; *"Development of Polymeric Cargo for Delivery of Photosensitizer in Photodynamic Therapy"*, Int. J. Photoenergy **2012**, 1(2011)

4. Battah S. H, Chee C E, Nakanishi H, Gerscher S, Mac Robert A. J, Edwards C; *"Synthesis and Biological Studies of 5-Aminolevulinic Acid-Containing Dendrimers for Photodynamic Therapy",* Bio conjugate Chem. **12**, 980(2001).

5. Dolmans DE, Fukumura D, Jain RK; *"Photodynamic therapy for cancer"*, Nature Reviews Cancer **3,** 380(2003)

6. Wilson BC; *"Photodynamic therapy for cancer: principles"*, Canadian. J. Gastro **16,** 393(2002)

7. Henderson B, and Dougherty T; *"How Does Photodynamic Therapy Work?"*, J.Photochem. Photobiol. B: Biol. **55**, 145 (1992).

8. Morgan J, and Oseroff A. R; *"Mitochondria-Based Photodynamic Anti-cancer Therapy"*, Adv. Drug Delivery Rev. **49**, 71 (2001).

9. Capella M A, Capella L S; *"A light in multidrug resistance: photodynamic treatment of multidrug-resistant tumors"*, J. Biomed. Sci. **10**,361(2003).

10. Bhawalkar J. D, Kumar N. D, Zhao C.F, Prasad P. N; *"Two-Photon Photodynamic Therapy"*, J. Clin. Laser Med. Surg. **15**, 201(1997).

11. Bassnett S, Reinisch L, Beebe D. C; *"Intracellular pH Measurement Using Single Excitation–Dual Emission Fluorescence Ratios"*; Am. J. Physiol. **258**, C171 (1990**).**

12. Nakamura T, Kawamura Y, Miyakawa H; "*Optical bioimaging: from living tissue to a single molecule: optical detection of synaptically induced glutamate transporter activity in hippocampal slices*", J. Pharmacol Sci. **93** 234(2003)

13. Bremer C, Tung C. H, Bogdanov A J, and Weissleder R; "*Imaging of Differential Protease Expression in Breast Cancers for Detection of Aggressive Tumor Phenotypes*", Radiology **222**, 814 (2002).

14. Yuen Yung Hui, Chia-Liang Cheng ,Huan-Cheng Chang; "*Nanodiamonds for optical bioimaging*", J. Phys. D: Appl. Phys. **43** 374021 (2010)

15. Gu, X, and Spitzer N.C; "*Distinct Aspects of Neuronal Differentiation Encoded by Frequency of Spontaneous Ca2+ Transients*", Nature **375**, 784 (1995).

16. Christopher GM Wilson, Thomas J Magliery ,Lynne Regan; "*Detecting protein-protein interactions with GFP-fragment reassembly", Nature methods*" **1** 255 (2005)

17. Chattoraj M, King B. A, Bublitz G. U, and Boxer S. G; "*Ultra-Fast Excited State Dynamics in Green Fluorescent Protein: Multiple States and Proton Transfer*", Proc. Natl. Acad. Sci. USA **93**, 8362 (1996).

18. Cubitt A. B, Heim R, Adams S. R, Boyd A. E, Gross, L. A,and Tsien R.Y; "Understanding,Improving and Using Green Fluorescent Proteins", Trends Biochem..**20**, 448 (1995).

19. Dickson R. M, Cubitt A. B, Tslen R. Y, and Moerner W. E; "*On/Off Blinking and Switching Behavior of Single Molecules of Green Fluorescent Protein",* Nature **388**,355 (1997).

20. Kirkpatrick S. M, Naik R. R, and Stone M. O; *"Nonlinear Saturation and Determination of the Two-Photon Absorption Cross-Section of Green Fluorescent Protein", J. Phys. Chem. B* **105**, 2867(2001).

21. Attila Nagy, András Málnási-Csizmadia, Béla Somogyi, Dénes Lorincz; *"Thermal stability of chemically denatured green fluorescent protein (GFP) A preliminary study"*, Thermochimica Acta **410**, 161(2004)

22. Yang F, Moss L. G, and Phillips J. G. N; *"The Molecular Structure of Green Fluorescent Protein"*, *Nat. Biotechnol.* **14**, 1246 (1996).

23. Choi J. W, Nam Y. S, Park S. J, Lee W. H, Kim D, and Fujihira M; *"Rectified Photocurrent of Molecular Photodiode Consisting of Cytochrome C/GFP Heterothin Films"*, Biosensors & Bioelectronics **16**, 819 (2001)

24. P.Syntichaki, N.Tavernarakis; "Genetic models of mechanotransduction: the nematode Caenorhabditis elegans", Physiol Rev. **84**,1097(2004)

25. Parker A. R, McPherson R. C, McKenzie D. R, Botten L. C, Nicorovici N. A. P, *"Aphrodite's Iridescence"*, Nature **409,** 36 (2001).

26. Atsuhiro Uetomo, Masatoshi Kozaki, Shuichi Suzuki, Ken-ichi Yamanaka, Osamu Itoand Keiji Okada; *"Efficient Light-Harvesting Antenna with a Multi-Porphyrin Cascade"*, J. Am. Chem. Soc.**133**, 13276(2011)

27. Ajay V. Singh, Bapurao M. Bandgar, Manasi Kasture, B. L. V. Prasad and Murali Sastry; *"Synthesis of gold, silver and their alloy nanoparticles using bovine serum albumin as foaming and stabilizing agent"*, J. Mater. Chem **15**(2005) 5115–5121

28. A. J. Steckl; *"DNA - a new material for photonics*?," Nat. Photon. **1**, 3(2007).

29. E. Heckman, P. Yaney, J. Hagen, J. Grote, and F. Hopkins; "*Processing techniques for DNA: a new biopolymer for photonics applications*", Appl. Phys. Lett. **87**, 211115(2005)

30. Kentaro Tanaka and Yoshio Okahat A; " *DNA−Lipid Complex in Organic Media and Formation of an Aligned Cast Film*", J. Am. Chem. Soc. 118, 10679(1996)

31. Wang L. Yoshida J, Ogata N, Sasaki S, Kajiyama T; "*Self-Assembled Supramolecular Films Derived from Marine Deoxyribonucleic Acid (DNA)- Cationic Surfactant Complexes: Large-Scale Preparation and Optical and Thermal Properties*", Chem. Mater. **13***, 1273(2001)

32. J. Hagen, W. Li, A. Steckl, J. Grote, and K. Hopkins; "*Enhanced emission efficiency in organic light emitting diodes using deoxyribonucleic acid complex as electron blocking layer*", Appl. Phys. Lett. **88**, (171109) 2006.

33. B. Singh, S. Sariciftci, J. Grote, F. Hopkins; "*Bio-organic semiconductor fieldeffect transistor (BiOFET) based on deoxyribonucleic acid (DNA) gate dielectric*", J. Appl. Phys. **100**, 24514(2006)

34. J. Grote, E. Heckman, J. Hagen, P. Yaney, D. Diggs, G. Subramanyam, R. Nelson J. Zetts, D. Zang, B. Singh, N. Sariciftci and F. Hopkins; "*DNA—new class of polymer*", Proc. SPIE **6117**, 0J1(2006)

35. E. Heckman, P. Yaney, J. Grote, F. Hopkins, M. Tomczak; "*Development of an all-DNA-surfactant electro-optic modulator*", Proc. SPIE 6117(2006).

36. P. Yaney, E. Heckman, A. Davis, J. Hagen, C. Bartsch, G. Subramanyam, J.Grote, F. Hopkins; "*Characterization of NLO polymer materials for optical waveguide*", *Proc. SPIE* **6117** 0W1(2006)

37. E. Heckman, J. Grote, F. Hopkins, and P. Yaney; "*Performance of an electro-optic waveguide modulator fabricated using a deoxyribonucleic-acid-based biopolyme*r", Appl.Phys. Lett. **89** (181116)2006.

38. C. Bartsch, G. Subramanyam, H. Axtell, J. Grote, F. Hopkins, L. Brott, and R. Naik; "*A new capacitive test structure for microwave characterization of biopolymers, temperature and bias dependent microwave dielectric properties of new biopolymers*", Microwave Opt. Technol. Lett. **49** 1265(2007)

39. E. Heckman, P. Yaney, J. Grote, and F. Hopkins; "*Development and performance of an all-DNA-based electro-optic waveguide modulator*", Proc. SPIE **6401**, 640108(2006)

40. G. Subramanyam, P. Mathala, C. Chevalier, A. Davis, P. Yaney, and J. Grote; "*Microwave characterization of electro-optic polymers*", Proc. Mater. Res. Soc. **734**, 249(2003)

41. G. Subramanyam, E. Heckman, J. Grote, and F. Hopkins; "*Microwave dielectric properties of DNA based polymers between 10 and 30 GHz*", IEEE Microwave Compon. Lett. **15,** 232(2005)

42. J. Hagen, W. Li, J. Grote, and A. Steckl; "*Red/blue electroluminescence from europium-doped organic light emitting diodes*", Proc. SPIE **6117** 0O1(2006)

43. J. Hagen, J. Grote,W. Li, A. Steckl, D. Diggs, J. Zetts, R. Nelson, and F. Hopkins; "*Organic light-emitting diode with a DNA biopolymer electron-blocking layer*", Proc. SPIE **6333**, 0J1(2006)

44. J. Hagen, W.-X. Li, H. Spaeth, J. Grote, and A. Steckl; "*Molecular beam deposition of DNA nanometer films*", Nano Lett. **7**,137(2007)

45. N. Kobayashi, S. Umemura, K. Kusabuka, T. Nakahira, H. Takashi; "*An organic red-emitting diode with a water soluble DNA-Polyaniline complex containing Ru(bpy)$_3^{2+}$ ",* J. Mater. Chem.**11**,1766(2001)

46. Z. Yu, W. Li, J. A. Hagen, Y. Zhou, D. Klotzkin, J. G. Grote, and A. J. Steckl; "*Photoluminescence and lasing from deoxyribonucleic acid (DNA) thin films doped with sulforhodamine*", Appl. Opt. **46**, 1507(2007).

47. Y. Kawabe, L. Wang, T. Nakamura, and N. Ogata; "*Thin-filmlasers based on dye–deoxyribonucleic acid–lipid complexes*", Appl. Phys. Lett. **81**, 1372 (2002).

48. G. S. He, Q. Zheng, P. N. Prasad, J. Grote, and F. K. Hopkins; "*Infrared two-photon-excited visible lasing from a DNA–surfactant–chromophore complex*", Opt. Lett**. 31**, 359(2006).

49. Y. Kawabe, L. Wang, S. Horinouchi, and N. Ogata; "*Amplified spontaneous emission from fluorescent-dye-doped DNAsurfactant complex films",* Adv. Mater. **12**, 1281(2000).

50. J. Chen, R. Deaton, and Y. Wang; "*A DNA-based memory with in vitro learning and associative recal,*", Proc. of Ninth Annual Meeting on DNA-Based Computers, **127** (2003)

51. A. Kameda, M. Yamamoto, H. Uejima, M. Hagiya, K. Sakamoto, and A. Ohuchi; "*Hairpin-based state machine and conformational addressing: Design and experiment*", Natural Computing **4**, 103 (2005).

52. A. Miniewicz, A. Kochalska, J. Mysliwiec, A. Samoc, M. Samoc, and J. G. Grote; "*Deoxyribonucleic acid-based photochromic material for fast dynamic holography"*, Appl. Phys. Lett. **91**, 041118(2007)

53. Mbindyo J. K. N, Reiss B. D, Martin B. R, Keating C. D, Natan M. J, and Mallouk T. E; "*DNA-Directed Assembly of Gold Nanowires on Complementary Surfaces",* Adv. Mater. **13**, 249 (2001).

54. Storhoff J. J *and Mirkin C. A; "Programmed Materials Synthesis with DNA",* Chem. Rev. **99,** 1849 (1999).

55. Braun E, Eichen Y, Sivan U, Ben-Yoseph G; *"DNA-templated assembly and electrode attachment of a conducting silver wire",* Nature **391**,775(1998)

56. Zhiguo Liu, Yuangang Zu , Yujie Fu, Yuliang Zhang, Huili Liang; *"Growth of the oxidized nickel nanoparticles on a DNA template in aqueous solution"* , Mater. Lett. **62**, 2315(2008)

57. Yong Yao, Yonghai Song and Li Wang; *"Synthesis of CdS nanoparticles based on DNA network templates"*, Nanotechnology **19,** 405601(2008)

58. Gang Wei, Li Wang, Zhiguo Liu, Yonghai Song, Lanlan Sun,Tao, Yang and Zhuang Liz; *"DNA-Network-Templated Self Assembly of Silver Nanoparticles and their application in Surface enhanced Raman scattering"*, J Phys Chem. B. **109**, 23941(2005)

59. Zhu, Xuehong Liao, Hong-Yuan Chen Junjie; *"Electrochemical preparation of silver dendrited in the presence of DNA",* Material Research Bulletin **36** 1687(2001)

60. Xiang Dong Liu, HongYan Diaob and Norio Nishi; *"Applied chemistry of natural DNA",* Chem. Soc. Rev., **37**, 2745(2008)

61. A. Rex and F. Fink; *"Applications of laser-induced fluorescence spectroscopy for the determination of NADH in experimental neuroscience"*, Laser Phys. Lett. **3**, 452(2006).

62. G. K. Giorgadze, Z. V. Jaliashvili, K. M. Mardaleishvili, T. D. Medoize, and Z. G. Melikishvili; *"Measurement of the abnormality degree in the biological tissue by the laser induced fluorescence",* Laser Phys. Lett. **3**, 89 (2006).

63. P. M. Sandeep, S. W. B. Rajeev, M. Sheeba, S. G. Bhat, and V. P. N. Nampoori; "*Laser induced fluorescence based optical fiber probe for analyzing bacteria*", Laser Phys. Lett.**1**, 5 (2007).

64. N D Gómez, V M Freytes, J Codnia, F A Manzano and M L Azcárate *"Implementation of laser induced fluorescence technique to study the kinetics of radicals generated in the IR multiphoton dissociation of chloroform*", J. Phys. Conf. Ser. **274** 012097(2011)

65. C. Neal Stewart Jr et.al; "Laser-Induced Fluorescence Imaging and Spectroscopy of GFP Transgenic Plants" , J. Fluorescence **15**, 697 (2005)

..........ᘓᘔ..........

Chapter 2

Studies on Dye –DNA-Poly Vinyl Alcohol system

Abstract

This chapter describes the results obtained from investigations on the effect of DNA on nonlinear optical properties of Rhodmine 6G-PVA solution and thin film using open aperture Z-scan. We observed saturable absorption (SA) at 532 nm for dye solution without DNA. A strong influence on SA behavior of dye solution is observed by adding DNA. As the concentration of DNA (2 wt %) increased, we observed RSA within SA. The sample shows SA behavior away from focus and RSA behavior near the focus. Theoretical analysis has been performed using a model based on nonlinear absorption coefficient and saturation intensity. In dye doped DNA –PVA film, complete switch over from SA to RSA is observed when concentration of DNA changes from 1 wt% to 1.5 wt%. Temperature dependence on structural and nonlinear optical properties of DNA in poly vinyl alcohol solution is studied, details of which are illustrated in this chapter. As temperature increases from $30^{0}C$ to $55^{0}C$ the nonlinear absorption coefficient decreases from approximately 0.5 cm/GW to 0.02 cm/GW.

2.1. INTRODUCTION

The bio-organic polymer, DNA is emerging as a novel exciting photonic polymer material due to its unique double-helix structure. From the rich world of organic materials, biomaterials are of particular interest as they often have unusual properties that are not easily replicated in conventional organic or inorganic materials in the laboratory. Furthermore, natural biomaterials are a renewable resource and are inherently biodegradable [1, 2]. DNA can be used as a photonic material for making optical waveguide, both on its own and also as a host material accepting appropriate chromophores. There have been numerous investigations on lumophore-doped DNA and laser emission from solid state thin film of DNA as well [3-6].

It is important to evaluate parameters which may be relevant for photonic device applications of DNA itself and the materials derived from it. Determination of second and third order nonlinearities are of fundamental importance for evaluation of the properties with respect to wave-guiding structures containing DNA based materials. In order to study the use of DNA for photonic applications, temperature dependence of relevant properties is important. In the present chapter we have studied the temperature dependence of nonlinear optical properties of DNA arising due to denaturation using Z-scan technique. In order to understand the detailed aspects of DNA interaction with dye, investigation on nonlinear optical properties of dye doped DNA matrix are carried out. Numerous organic chromophores show extremely large and fast nonlinearities [7]. We have used poly vinyl alcohol (PVA) - for dissolving DNA and dye for carrying out most of the experiments. Since DNA and PVA are water soluble, it is very easy to make thin film of DNA-PVA mixture by allowing it to get dry. Polyvinyl alcohol (PVA) has excellent film forming, emulsifying and adhesive properties. In the DNA-PVA system we have incorporated Rhodamine 6G dye, which is frequently investigated to

characterize dye lasers in a variety of liquid and solid hosts, on account of its high fluorescence quantum yield, low intersystem crossing rate and low excited state absorption at both pump and lasing wavelength [8]. To make the thesis self contained, relevant aspects of nonlinear optics are described in the following section.

2.2. NONLINEAR OPTICS

Nonlinear optical response has been studied for a long time in relation to the photonic device application. Nonlinear optics has been a rapidly growing field in the past few decades. It is based on the study of effects and phenomena related to the interaction of intense coherent light radiation with matter. Nonlinear optics is observed with lasers which have high degree of spectral purity, coherence and directionality with which atoms and molecules can be irradiated with an equivalent electric field that is comparable to inter atomic field. Studies on optical nonlinearity and related dynamics are useful for the development of new materials for applications in ultra fast optical devices [9-15].

The property of optical nonlinearity can be well understood by considering the dependence of dipole moment per unit volume or polarization **P(t)** of the material on the strength **E(t)** of the applied electric field associated with electro magnetic field (EMF). In the case of linear optics the induced polarization has a linear dependence on the electric field strength which can be described as

$$\mathbf{P}(t) = \chi^{(1)}\mathbf{E}(t) \qquad \qquad ......(2.1)$$

where the constant of proportionality $\chi^{(1)}$ is the linear optical susceptibility. When the electric field is significantly high, nonlinear interaction occurs and the observed nonlinear optical effects can be described by expressing the induced polarization **P (t)** as a power series in the field strength **E(t)** as

$$\mathbf{P(t)} = \chi^{(1)}\,\mathbf{E(t)} + \chi^{(2)}\,\mathbf{E}^2\,\mathbf{(t)} + \chi^{(3)}\,\mathbf{E}^3\,\mathbf{(t)} + \ldots\ldots \qquad \ldots(2.2)$$

$$= \mathbf{P}^{(1)}\mathbf{(t)} + \mathbf{P}^{(2)}\,\mathbf{(t)} + \mathbf{P}^{(3)}\,(\mathbf{t}) + \ldots\ldots \qquad \ldots(2.3)$$

where $\chi^{(2)}$, $\chi^{(3)}$ are the second and third order nonlinear optical susceptibilities respectively. The second and third order polarizations can be expressed as

$$\mathbf{P}^{(2)}\mathbf{(t)} = \chi^{(2)}\,\mathbf{E}^2\mathbf{(t)} \qquad \ldots(2.4)$$

$$\mathbf{P}^{(3)}\mathbf{(t)} = \chi^{(3)}\,\mathbf{E}^3\mathbf{(t)} \qquad \ldots(2.5)$$

The physical processes that occur due to second and third order polarizations are distinct from each other. Unlike in the case of 3rd order nonlinearity, second order nonlinear effects occur only in non centrosymmetric crystals. Third order nonlinear processes are of special importance because they belong to the nonlinearity which is the lowest order nonlinear effect in majority of the materials. In resonant media the third order optical susceptibility is considered to be a complex quantity having both real and imaginary components. $\chi^{(3)} = \chi_R^{(3)} + \chi_I^{(3)}$. The real and imaginary parts are related to n_2 and β respectively, where n_2 is the nonlinear refractive index and β is the nonlinear absorption coefficient [10, 11].

2.2.1. Nonlinear Optical Absorption (NLA)

In the low intensity field the amount of light absorbed by any absorbing medium increases linearly with input intensity and is termed as linear absorption. At sufficiently high intensities the probability of a material absorbing more than one photon before relaxing to the ground state is greatly enhanced. Other than two or more photon absorption, many other complicated phenomena like population redistribution, complicated energy transitions in complex molecular systems and the generation of free carriers are accompanied by the intense optical fields. These phenomena are manifested optically in a reduced (saturable) or increased (reverse saturable) absorption.

The two absorptive mechanisms resulting in reverse saturable absorption (RSA) are the two or multiphoton absorption and the excited state absorption (ESA). Two photon or multiphoton absorption involves a transition from the ground state of a system to a higher lying state by the simultaneous absorption of two or more photons from an incident radiation. This process involves different selection rules than those of single photon absorption. Fig. 2.1 shows the schematic representation of TPA. The intermediate state is the virtual level and hence the system must absorb two photons simultaneously.

The nonlinear absorption in this case is proportional to the square of the simultaneous intensity (I) and is given by

$$\frac{dI}{dz} = -\alpha I - \beta I^2 \qquad \qquad \text{......2.6}$$

Where α is the linear absorption coefficient and β is the two photon absorption coeficient.

The absorption of (n+1) photons (multi photon) from a single optical beam is given by

$$\frac{dI}{dZ} = -(\alpha + \gamma^{(n+1)} I^n) I \qquad \qquad \text{......2.7}$$

Where γ^{n+1} is the (n+1) photon absorption coefficient.
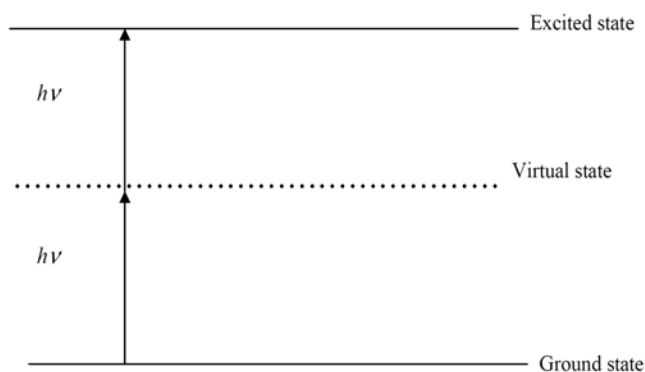
Figure: 2.1. *Schematic diagram of two photon absorption*

When the incident intensity is well above the saturation intensity, the excited state can become significantly populated. The excited electrons can rapidly make a transition to higher excited states before it eventually makes transition back to the ground state. In organic molecules, transitions are possible to higher energy singlet and triplet manifolds. Depending on the pulse duration, pump intensity and wavelength the excited electrons from the first excited singlet state S_1 can make transition to higher excited singlet states S_n or from the T_1 to T_n states in the triplet manifold. This is known as the excited state absorption (ESA). When the cross section for TPA or ESA is greater than that of linear absorption, reverse saturable absorption (RSA) occurs. It is observable when the incident beam intensity is sufficiently high to deplete the ground state significantly. In the case of ESA the absorption cross section σ_{01} from ground state to first excited state will be lower than the excited state absorption cross section σ_{12}.

The nonlinear process associated with real energy level is the saturable absorption (SA). In this process, absorption of light by the material decreases with increasing light intensity. Here, the absorption cross section of material $\alpha(I)$ decreases with intensity. On the other hand, when the absorption cross section increases with intensity, the system will be less transmissive when excited. This gives the opposite effect of SA and the phenomenon is termed as reverse saturable absorption (RSA).

Third order nonlinearity effect can be easily studied in Z-scan technique and details of which are given in the following section.

2.2.2. Open Aperture Z-scan to Study NLA

The Z-scan technique is a simple and sensitive single beam method developed by Sheik Bahae [15] to measure the sign and magnitude of both real and imaginary part of third order nonlinear susceptibility $\chi^{(3)}$. When a high intensity laser beam propagate through any nonlinear material, photo induced refractive index variations may lead to self focusing of the beam. The propagation of laser beam inside such a material and the ensuing self refraction can be studied using the Z-scan technique.

The experimental set up for single beam Z-scan technique is given in Fig. 2.2. In the single beam configuration, the transmittance of the sample is measured, as the sample is moved along the propagation direction of a focused Gaussian beam. In Z-scan measurement, it is assumed that the sample is thin and the sample length is much less than the Rayleigh's range z_0 which is given by

$$z_0 = \frac{k\omega_0^2}{2} \qquad ...(2.8)$$

where k is the wave vector and ω_0 is the beam waist. This is essential to make sure that the beam profile does not vary appreciably inside the sample. The refractive nonlinearity is obtained by measuring the transmittance through a finite aperture in the far field as function of the sample position z from the focal plane. This is the closed aperture Z-scan technique by which the sign and magnitude of nonlinear refractive index n_2 can be determined. In this method, the phase distortion suffered by the beam while propagating through the nonlinear medium is converted into corresponding amplitude variation.

The absorptive nonlinearities are determined by the open aperture Z-scan technique where the entire light is collected by removing the aperture from the experimental setup. Since Z-scan measurements are very sensitive to nonlinear refractive index effects that will spread the transmitted beam, care must be taken

in the case of open aperture scheme to collect the whole transmitted energy. When the entire light is collected, the throughput is sensitive only to nonlinear absorption resulting from the intensity dependent refractive index. Nonlinear absorption present in the sample is manifested in the measurements as a transmission minimum at the focal point [16-20]. Since we are interested only in intensity dependent optical absorption, experiments were restricted only to open aperture Z-scan technique in the present case.
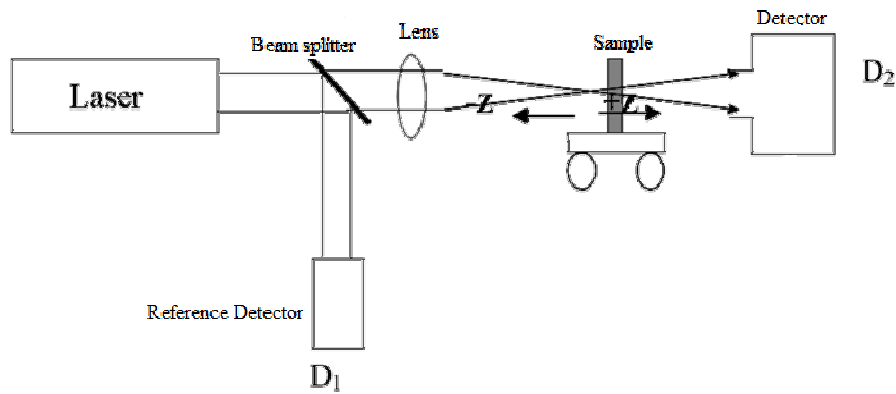
Figure 2.2. *Schematic representation of the experimental set up for Z-scan technique.*

2.2.3. Theory of Open Aperture Z-scan Technique

When the absorption coefficient of a medium has a dependence on laser beam intensity, one can write

$$\alpha(I) = \alpha_0 + \beta\, I \qquad\qquad \text{.... (2.9)}$$

where α_0 is the linear absorption coefficient and β is the nonlinear absorption coefficient of the medium.

The irradiance at the exit surface of the sample can be written as

$$I_r(z,r,t) = \frac{I_{(z,r,t)}e^{-\alpha_0 l}}{1 + q(z,r,t)} \qquad \text{.... (2.10)}$$

where $\quad q(z,r,t) = \beta\, I(z,r,t) L_{eff}$ $\qquad$ ....(2.11)

L_{eff} is the effective length and is given in terms of sample length l and α_0 by the relation

$$L_{eff} = \frac{(1 - e^{\alpha_0 l})}{\alpha_0} \qquad \text{.... (2.12)}$$

The total power transmitted P (z,t) is obtained by integrating equation 2.10 over z and r and is given by

$$P(z,t) = P_1(t)e^{-\alpha_0 l}\,\frac{\ln[1 + q_0(z,t)]}{q_0(z,t)} \qquad \text{.... (2.13)}$$

$P_1(t)$ and $q_0(t)$ are given by the equations

$$P_1(t) = \frac{\pi\omega_0^2 I_0(t)}{2} \qquad \text{.... (2.14)}$$

$$q_0(z,t) = \frac{\beta_f I_0(t) L_{eff}\, z_0^2}{z^2 + z_0^2} \qquad \text{.... (2.15)}$$

Where z_0 is the Rayleigh's range, equation 2.13 can be integrated to give the transmission as

$$T(z) = \frac{C}{q_0\sqrt{\pi}} \int_{-\infty}^{\infty} \ln(1 + q_0 e^{-t^2})\, dt \qquad \text{.... (2.16)}$$

If $|q_0| \angle 1$, equation 2.16 [16] can be simplified as

$$T(z) = \sum_{m=0}^{\infty} \frac{[-q_0(z,0)]^m}{(m+1)^{\frac{3}{2}}} \qquad \text{....(2.17)}$$

where m is an integer. Once open aperture Z-scan is performed, the parameter q_0 can be obtained by fitting the experimental results to equation 2.16.Then the nonlinear absorption coefficient β can be unambiguously deduced using equation 2.11.

The nonlinear absorption coefficient is related to Im(χ^3) by the relation

$$\text{Im}(\chi^3) = \frac{\varepsilon_0 n_0^2 c^2 \beta}{\omega} \ (\text{m}_2 \text{V}^2) = \frac{n_0^2 c^2 \beta}{240\pi^2 \omega} \ (\text{esu}) \qquad \dots (2.18)$$

where ω is the excitation frequency, n_0 is the linear refractive index, ε_0 is the permittivity of free space and c the velocity light in vaccum [16].

2.3. MATERIALS AND METHODS

DNA powder (SRL, extracted from herring sperm) at appropriate amount in polyvinyl alcohol solution (PVA-Merck) is taken to study the effect of temperature on nonlinear optical properties of the DNA. We have studied variation in absorption spectra of DNA at different temperature using UV-VIS NIR spectrophotometer (Jasco V-570). Nonlinear studies are carried out by Z-scan technique. Rhodamine 6G at appropriate concentration is dissolved in polyvinyl alcohol (PVA). In order to study the effect of DNA on the dye solution, DNA was added at different concentration in the range of 1 to 2 wt%. Effect of DNA on the nonlinear optical properties Rhodamine 6G solution was carried out by Z-scan technique. A mode locked Nd:YAG laser (Spectra Physics LAB-1760) having 10 ns pulses at a repetition rate of 10 Hz giving second harmonic at 532 nm was used in the Z-scan experiment to study the optical nonlinearity. The sample is moved along the axis of light beam which is focused

with a lens of focal length 200 mm. The radius of the beam waist w_0 is calculated to be 42.56 μm. The Rayleigh length $z_0 = \pi a_0^2 / \lambda$, is estimated to be 10.6 mm, which is much greater than the thickness of the sample cuvette (1mm), which is an essential condition for Z-scan experiments. The transmitted beam energy, reference beam energy and their ratio are measured simultaneously by an energy ratiometer (Rj620, Laser Probe Corp.) having two identical pyroelectric detector heads (Rjp 735). The complete experimental setup is automated using labview. The effect of fluctuations of laser power is eliminated by dividing the transmitted power by the power obtained at the reference detector.

Absorption spectra and Z - scan experiment are performed in Rhodamine 6G- DNA-PVA film also. The required film is fabricated by dissolving certain amount of PVA (8 wt%) into distilled water at 80 ^{0}C under continuous stirring for 3 hr. DNA solution were prepared in water by dissolving required amount of DNA in distilled water in which Rhodamine 6G dye at concentration of 2×10^{-3} M was added. PVA and DNA solutions were then mixed for 4 hr. After mixing the solutions, thin film is fabricated on glass substrate by dip coating technique. Film thickness can be varied either by changing the viscosity of solution or by increasing the number of coating layers.

2.4. RESULTS AND DISCUSSIONS

Fig. 2.3 shows absorption spectra of DNA- PVA solution measured at different temperature (30-55 ^{0}C). In all temperature DNA shows absorption peak at 260 nm which is the characteristics of DNA absorption and is consistent with reported result of enhancement in absorption at 260 nm with increase in temperature. This band is due to the absorption of light by nucleic acid bases of DNA. Significant increase in absorption peak in the absorption spectra of the

sample describe temperature increased hyperchromic shift on increase in light absorbance at 260 nm region. Both native and denatured DNA are capable of absorbing UV light at a wavelength of 260 nm due to the aromaticity of nitrogenous bases. However, the stacking of nitrogenous bases in native DNA interferes with UV absorption, resulting in a lower absorbance. Denaturation disrupts such stacking, allowing for more absorbance by the bases. Thus increase in absorbance indicates the degradation or unwinding of DNA molecule from double stranded structure [21].

Open aperture Z-scan is plotted in Fig. 2.4 for three temperature at intensity 50 MW/cm^2. Transmittance is minimum at the focus and increases steadily on both sides of the focus indicating RSA. Fitting of the experimental open aperture Z-scan plot to theoretical curve describes the TPA induced RSA. Two-photon absorption is possible in DNA at 532 nm corresponding to twice the wavelength of the main absorption peak (260 nm) [22-24]. From analysis it is found that two photon absorption coefficient of DNA varies in the range approximately 0.5 cm/GW to 0.02 cm/GW as temperature varies from 30 to 55^{0}C. Thus our studies show the decrease in two photon absorption cross section as temperature is increased. The absorbance at 260 nm leads to more atoms in excited state compared to lower state. This leads to saturation in ground state absorption thereby leading to decrease in two photon absorption coefficient. From absorption spectra it is clear that increase in temperature leads to denaturation or unwinding of the DNA molecule. Also Z-scan curve shows decrease in two photon absorption coefficients which is a measure of loss of double stranded structure.
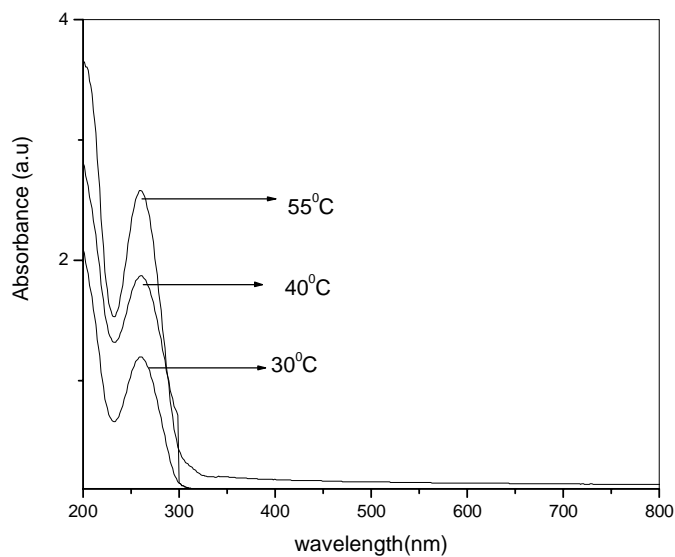
Figure: 2.3. *Absorption spectra of DNA in PVA at different temperatures*
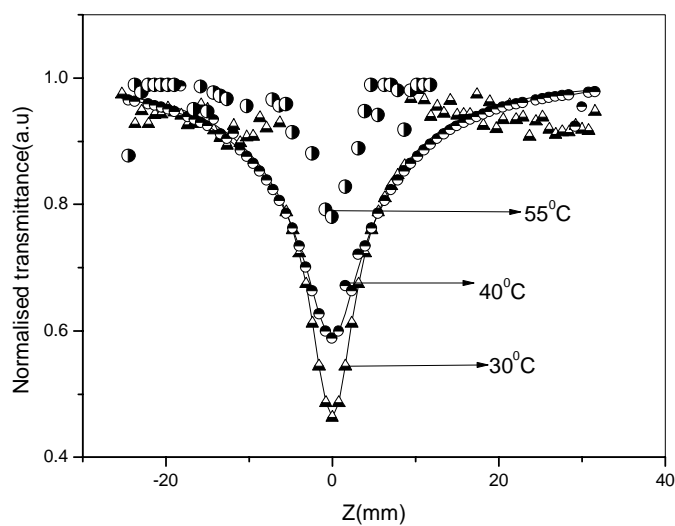
Figure: 2.4. *Open aperture Z-scan curve of and DNA in PVA solution at different temperatures*
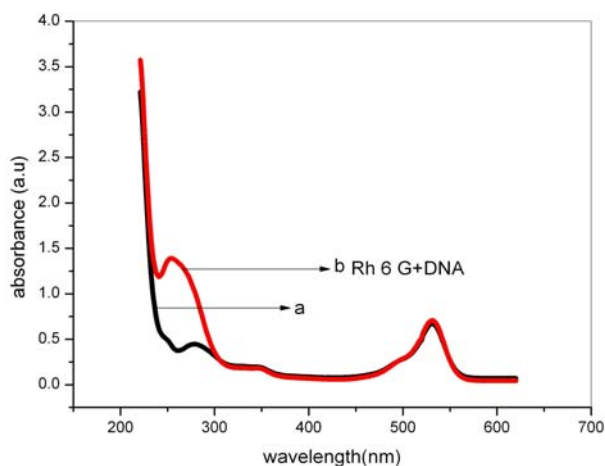
Figure: 2.5. *Absorption spectra of dye doped DNA-PVA solution*

      a. *Rhodamine 6G -PVA alone*

      b. *Rhodamine 6G –DNA-PVA*

The linear absorption spectra for Rhodamine 6G solution (2×10^{-3} M) and DNA doped Rhodamine 6G solution in polyvinyl alcohol are shown in Fig. 2.5. Absorption peak of the Rhodamine 6G is prominent in the visible region around 532 nm. The curve b shows the presence of DNA in dye solution as is confirmed by the presence of the absorption band 260 nm which is characteristics of DNA.

Fig. 2.6 shows the plot related to open aperture Z - scan experiment in Rhodamine 6G solution at resonance wavelength of 532 nm with typical laser fluence of 175 MW/cm^2. At this wavelength, which is close to peak of the absorption band, saturable absorption (SA) behavior is observed. Since increase in transmission with increased intensity is observed at this wavelength. In this wavelength the linear absorption coefficient is very large, and strong pumping leads to saturation rather than RSA. Fig. 2.7 shows the open aperture curve of dye solution doped with 1 wt% of DNA. An important point to be noted is a small dip at the focal point. As the concentration of DNA increased to 2wt % (Fig. 2.8) the dip develops into a well defined RSA structure within the SA

pattern. In other words the sample shows SA behavior away from focus and RSA behavior near the focus. Similar observations of switching from SA to RSA have been observed in other studies. For example Rhodamine B dye in methanol and water, Zinc meso-tetra tetrabenzoporphyrin (ZnmpTBP), polymethine dye and coordination compound [25-28]. In Rhodamine B the behaviour is due to the aggregation of dye moleules in higher concentration [25]. In ZNmpTBP the behavior was attributed to the excitation of population into higher excited state at higher intensities, giving rise to RSA and the SA behavior was given as due to the saturation of the triplet state T1[26]. In polymethine dye this behavior was attributed to irreversible damage induced by the input pulses [27]. For Ruthenium and Osmium complexes of modified terpydines, the saturation behavior was explained due to the formation of compounds and the RSA portion as being due to TPA of the solvent [28]. In the present case, the observed behavior is due to the effect of DNA.

To estimate saturation intensity and nonlinear absorption coefficient, experimental data were fitted with numerical simulations. To analyse the flip of saturable absorption around focus, we combine a saturable absorption coefficient and the two photon absorption coefficient (TPA) as

$$\alpha(I) = \frac{\alpha_0}{1 + \dfrac{I}{I_s}} + \beta I \qquad \qquad \text{.... (2.19)}$$

where the first term describes saturable absorption and the second term describes reverse saturable absorption resulting from two photon absorption, α_0 is the low intensity absorption coefficient, I and I_s are laser radiation intensity and saturation intensity, respectively, while β is nonlinear absorption coefficient.

The normalized transmittance for open aperture Z-scan is given by the equation

$$T(Z) = \sum_{m=0}^{\infty} \frac{\left[\dfrac{-\alpha I_0 L_{eff}}{1 + z^2/z_0^2}\right]^m}{m+1} \qquad \qquad \textbf{....(2.20)}$$

where $L_{eff} = \left(1 - e^{-\alpha_0 L}\right)/\alpha_0$ z is the longitudinal displacement of the sample from focus (Z=0), α is the nonlinear absorption coefficient. I_0 is the peak intensity at focus, L_{eff} is the effective interaction length, α_0 is the linear absorption coefficient, L is the sample length z_0 is the Rayleigh length.

Theoretical fit of the experimental data is obtained by the substitution of Eq.2.19 into Eq.2.20 [29]. In Fig. 2.6 - 2.8 solid line show theoretical fit to the experimental data. In Fig. 2.6 theoretical fit give saturation intensity, I_5 =105 MW/cm^2 and two photon absorption coefficient, β = -0.24 cm/GW. In Fig. 2.9 saturation intensity, I_s =140 MW/cm^2 and two photon absorption coefficient, β is 0.54 cm/GW.
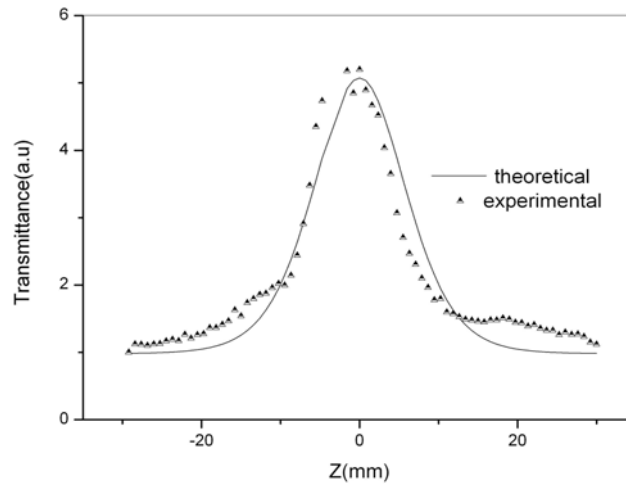
Figure: 2.6. *Open aperture Z-scan curve of Rhodamine 6G in Polyvinyl alcohol solution*
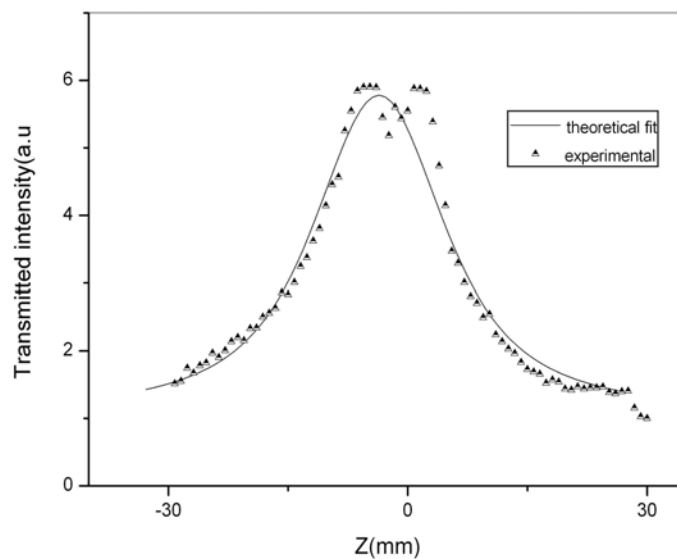
Figure: 2.7. *Open aperture Z-scan curve of DNA (1 wt%) doped in Polyvinyl alcohol solution of Rhodamine 6G (Note a small dip in the transmission peak at the focal point.)*
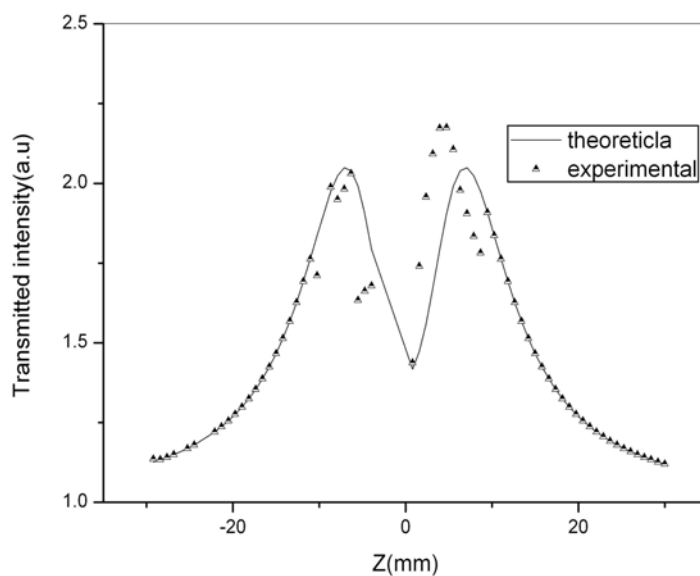
Figure: 2.8. *Open aperture Z-scan curve of DNA (2 wt %) doped Polyvinyl alcohol solution of Rhodamine 6G.*

To estimate the role of DNA in Rhodamine 6G, we also carried out open aperture Z-scan measurements on DNA (2 wt %) in PVA and PVA alone at the same laser power. As shown in Fig. 2.9 no obvious nonlinear absorption effect was found for PVA alone. But DNA in PVA shows strong nonlinear absorption leading to two photon absorption (β =0.01 cm/GW). This indicates that the switch over from SA to RSA is due to extra absorption arising due to two photon absorption in DNA. The absorption saturation of Rhodamine 6G at 532 nm is represented as the SA behavior in Rhodamine 6G-PVA system. The influence of DNA on the nonlinear character of the Rhodamine 6G-PVA solution lead to RSA near the focal point.
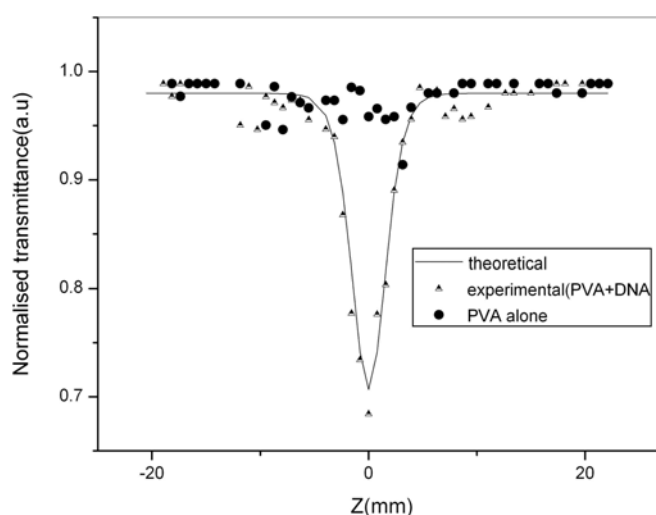
Figure: 2.9. *Open aperture Z-scan curve of polyvinyl alcohol solution (PVA) and DNA –PVA solution*

Fig. 2.10 shows the absorption spectra of dye DNA – PVA thin film and dye –PVA thin film structures. The characteristic absorption peak of the DNA at 260 nm is shifted to 280 nm. This may be due to the change in micro environment of DNA molecule in the thin film. DNA based films are promising candidates for optoelectronic applications due to observed amplified

spontaneous emission ASE enhanced fluorescence, low optical loss and nearly zero background emission. Fig. 2.11 is the open aperture Z-scan curve of the dye doped DNA –PVA film. Curve "a" is Z-scan curve of Dye-PVA alone exhibiting SA behaviour. As we increase the concentration of DNA (0.5 wt% to 2 wt %), film shows switching over from SA to RSA.
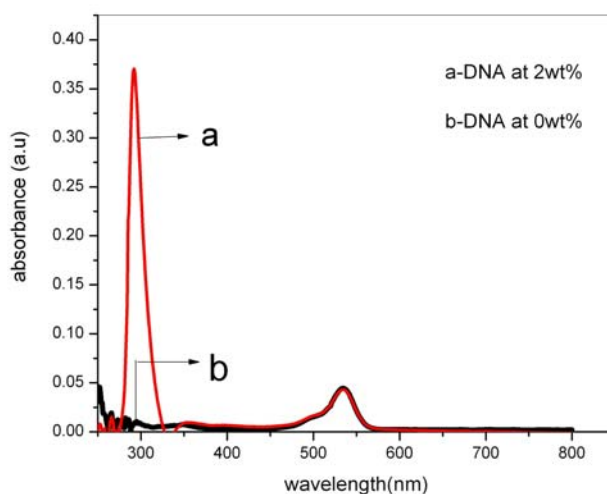
Figure: 2.10. *Absorption spectra of dye doped DNA- PVA thin film*
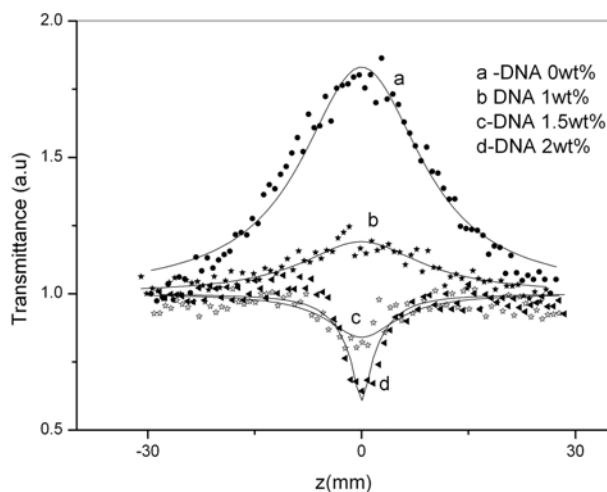
Figure: 2.11. *Open aperture Z-scan curve of DNA doped Rhodamine 6G   Polyvinyl alcohol thin film of thickness 500 μ m*

2.5. CONCLUSIONS

In summary, the absorption spectra and Z-scan studies show DNA-PVA matrix is very sensitive to temperature and gets denatured as we increase the temperature. Two photon absorption coefficient of DNA-PVA matrix decreases from 0.5 cm/GW to 0.02 cm/GW as temperature increases from $30\,^0$C to $55\,^0$C. Our Z-scan experiments have revealed interesting features of the nonlinear absorption properties of DNA doped rhodamin6G-PVA solution. At 532 nm excitation SA behavior was observed for Rhodamine 6G –PVA solution. On doping DNA at 2 wt% in Rhodamine 6G –PVA solution, we have observed RSA behavior near focus and SA behavior away from focus. Saturation intensity and nonlinear absorption coefficients were estimated by performing numerical fitting to the experimental data. DNA plays good role in the nonlinear behavior of Rhodamine 6G-PVA solution. The simultaneous occurrence of several nonlinear processes in dye-DNA- PVA system can be made use of in developing various photonic devices. In thin film of dye –PVA matrix we observed direct switch over from SA to RSA by increasing the concentration of DNA.

REFERENCES

1. P. N. Prasad, "*Introduction to Bio Photonics*", (Wiley-Interscience, 2003),

2. A. J. Steckl; "DNA - a new material for photonics?", Nat. Photon. **1**, 3 (2007).

3. Y. Kawabe, L. Wang, S. Horinouchi, and N. Ogata; "*Amplified spontaneous emission from fluorescent-dye-doped DNAsurfactant complex films*"; Adv. Mater. **12**, 1281 (2000).

4. Z. Yu,W. Li, J. A. Hagen, Y. Zhou, D. Klotzkin, J. G. Grote, and A. J. Steckl; "*Photoluminescence and lasing from deoxyribonucleic acid (DNA) thin films doped with sulforhodamine*", Appl. Opt. **46**, 1507(2007).

5. Y. Kawabe, L. Wang, T. Nakamura, and N. Ogata; *"Thin-film lasers based on dye–deoxyribonucleic acid–lipid complexes"*, Appl. Phys. Lett. **81**, 1372 (2002).

6. G. S. He, Q. Zheng, P. N. Prasad, J. Grote, and F. K. Hopkins;*"Infrared two-photon-excited visible lasing from a DNA–surfactant–chromophore complex"*, Opt. Lett. **31**, 359(2006).

7. K Geetha, M Rajesh, V P N Nampoori1, C PGVallabhan and P Radhakrishnan; *"Laser emission from transversel ypumped dye-doped free-standing polymer film"*, J .Opt. A: Pure Appl. Opt. **8** ,189(2006)

8. C. V. Bindhu, S. S. Harilal, V. P. N. Nampoori and C. P. G. Vallabhan; *"Studies of nonlinear absorption and aggregation in aqueous solutions of Rhodamine 6G using transient thermal lens technique"*; J. Phys. D **32**, 407(1999)

9. R. L. Sutherland, *"Hand book of nonlinear optics"*, Marcel Dekker (1996)

10. Y. R. Shen, *"The Principles of nonlinear optics"*, John Wiley and sons, New York (1991)

11. R. A. Gannev; *"Nonlinear refraction and nonlinear absorption of various media"*, J. Opt. A: pure and Appl. Opt. **7,** 717(2005)

12. J. S. Shirk, R.G.S.Pong, F. J. Bartoli A. W. Snow; *"Optical limiter using a lead phthalocyanine"* , Appl. Phys. Lett. **63**, 1880 (1993)

13. H. Ditlbacher, J.R. Krenn, B. Lamprecht, A. Leitner, F.R. Aussenegg; *"Spectrally coded optical data storage by metal nanoparticles"*, Opt.Lett. **25**, 563(2000)

14. H. Hashimoto, T. Nakashima, K. Hattori, T. Yamada , T. Mizoguchi, Y. Koyama, T. Kobayashi; *"Structures and non-linear optical properties of polar carotenoid analogues"*, Pure Appl. Chem. **71**, 2225(1999)

15. M. Sheik Bahae, A. A. Said, T. Wei, D. J.Hagan, E. W. Van Stryland ; *"Sensitive measurements optical nonlinearities using a single beam",* IEEE **26**, 760 (1990)

16. W. Zang, J. Tian, Z. Liu, W. Zhou, F. Song, C. Zhang, J. Xu; *"Accurate determination of nonlinear refraction and absorption by a single Z-scan method",* J. Opt. Soc. Am. B **21**, 439(2004)

17. U. Tripathy, R. J. Rajesh, P. B Bisht, A. Subrahamanyam; *"Optical nonlinearity of organic dyes as studied by Z-scan and transient grating techniques",* Proc, Indian Acad. Sci.(Chem.Sci) **114** 557(2002)

18. Q. Mohammed Ali, P. K. Palanisamy; *"Investigation of nonlinear optical properties of organic dye by Z-scan technique using He-Ne laser",* Optik. **116**, 515(2005)

19. W. Van Stryland, M. Sheik-Bahae, *"Z.scan measurements of optical nonlinearities",* Characterization Techniques and tabulation for organic nonlinear materials*,* E Marcel dekker. Inc 655 (1998)

20. Jiaxi Wu and Leroy F. Liu; *"Processing of topoisomerase I cleavable complexes into DNA damage by transcription", Nucl. Acids Res. 25, 4181 (1997)*

21. James G. Grote et.al; *"DNA-based materials for electro-optic applications: current status",* Proc. SPIE, **5934**, 593406 (2005);

22. G. Zhang, H. Takahashi, L. Wang, J. Yoshida, S. Kobayathi, S. Horinouchi and N.Ogata;*"Nonlinear optical materials derived from Biopolymer DNA – surfactant –Azo Dye Complex*", Proc. SPIE. **4905**, 375(2002**)**

23. Andrzej Miniewicz , Anna Kochalska, Jaroslaw Mysliwiec, Anna Samoc , Marek Samoc James and G. Grote; *"Deoxyribonucleic acid-based photochromic material for fast dynamic Holography",* Appl. Phys. Lett. **91**, 041118 (2007)

24. N. K. M. Naga Srinivas, S. Venugopal Rao, and D. Narayana Rao ;"*Saturable and reverse saturable absorption of Rhodamine B in methanol and water*", J. Opt. Soc. Am. B **20,** (2003)

25. Kimball, M. Nakashima, B. S. Decristofano, and D. N. Rao;''*Wavelength dependent studies of nonlinear absorption in zinc meso-tetra(p-methoxyphenyl)tetrabenzoporphyrin (Znmp TBP) using Z-scan techniqu,',*' J. Porphyri. Phthalocyn. **5**, 549 (2001).

26. O. V. Przhonska, J. H. Lim, D. J. Hagan, E. W. Van Stryland, M. V. Bondar, and Y. L. Slominsky; *''Nonlinear light absorption of polymethine dyes in liquid and solid media'',* J. Opt. Soc. Am. B **15**, 802 (1998).

27. M. Konstantaki, E. Koudoumas, S. Couris, P. Laine, E.mouyal, and S. Leach; *''Substantial non-linear optical response of new polyads based on Ru and Os complexes of modified terpyridines''*, J. Phys. Chem. B **105**,797 (2001).

28. Yachen Gao, Xueru Zhang, Yuliang Li, Hanfan Liu,Yuxiao Wang, Qing Chang, Weiyan Jiao, Yinglin Song; "*Saturable absorption and reverse saturable absorption in platinum nanoparticles*", J. Optcom. **251** 429(2005)

...........ড়ঌ৪ঌ..........

Chapter 3

Amplified spontaneous emission of radiation from Dye –PVA-DNA system

Abstract

Studies on amplified spontaneous emission from Dye-PVA-DNA systems are described in this chapter. The light amplification and optical gain studies in different dye doped DNA-PVA matrices are carried out by varying the pump intensity, concentration of dye and DNA etc. Amplified spontaneous emission (ASE) intensity and lasing threshold are compared in dye doped PVA samples with and without DNA molecule. Lasing is obtained by pumping with a frequency doubled Nd:YAG laser at 532 nm with 10 ns pulse width. Enhanced light amplification and optical gain of the dye –PVA medium are observed. As the concentration of DNA increases, there is a decrease in the lasing threshold and enhancement in ASE intensity. Thin solid film of DNA has been fabricated by treating with polyvinyl alcohol PVA) and used as host for the laser dye Rhodamine 6G. The edge emitted spectrum clearly indicated the existence of laser modes and amplified spontaneous emission (ASE). This film produces a Fabry-Perot optical cavity effect enabling laser emission with FWHM of 0.2 nm. A solid state laser based on dye doped deoxyribonucleic acid (DNA) matrix is described.

3.1. INTRODUCTION

The continued development of photonics technology is crucially dependent on the availability of suitable optical materials. Biomaterials are emerging as an important class of materials for a variety of photonic applications. The most important and famous biomaterial known to man is DNA, the polymeric molecule that carries the genetic code in all living organisms. It is clear that the unique structure of DNA results in many optical and electronic properties that are extremely interesting for photonic applications. DNA is reported to be an efficient host for certain luminescent organic and organometallic molecules in both solution and solid state thin films [1-5]. For example, Kawabe et al. have reported synthesis and film formation method of complexes composed of DNA, lipid and Rhodamine 6G and have observed amplified spontaneous emission (ASE) from relatively highly doped DNA films under pulsed laser excitation [4]. DNA – CTMA thin-films doped with the luminescent dye sulforhodamine (SRh) have been reported to exhibit photoluminescence intensity more than an order of magnitude higher than that of SRh in (poly methyl methacrylate), which is a popular polymer host. Other lumophores have also been reported to luminescence very efficiently in DNA thin films [3].

Qualitative investigations of amplified spontaneous emission of light from organic dyes have been reported by a number of authors. In most cases nano second and pico second light pulses are used as a pump source to get ASE [6-10]. The important features of dye lasers are wide range of their tunability (near ultraviolet to the near infrared), high gain and the possibility of pulsed and continuous wave operation. These properties make dye lasers as attractive sources of coherent tunable radiation. It is showed that most of the dyes lase in the solid, liquid or gas phases [11].

The dye lasers in liquid form cause a number of practical difficulties mainly related to the need of employing large volumes of organic solutions of dyes that are both toxic and expensive. Also, each dye has a limited range of tunability (5 nm to 20 nm) so that the dye has to be changed for different wavelength regions. This, together with the need for complex and bulky cell designs for the continuous circulation of the solution, has restricted the use of these laser systems outside the laboratory. A solid-state dye laser avoids the problems of toxicity and flammability and they are compact, versatile and easy to operate and maintain. The importance of organic solid-state lasers using variety of host and lumophore combinations are discussed in various reviews [12-18]. The first observations of stimulated emission from solid matrices doped with organic dyes were reported as early as 1967 by Soffer and Mcfarland [16]. The synthesis of high performance dyes and the implementation of new ways of incorporating the organic molecules into the solid matrix have resulted in significant advances towards the development of practical tunable solid state lasers. Organic materials, in particular, offer advantages such as ease of processing, which permits the fabrication of devices in virtually any shape and potentially at a very low cost. The combination of the tunability and high efficiency of laser dyes with the high power density that can be easily achieved in waveguide structures make devices based on dye-doped organic material waveguides and fibers very promising [19,20]. There have been numerous investigations on laser emission from polymer planar micro cavities and polymer micro ring lasers, as well [21-23]. Recently, a tandem organic light-emitting diode structure, excited electrically in the pulsed domain and confined within a double interferometric configuration, was observed to emit a low-divergence beam with a near-Gaussian spatial distribution. The emission originates from the laser dye Coumarin 545 T used as dopant [24].

In the present chapter we report the observation of amplified spontaneous emission (ASE) and multimode laser emission from DNA -Poly Vinyl Alcohol solution and PVA -DNA blended film doped with Rhodamine 6G. Polyvinyl alcohol (PVA) has excellent film forming, emulsifying and adhesive properties. Since DNA and PVA are water soluble, it is very easy to make thin film of DNA-PVA mixture by allowing it to get dry. In the DNA-PVA system we incorporated Rhodamine 6G (Rh 6G) dye, which is usually employed to characterize solid –state dye lasers in a variety of solid hosts. Spectroscopic and stimulated emission measurements were performed in liquid and solid samples of Rh 6G-PVA system and Rh 6G-DNA-PVA matrix.

3.2. MATERIALS AND METHODS

Poly Vinyl alcohol solution of 8 wt% concentration was prepared by dissolving appropriate amount of PVA into distilled water at $80^{0}C$ under continuous stirring for 3 hr. Weighed DNA powder (SRL, extracted from herring sperm) were added to prepared PVA solution. Rhodamine 6G dye was then added to PVA -DNA solution in desired concentration. After mixing the solutions by stirring for 4 hr, thin film waveguides were fabricated on glass substrates by dip coating technique. These films show best optical transparency in the visible spectral range. Film thickness can be varied either by changing the viscosity of solution or by increasing the number of coating layers.

Fig. 3.1 shows the schematic diagram of the experimental set up. The samples were transversely pumped using 10 ns pulses from a frequency doubled Nd:YAG laser (Spectra Physics LAB-1760, 532 nm,10Hz). A set of calibrated neutral density filters were used for varying the pump energy. The laser beam was focused on to a stripe shape on the samples from normal incident angle using cylindrical lens. The size of the strip was 1 x 4 mm. Fluorescence emission from the sample was collected from the edge by a fiber and directed to a 0.5 m

spectrograph (Spectra Pro-500i) coupled with a cooled CCD array. The distance between collecting fiber and waveguide edge was 1cm. We kept one end of the excitation strip at the edge of the waveguide. The intensity of fluorescence emission is measured as a function of pump pulse energy. This helps us to determine the threshold energies and confirm spectral narrowing of the emission spectra as excitation intensity is enhanced. The emitted beam from the edge of the sample is so strong and highly directional that we could collect it even without any focusing.
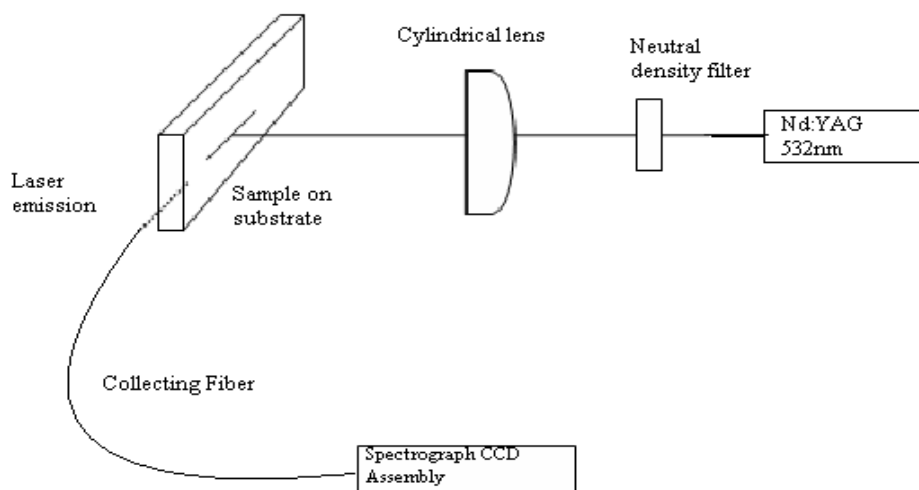
Figure.3.1. *Schematic diagram of experimental set up.*

3.3. THEORY OF AMPLIFIED SPONTANEOUS EMISSION

Amplified spontaneous emission is a phenomenon readily observed in organic dye solution when the sample is excited by intense light pulses. The spontaneously emitted light is amplified through a single pass in the gain medium by stimulating the emission of more photons as it travels down the length. It does not require a population inversion but needs a sufficient number

of excited state molecules along the optical path length. The favourable condition for strong ASE is a high gain medium combined with a long path length in the active material. ASE occurs in a gain medium with long path length either by internal multiple reflections or extended medium. In contrast to spontaneous emission, ASE possesses certain distinctive features of laser emission such as directionality, spectral narrowing, limited coherence, reduced pulse width, low threshold, intense beam and saturation of gain [19]. The gain is strongest at the wavelength where the cross section for stimulated emission is highest. This leads to narrowed spectral line width. The ASE threshold behaviour arises from the saturation. If the travelling wave becomes strong enough to extract all the stored energy (I_{SAT}), the output grows linearly with the pump power as observed in an ordinary laser. Since the ASE shows features of laser emission to some extent even in the absence of any external cavity, it is also known as a mirrorless lasing [25-27].

The measurement of optical gain in terms of the ASE intensity exhibited by extended length of the gain medium is an efficient way of analyzing the potential of the material as a laser medium. A single pass gain measurement proposed by Shaklee et al. is the widely used method to determine the gain of a medium [27]. In this method, gain medium is excited with a cylindrical lens to form a stripe like structure. As mentioned above, it does not require a population inversion but a sufficient number of excited states along the optical path length. Gain occurs when the amplified spontaneous emission of photons exceeds the loss due to reabsorption and scattering. ASE gain is the ratio of light intensity emitted to incident intensity per unit length of the pumped gain material. In materials with high gain, ASE intensity can be high similar to that of multiple pass gain build up in a cavity with mirrors. A signature of ASE is the gain

narrowing of the fluorescence spectrum. As the pump energy increases the spectrum changes from a normal fluorescence to pure ASE.

According to the theory described by Shaklee et al. the rate of change of fluorescence intensity with the length of the pumped region in one dimension is

$$\frac{dI}{dx} = AP_0 + gI \qquad\qquad ....(3.1)$$

Where I is the fluorescence intensity propagating along the x axis.

$g = g' - \alpha$, is the net optical gain where g' is the gain due to stimulated emission and α account for all the optical losses.

AP_0 – the spontaneous emission proportional to pump intensity.

The solution of this equation with respect to pump length is;

$$I = \frac{AP_0}{g(\lambda)}[\exp(g(\lambda)l) - 1] \qquad\qquad ....(3.2)$$

where P_0 – pump intensity

      A – a constant related to spontaneous emission cross section

      l – length of the pumped stripe.

The relation(3.2) shows the exponential growth of the output emission intensity from the dye doped films with the excitation length of the gain medium. For positive values of $g(\lambda)$ the output intensity will exponentially grow and correspondingly a spectral narrowing will be observed since the amplification occurs to a greater extent in certain wavelengths. Thus gain coefficient is wavelength dependent. Shaklee et al. measured the single pass gain of dye medium by comparing the intensities of ASE for two excited stripes of

length *l* and *l*/2 for a constant wavelength [27]. The gain equation for a length of *l*/2 can be written.

$$I(\lambda, l/2) = \frac{P_0 A(\lambda)}{g(\lambda)}[\exp(g(\lambda)l/2)) - 1] \qquad \text{....(3.3)}$$

From equations (3.1) and (3.2), the net gain can be obtained as,

$$g = \frac{2}{l}\ln\left[\frac{I(l)}{I(l/2)} - 1\right] \qquad \text{....(3.4)}$$

Equation (3.4) applies only for pump powers up to the onset of saturation.The gain coefficient can also be calculated by fitting the function for emission intensity of ASE with the experimental data.

3.4. RESULTS AND DISCUSSIONS

3.4.1. Light Amplification from Dye Doped DNA-PVA Solution

To study the nature of emission from the Rhodamine 6G dissolved in PVA, the emission spectra are recorded for various pump intensities starting from 0.5 mJ/pulse with the excitation length of 4 mm. Dye concentration is varied from 0.5×10^{-4} to 5×10^{-3} M. Fig. 3.2 shows the emission spectra from Rhodamine 6G (0.5×10^{-4} M) doped PVA solution under different values of pump intensity. At low pump intensities fluorescence spectra recorded is highly broad with a spectral width of 40 nm. At 2.5 mJ there is a tendency for spectral narrowing and amplification of intensity. The spectral width is reduced to 30nm in this pump energy. DNA at 1.5 wt% is added to study the effect of DNA on ASE of Rhodamine 6G in PVA. The result of the amplification measurements in

the DNA –PVA sample are shown in Fig. 3.3 for the same dye concentration. With the increase in pump intensity, the fluorescence emission spectra become narrow and give amplified spontaneous emission and sharp peak appeared when pump energy increased to 2.5 mJ. This shows DNA plays important role in ASE of dye in PVA. Fig. 3.4 and 3.5 shows emission spectra of dye – PVA and DNA added system of dye concentration 1.5×10^{-4} M at different pump intensity. As we increase the concentration of dye both systems show ASE while increasing pump intensity. However sharp ASE peak is appeared at DNA added system at lower pump intensity. This indicates that presence of DNA reduces ASE threshold value in dye PVA system.

Figure:3.2. *ASE from Rhodamine 6G (0.5×10^{-4} M) doped PVA for different pump intensities at excitation lengths of the pump beam 4mm, where a, b, c, d, e, f are ASE spectrum at 1, 1.5, 2, 2.5, 3, 3.5 mJ respectively.*

Figure: 3.3. *ASE from Rhodamine 6G (0.5x10^{-4} M) doped DNA-PVA for different pump intensities at excitation lengths of the pump beam 4mm, where a, b, c, d are ASE spectrum at 1, 1.5, 2, 2.5 mJ respectively.*

Further investigations are done by changing the concentration of DNA. Fig. 3.6 contains the plots of amplified emission of Rhodamine 6G (1.5x10^{-4} M) at different concentration of DNA with increasing pump intensity. It is clear that as concentration of DNA increases the emission intensity increases and lasing threshold decreases. The threshold pump power for observing laser oscillation is significantly less for DNA added system. The most remarkable feature of this experiment is that the presence of DNA lowers lasing threshold leading to higher gain characteristics in comparison with pure dye in PVA.

Figure: 3.4. *ASE from Rhodamine 6G (1.5x10 $^{-4}$ M) doped PVA for different pump intensities at excitation lengths of the pump beam 4mm, where a, b, c, d, e are ASE spectrum at 1, 1.5, 2, 2.5, 3 mJ respectively.*
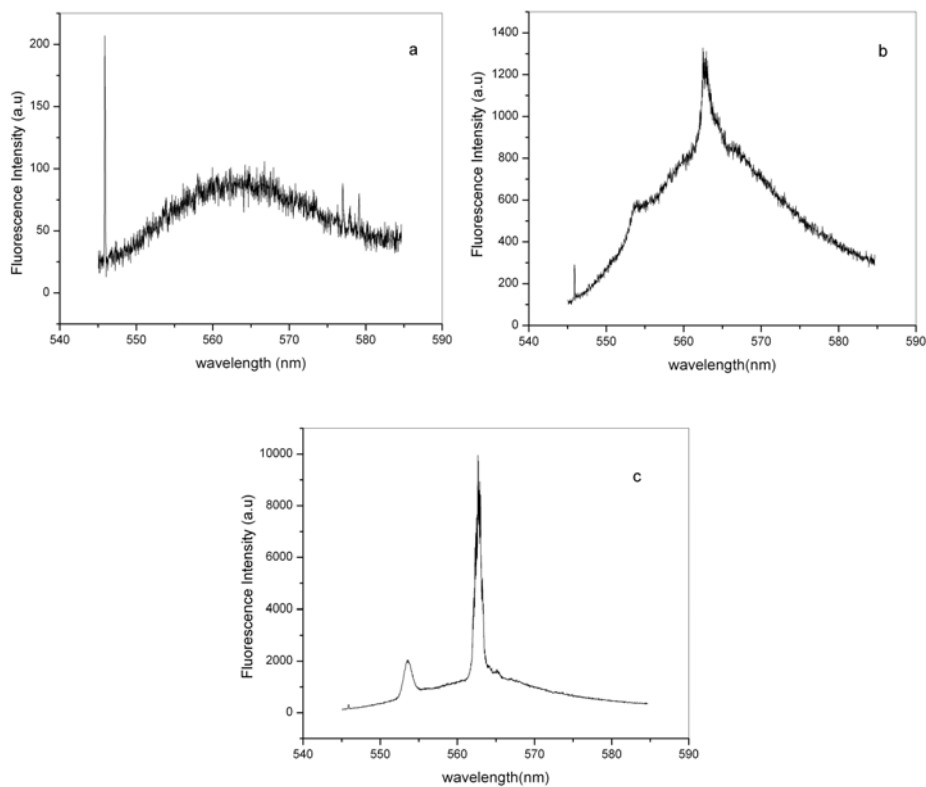
Figure: 3.5. *ASE from Rhodamine 6G (1.5x10^{-4} M) doped DNA-PVA for different pump intensities at excitation lengths of the pump beam 4mm, where a, b, c are ASE spectrum at 1, 1.5, 2, mJ respectively*
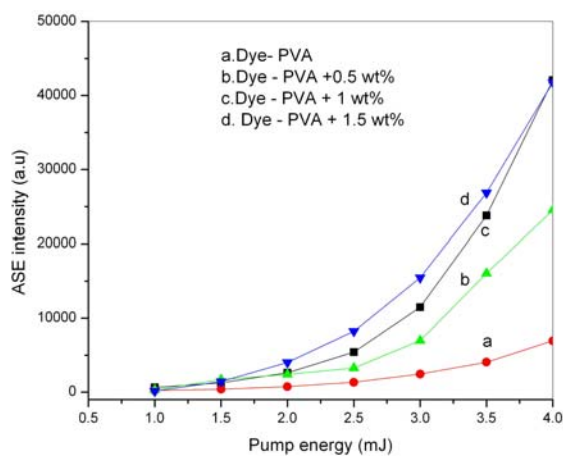
Figure: 3.6. *Shows the effect of DNA on the ASE from dye-DNA-PVA system, clear dependence of DNA on ASE in dye PVA is observed*

Fig. 3.7 shows change in Full width half maximum of ASE spectrum of above mentioned system. Spectral narrowing power of the sample is high for DNA added system compare to its counterpart Dye –PVA system. At particular pump power the FWHM is less for DNA added system. The spectral narrowing is very prominent at higher pump intensities where the FWHM was reduced to a value of 0.3 nm.

Our studies show that the DNA plays an important role in laser emission from dye-PVA-DNA system. Many fluorescent dyes can readily be intercalated into helices of DNA. These dye molecules can be situated inside the double helix structure or at some grooves (minor or major) beside the main chains. The intercalation or groove binding of dyes in the DNA strand make molecules getting isolated from each other thereby reducing the fluorescence quenching caused by aggregation. In the case of Rhodamine 6G, there has not been any evidence of complete intercalation. More studies are required to clarify the microscopic structure and the effects of intercalation on the spectral properties of laser dyes. To understand the fluorescence enhancement due to Rhodamine 6G – DNA intercalation we have measured fluorescence spectra of dye-PVA system and DNA added system using non coherent source at 532 nm. Significant enhancement in the fluorescence is not observed in this case even though there is a slight tendency to enhance intensity. In this context we assume that the reason for gain enhancement may be due to the nonlinear absorption of DNA molecule in dye-PVA system. In chapter 2 we have discussed the effect of DNA on nonlinear absorption of Rhodamine 6G. In the presence of DNA the pump beam 532 nm will excite both dye and DNA molecule by one photon absorption and two photon absorption respectively. The two photon absorption (TPA) of DNA induces RSA thereby exciting DNA molecules to a level which matches with one of the higher state of Rhodamine 6G. The excited DNA molecules will transfer their energy to Rhodamin6G leading to enhancement in the gain of Rhodamine 6G-PVA system in the presence of DNA molecules.
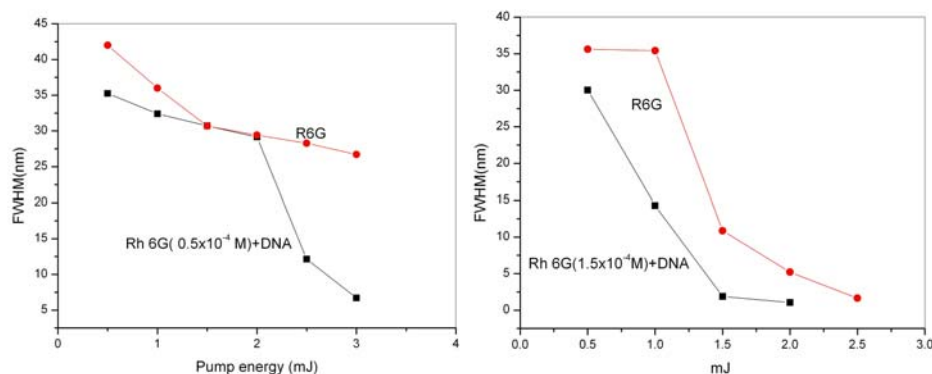
Figure: 3.7. *Full width half maximum of ASE spectra vs pump intensity*

ASE spectrum of highly concentrated dye solutions are shown in Fig. 3.8. It is clear from the figures that dual band is appeared by increasing pump energy. Simultaneous occurrence two distinct peaks are observed when pump energy reaches 2 mJ. The dual ASE should be attributed to the existence of two distinct molecular species in the excited state producing gain independent of each other at different wavelength. The two excited species responsible for the dual ASE differ only on their vibronic mode. The measurements ASE spectra give evidence that the system consists of two fluorescent species monomers and dimers. At high concentrations the dye molecules come near together by random motion and they interact with one another and forms closely spaced pairs. As the dye concentration increases, apart from dye monomers also dimmers and aggregates of higher order may form in a solution [28, 29]. Fig. 3.9 is the ASE spectra of the same system with DNA at 1.5 wt% with various pump power. In this system the occurrence of multiple ASE bands is not significant compared to previous one. This indicates less aggregation of dye molecules in DNA-PVA solution. This analysis shows that DNA effectively prevents aggregation of dye molecules at higher concentration. The reason for this phenomena is explained in chapter 1.
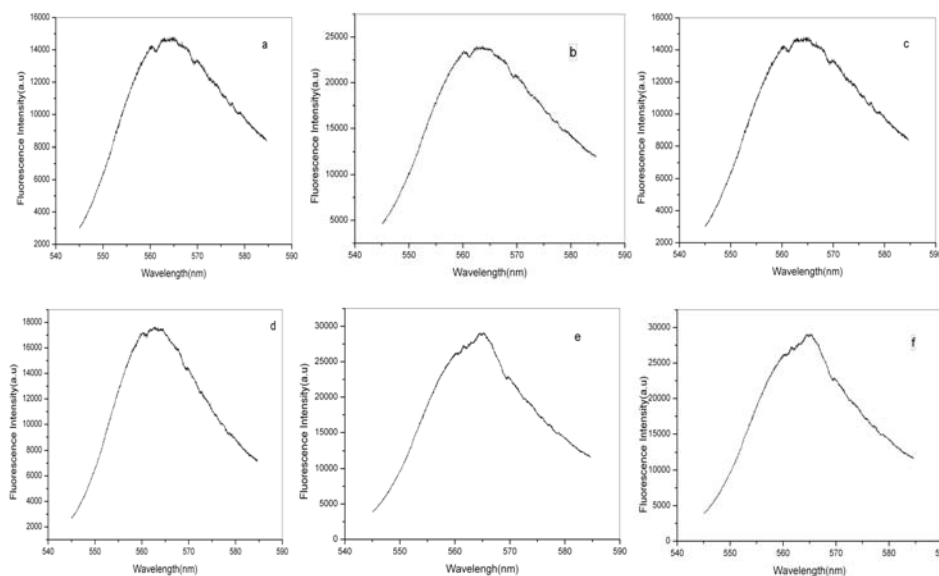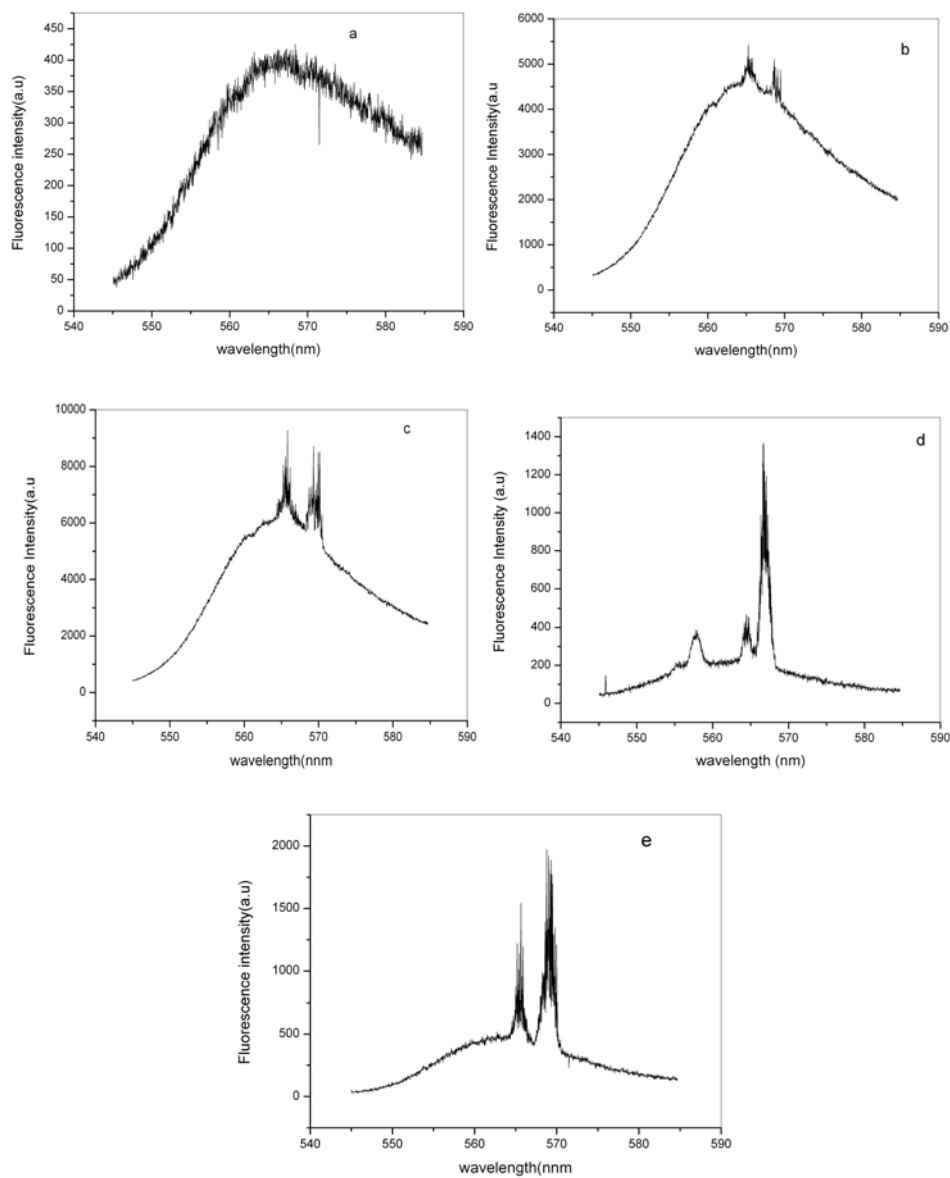
Figure: 3.8. *ASE from Rhodamine 6G (1.5x10^{-3} M) doped PVA for different pump intensities at excitation lengths of the pump beam 4mm, where a, b, c, d, e are ASE spectrum at 1, 1.5, 2, 2.5, 3 mJ respectively.*
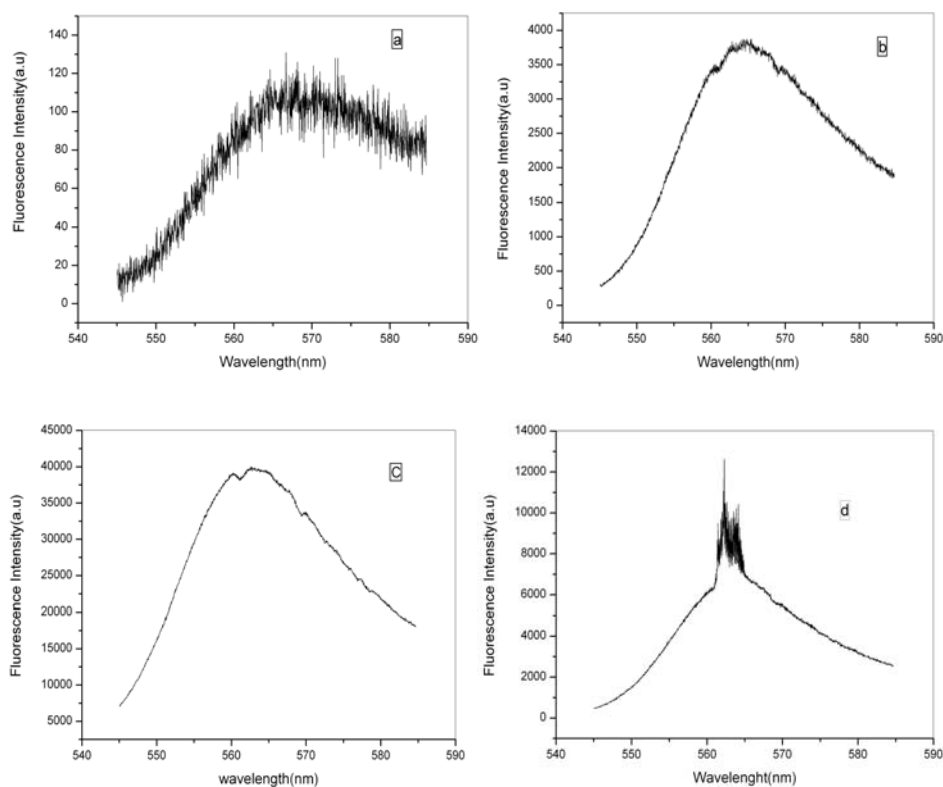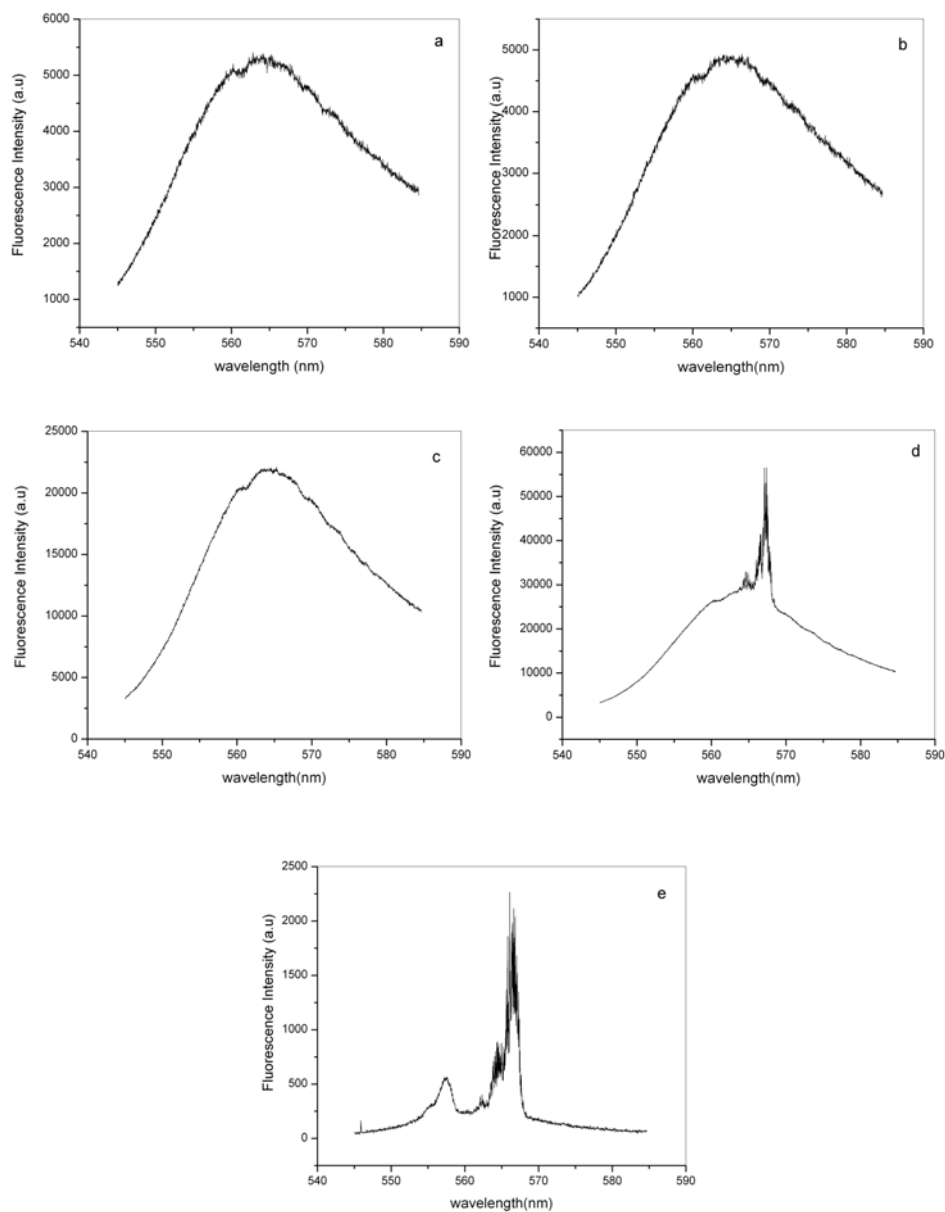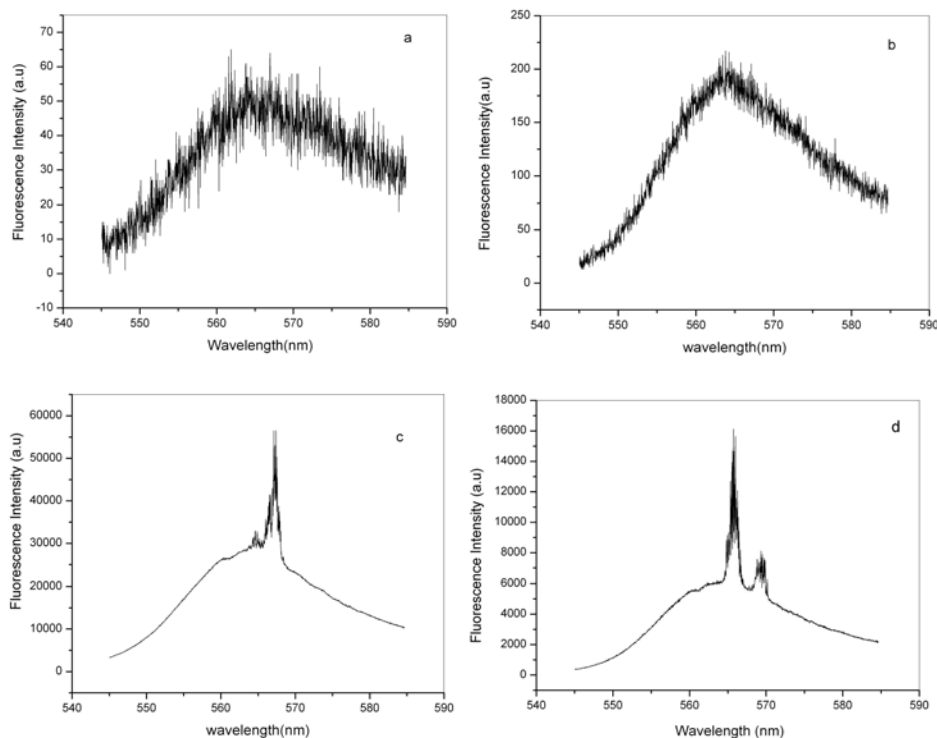
Figure: 3.9. *ASE from Rhodamine 6G (1.5x10^{-3} M) doped DNA-PVA for different pump intensities at excitation lengths of the pump beam 4mm, where a, b, c, d, e are ASE spectrum at 1, 2, 2.5, 3 mJ respectively.*

3.4.2. Light Amplification from Dye Doped DNA-PVA Film

Thin film based studies are important in device fabrication point of view. To study the nature of emission from the dye doped (1x10^{-4} M) DNA-PVA blended film; the emission spectra are recorded for various pump intensities starting from 3 mJ/pulse. Fig. 3.10 shows the emission spectra film thickness 530 μm for different values of pump energy. At lower pump intensities fluorescence spectra are broad with a spectral width of 25 nm. Amplification of the light emission and spectral narrowing are observed when the pump intensity is gradually increased. To understand the nature of amplified spontaneous emission (ASE) in detail, the dependence of peak emission intensity on incident

pump intensity is studied (Fig.3.11).As is evident from the plots, threshold pump energy of around 6 mJ/pulse is observed for the occurrence of ASE. Similar observations were made by previous workers also. However, in contrast to the reports available in the literature we observed mode structure at higher pump power (Fig.3.12). It is observed that at higher pump power one mode selectively gets excited to high intensity with narrow width about 0.2 nm.
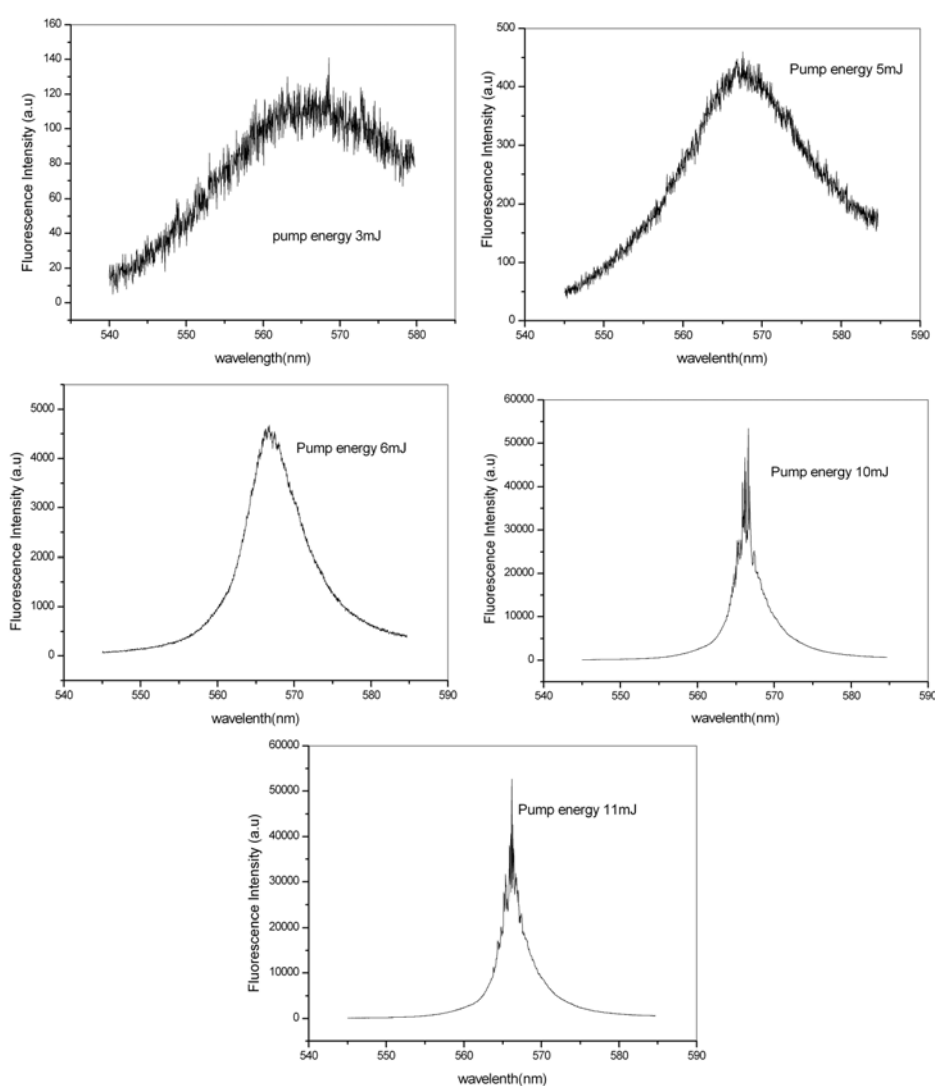
Figure: 3.10. *ASE from dye doped PVA-DNA thin film for different pump intensities.*
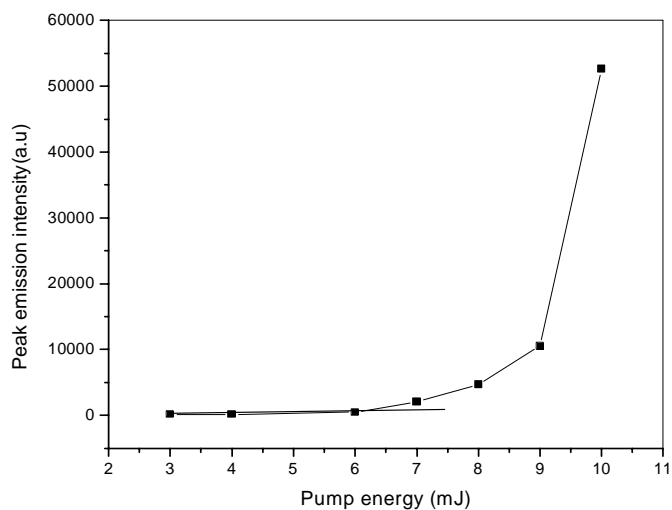
Figure: 3.11. *Dependence of peak emission intensity of ASE on incident pump energy*
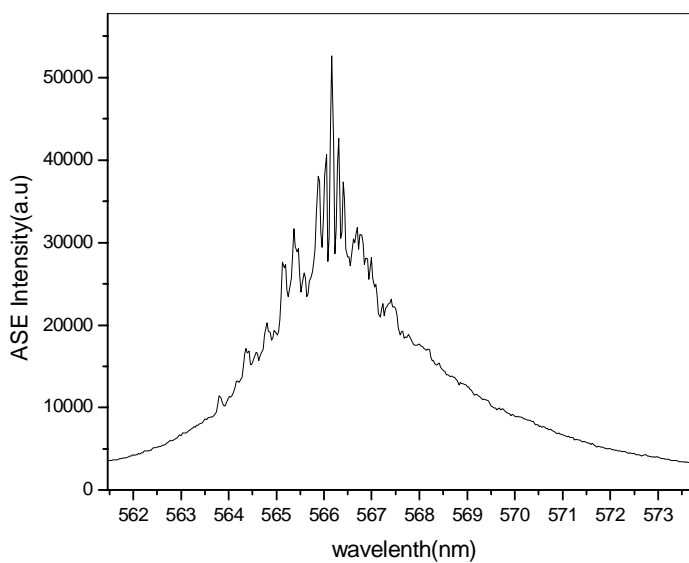
Figure: 3.12. *Laser modes with a spacing of   0 .2 nm from a dye doped DNA –PVA thin film.*

Laser emission requires an external feed back. In the present structure, there are no external mirrors to provide the feedback. Lasing studies are performed in the film along with the substrate. With this arrangement the film acts as an asymmetric waveguide with air and glass on both sides of the film.

The Fabry-Perot like behavior of an asymmetric thin-film waveguide was explained to be quite similar to that of thin film micro cavities [30-33] .Considering the sample geometry and pumping scheme, the modes of this cavity are analogous to the transverse modes of Fabry-Perot type cavity. Thin film structure can be modeled as a serially connected Fabry-Perot etalon. In this case stimulated emission occurs in the direction along the stripe. Both the stimulated emission along with the propagation in the guiding gain medium and the feedback at the lateral faces induces high gain for laser action. The system can also be thought of as the distributed feed back (DFB) device [34]. The mode spacing at λ can be calculated using equation for mode spacing in Fabry–Perot cavity, namely,

$$\Delta\lambda = \frac{\lambda^2}{2nL} \qquad\qquad ....(4.1)$$

Where λ is the wavelength of the strongest emission line, n is the refractive index and L is the length of the resonator cavity. In the present case, the length of the Fabry–Perot cavity corresponds to the thickness of the polymer film with the values for λ, n and thickness as 566 nm, 1.5 and 530 μm respectively, we get the mode spacing as 0.201 nm, which is same as the observed value 0.2 nm. To confirm this observation, dye doped films with different thicknesses were studied. With the film of thickness 213 μm, the spacing observed was 0.48 nm against the theoretical value of 0.50 nm.

The spectral width of the emission (FWHM) is summarized in Fig. 3.13 as a function of pump energy. It is clear from the figure that the line width is converged to 0.2 nm in strong pumping region. This value is also found to be very small when compared with other dye doped DNA matrix.
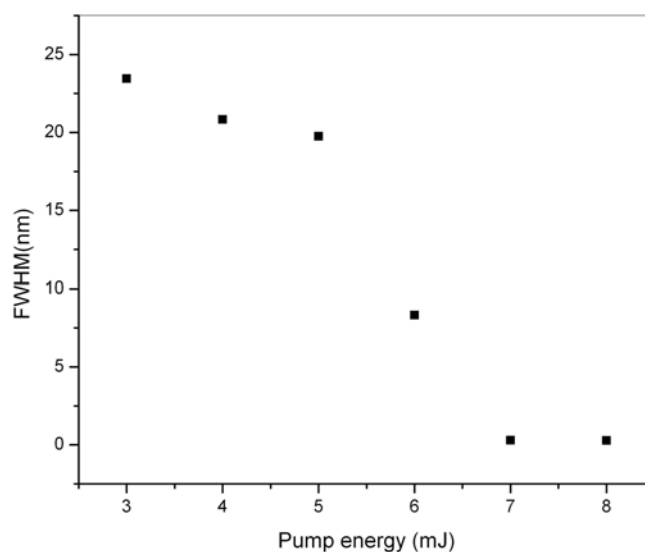
Figure: 3.13. *Line width of emission spectra at different pump energy levels*

In order to study the effect of DNA as a host material for thin film lasers, we performed same experiment on dye doped PVA film under the same experimental conditions. Although the film showed strong fluorescence under the same pumping condition, mode structure is absent (Fig.3.14) even though there is a tendency to reduce line width in fluorescence emission spectra. By comparing the figures 3.10 and 3.11 it is clear that DNA plays important role in laser emission. The ASE not only depends on the type of host material, but on the quality and morphology of the films. In our case morphology of the PVA film may be modified by adding DNA, which may favour the ASE.
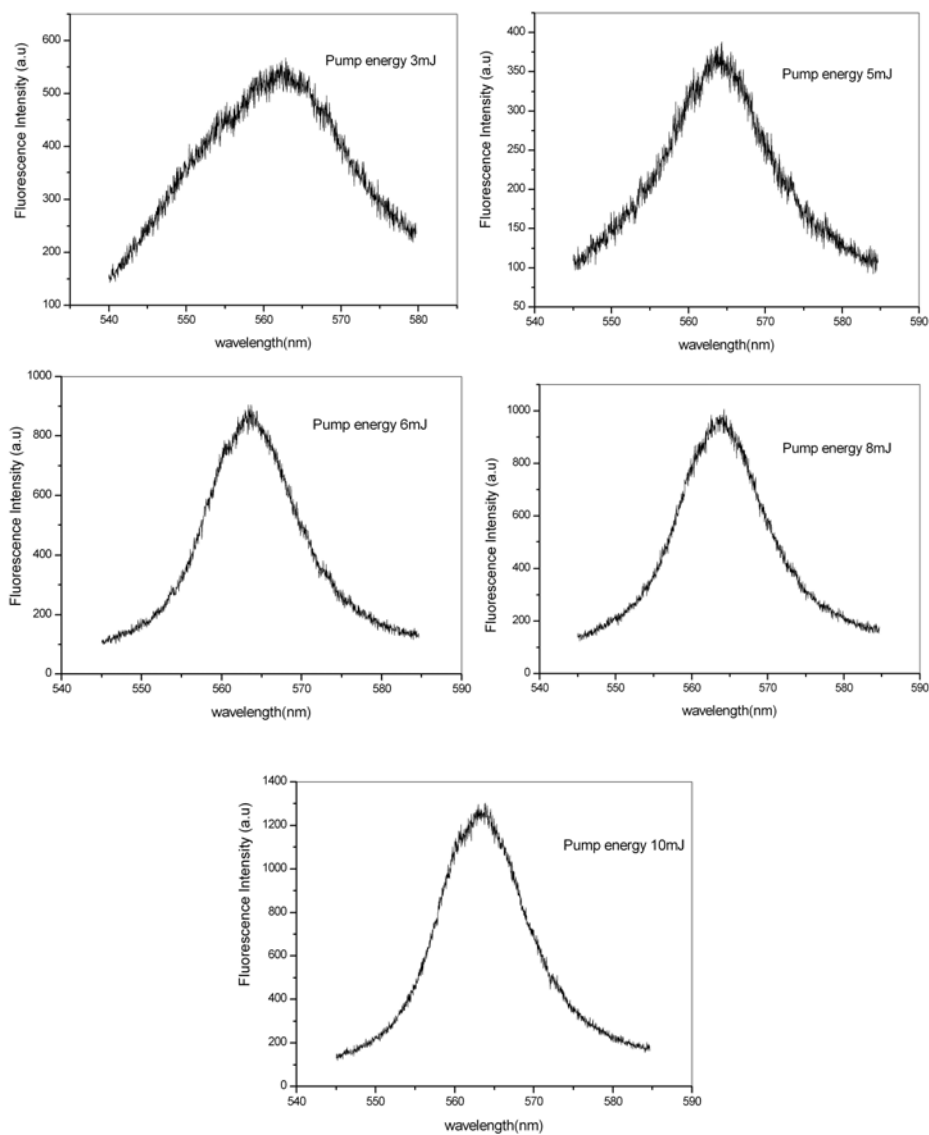
Figure: 3.14. *Emission spectra from dye doped PVA thin film for different pump intensities*

3.5. CONCLUSIONS

DNA-PVA matrix has been found to be an excellent host material for the laser dye Rhodamine 6G. The intensity of amplified spontaneous emission is enhanced with the addition of DNA is observed. The threshold value of ASE is found to be less compared to system without DNA. We have observed multimode laser emission from transversely pumped dye-doped DNA-PVA blended film. Reflections from the lateral faces of the film provided optical feedback. This together with the guidance through the gain medium gave rise to intense narrow emission lines. For pump energy of 6 mJ/pulse an intense line with FWHM was observed at 0.2 nm due to energy transfer from other modes. This value is found to be very small when compared with other dye doped DNA matrix. These results establish the occurrence of lasing action in dye doped DNA-PVA system could be of considerable application in the design of different optical elements.

REFERENCES

1.   J. Hagen, W. Li, A. Steckl, J. Grote, and K. Hopkins; *"Enhanced emission efficiency in organic light emitting diodes using deoxyribonucleic acid complex as electron blockinglaye*r", Appl. Phys. Lett. **88**, 171109 (2006).

2.   J. Hagen, W. Li, J. Grote, and A. Steckl; "*Red/blue electroluminescence from europium-doped organic light emitting diodes"*, Proc. SPIE **6117,** 0O1(2006)

3.   Z. Yu,W. Li, J. A. Hagen, Y. Zhou, D. Klotzkin, J. G. Grote, and A. J. Steckl; "*Photoluminescence and lasing from deoxyribonucleic acid (DNA) thin films doped with sulforhodamine*"; Appl. Opt. **46,** 1507 (2007).

4. Y. Kawabe, L. Wang, T. Nakamura, and N. Ogata; "*Thin-film lasers based on dye-deoxyribonucleic acid-lipid complexes*", Appl. Phys. Lett. **81**,1372(2002)

5. He G. S, Zheng Q, Prasad P. N, Grote J, Hopkins F. K; "*Infrared two-photon-excited visible lasing from a DNA-surfactant-chromophore complex*", Opt. Lett. **31**, 359 (2006)

6. M.E Mack; "*Super radiant travelling –wave dye laser*"; Appl. Phys. Lett. **15**,166(1969)

7. M. M. Malley and P.M. Rentzepis; "*Picosecond time-resolved stimulation light emission*" ,Chem. Phys. Letters **7**, 57 (1970)

8. H. Soffer, B. B. McFarland; "*Continuously tunable, narrow-band organic dye lasers*", Appl. Phys. Lett**. 10**, 266 (1967).

9. P. Schafer, W. Schmidt, K. Marth; "New *dye lasers covering the visible spectrum*", Appl. Phys. Lett. **24A**, 280 (1967)

10. F. J. Duarte, L.W.Hillman, "*Dye laser principles*", Academic Press, New York,(1990)

11. O. G. Peterson B. B. Snavely; "*Stimulated emission from flash lamp excited organic dyes in polymethyl methacrylate*", Appl. Phys. Lett. **12**, 238 (1968)

12. A. Costela, I. Garcia-Moreno J. M. Figuera, F. Amat-Guerri, R Satre; "*Polymeric matrices for lasing dyes: recent developments*", Laser Chem.**18**, 63(1998)

13. R. Satre, A. Costela; "*Polymeric solid-state dye lasers*", Adv. Materials, **7**, 198(1995)

14. D. Lo, J. E. Parris, J.L.Lawless; *"Multi-megawatt superradiant emission from coumarin doped sol-gel derived silica"*, Appl. Phys. B**. 55**, 365 (1992)

15. H. Soffer, B. B. McFarland; *"Continuously tunable, narrow-band organic dye lasers"*, Appl. Phy. Lett.**10** 266(1967)

16. B. B. Snavely, O.G.Peterson, R.F.Reithel; *"Blue laser emission from a flashlamp –excited organic dye solution"*, Appl. Phys. Lett. **11**275(1967)

17. F J Duarte, R O James; *"Tunable solid-state lasers incorporating dye-doped,polymer nanoparticle gain media"*, Opt. Lett. **28** 2088(2003)

18. V. Dumarcher, L. Rocha, C. Denis, C. Fiorini, J.-M. Nunzi, F.Sobel, B. Sahraoui, and D. Gindre; *"Polymer thin-film distributed feedback tunable lasers"*, J. Opt. A: Pure Appl. Opt **2**, 279(2000).

19. M. Karimi, N. Granpayeh, and M. K. Morraveg Farshi; *"Analysis and design of a dye-doped polymer optical fiber amplifier,"* Appl. Phys. B **78**, 387 (2004).

20. N. Tessler, G. J. Deenton, and R. H. Friend; *"Lasing from conjugated polymer microcavitie",* Nature **382**, 695(1996).

21. H. Becker, R. H. Friend, and T. D. Wilkinson; *"Light emission from wavelength tunable microcavitie",* Appl. Phys. Lett. **72**, 1266 (1998).

22. M. Kuwata-Gonokami, R. H. Jordan, A. Dobalapur, H. E. Katz, M. L. Schilling, and R. E. Slusher; *"Polymer microdisk and microring lasers"*, Opt. Lett. **20**, 2093(1995).

23. F. J. Duarte; *"Coherent electrically-excited organic semiconductors: visibility of interferograms and emission linewidth"*, Opt. Lett. **32**, 412–414 (2007).

24.   M. D McGehee, R Gupta, S. Veenstra, E K Miller , M. A. Diaz-Garcia, A. J. Heeger ; *"Amplified spontaneous emission from photopumped films of a conjugated polymer",* Phy. Rev. B, **58** 7035(1998)

25.   A V Deshpande, E. B. Namdas; *"Lasing action of Rhodamine B in polyacrylic acid films"*, Appl. Phys. B: Lasers & Opt. **64**, 19(1997)

26.   Kretsch K P, Belton C, Lipson S, Blau W J , Henari F Z, Rost H, Pfeiffer S, Teuschel A, Tillmann H and Horhold H; *"Amplified spontaneous emission and optical gain spectra from stilbenold and phenylene vinylene derivative model compound*s", J. Appl. Phys. **86**, 6155 (1999)

27.   K. L. Shaklee, R. F. Leheny; *"Direct determination of optical gain in semiconductor crystals"*, Appl. Phys. lett, **18**, 475(1971)

28.   A. Penzkofer and W. Leupacher; *"Fluorescence behaviour of highly concentrated rhodamine 6G solutions",* J. Lumi. **37,** 61(1987)

29.   T. N. Kopylova, V. A. Svetlichnyi, G. V. Mayer, E. N. Tel'minov and I. N. Lapin; *"Emission of Concentrated Solutions of Organic Compounds Excited with High-Power Laser Radiation",* Russian Physics Journal *46,* 470*(2003)*

30.   J Brouwer, V. V. Krasnikov, A. Hilberer, G. Hadziioannou; *"Stimulated emission from neat polymer films",* Adv. Mater. **8,** 61(1997)

31.   S. Yap, W. Siew, T.Tou, S. Ng, *"Red-green-blue laser emissions from dye-doped poly vinyl alcohol films*", Applied optics **41**, 1725 (2002)

32.   Otomo A, Yokoyama S, Nakahama T and Mashiko S; *"Supernarrowing mirrorless emission in dendrimer–doped polymer waveguides",* Appl. Phys. Lett.**77**, 3881(2000)

33.   A. Penzkofer, W. Holzer, H. Tillmann, and H. H. Horhold; "*Leaky mode emission of luminescent thin films on transparent substrate",* Opt. Commun. **229**, 279 (2004).

34.   S. V. Frolov, Z. V. Vardeny, K. Yoshino, A. Zakhidov, and R. H Baughman; "*Stimulated emission in high gain organic media",* Phys. Rev. B **59**, 5284(1999).

...........ॐ..........

.

<div align="right">

$Chapter$ **4**

</div>

Synthesis and optical characterization of silver nanoparticles in DNA template

Abstract

Highly fluorescent colloidal silver nanoparticles are prepared in aqueous solution of DNA at room temperature by standard reduction method. The absorption spectrum of silver nanoparticles showed the appearance of a broad surface plasmon resonance peak centered at 410 nm at higher concentration of DNA. The nonlinear optical properties of above nanoparticles are investigated using Z-scan technique at 532 nm. The nonlinear absorption coefficient of Ag nanoparticles depend on the concentration of DNA at low pump power of $50 MW/cm^2$. It is observed that at high pump power of 175 MW/cm^2, nonlinear absorption coefficient has less dependence on the concentration of the DNA. The photoluminescence study shows emission of silver nanoparticles is getting enhanced as concentration of DNA increases. At higher concentration of DNA the fluorescence maximum of silver nanoparticles shifts towards red as the excitation wavelength is increased.

4.1. INTRODUCTION

In recent years, there has been growing interest in developing photonic devices based on organic materials. Biomaterials often show unusual properties which are not replicated in conventional organic or inorganic materials. Among biological molecules deoxyribonucleic acid (DNA) has been used extensively as a biotemplate to grow inorganic quantum confined structures because of its well defined sequence of DNA base and a variety of super helix structures [1-5]. DNA template has also been described as smart glue for assembling nano particles. In general, synthesis of nano particles based on DNA template has been done by incubating metal ion coated DNA in a reducing agent solution. The ion DNA complexes control the release of metal ions, slow down their reduction and effectively inhibit metal ions from growing into big clusters. Nano-structures of metals such as silver, gold, palladium, platinum, copper, and nickel have been successfully synthesized by using DNA network templates [1-5].

Nonlinear optical and electronic properties of colloidal suspensions of metal nanoparticles have drawn special attention because of their strong and size-dependent plasmon resonance absorption and their applications as nonlinear materials for optical switching, optical limiting, beam flattening and computing because of their relatively large third-order nonlinearity and ultra fast response time [6-8]. Silver nanoparticles have received increased attention in the past few years due to its large third order nonlinearity. A large number of investigations have been carried out to study nonlinear optical properties of metal nano particles dispersed in different optically transparent solid matrices and liquids [9-14]. However, not much work has been done on nonlinear optical property of the metal nanoparticles in aqueous solution of DNA. An advantage of colloidal suspensions compared with fabrication of structures in solid matrix is that the nanoparticles in suspension are easily reconfigurable. The nanoparticle

environment in colloidal system is composed of the solvent and stabilizing agents adsorbed on the nanoparticles surface to avoid aggregation. The solvent and the stabilizing agent may change the optical properties of the nanoparticles in different ways [14, 15]. In this chapter we report the results obtained from investigation of nonlinear optical properties of silver nanoparticles prepared in aqueous solution of DNA.

A large number of reports are available in literature dealing with study of photo luminescence properties of silver nanoparticles dispersed in different optically transparent solid matrices and liquids [16-19]. Fluorescent dyes can be easily intercalated into the helices of the DNA biopolymer whereby the intensity of the fluorescence is greatly enhanced. In this chapter we also discuss photo luminescence (PL) properties of silver nanoparticles at different concentrations of DNA and at different excitation wavelength.

4.2. SYNTHESIS

Silver nano particles are synthesized in aqueous solution of DNA (SRL, extracted from Calf thymus) by standard reduction technique. A 20mL solution with a concentration of 0.25 mM AgNO3 (Alfa Aesar) and DNA with different concentration (0.05 wt%, 0.1 wt%, 0.15 wt %,) in water is prepared. While stirring vigorously 0.6 ml of 10 mM NaBH4 (Merck) was added at once. Stirring was stopped after 30 s when the silver nano colloid is formed. The addition of DNA results in stable solutions of silver nano particles at room temperature and found to be stable for several months. Two major challenges often faced in the preparation of nano crystals in solution are Ostwald ripening and agglomeration. Use of capping agents prevent these by effectively shielding the surface of the nuclei as soon as they are formed and thus preventing them from coming into direct contact with solution. Often molecules with longer chains are used as capping agents [12]. In our case DNA acts as a capping agents as well as

template for nano particles using the double helix nature of DNA. Per helix turn of the DNA can produce one major groove and one minor groove. Based on this structural mode, major groove of the DNA is the suitable place for the nanoparticles growth where the space is big enough to accommodate nanoparticles. The nucleation may occur first starting from the Ag+ bound on the DNA base or the phosphate groups, and then the silver ions are slowly reduced to the metallic silver on the nucleation site. The growth of the silver nanoparticles are finally blocked by the major groove of DNA [13].

4.3. ABSORPTION SPECTROSCOPY

Before carrying out the characterization of the optical nonlinearities, the linear absorption spectra of silver nanosol in different concentrations of DNA is obtained. Optical absorption measurement is an initial step to observe the nano sol behavior. For silver nano colloid, the surface plasmon absorption band lies in the 410 nm region. Metal nanoclusters have close-lying bands and electrons move quite freely. The free electrons give rise to surface plasmon absorption band in metal clusters, which depends on both the cluster size and chemical surroundings. Absorption spectra of silver nanosol in three concentrations of DNA (0.05 wt%, 0.1 wt%, and 0.15 wt% respectively) are shown in Fig. 4.1. It is clear from the figure that, the Ag plasmon resonance lies around 410 nm and absorption is less for higher concentration of DNA. This indicates that silver nanoparticles are formed in all concentrations of DNA even though the number of silver nano-particles formed at higher concentrations is less. The surface plasmon resonance (SPR) peak of silver nanoparticles mentioned in many other previous reports is around 410 nm [4, 5] which is consistent with our observation.
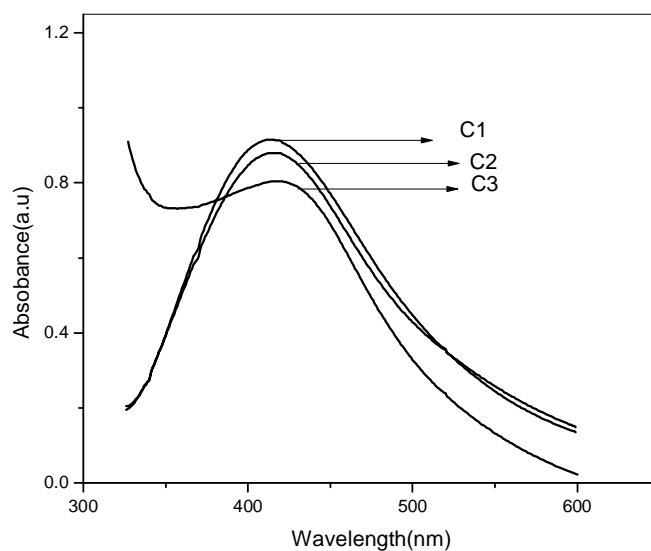
Figure: 4.1. *Absorption spectra of silver nanoparticles in aqueous solution of DNA, (where C1, C2, C3 represent 0.05 wt%, 0.1 wt%, 0.15 wt% of DNA respectively).*

4.4. SCANNING ELECTRON MICROSCOPY (SEM)
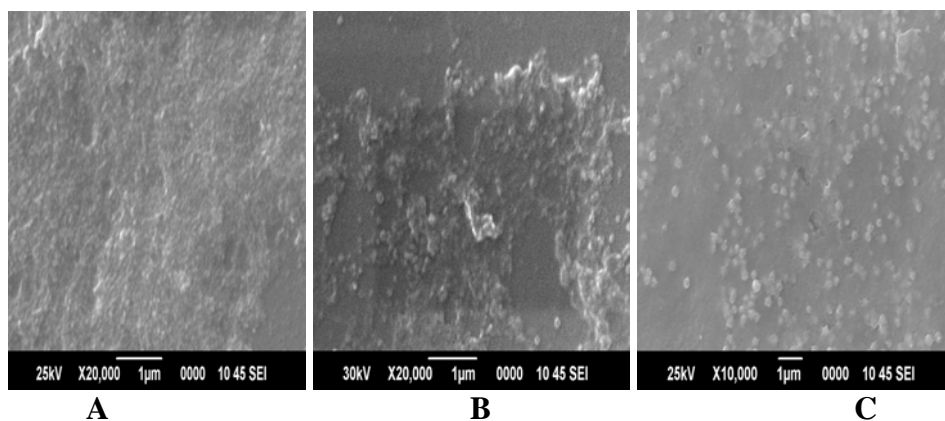
Figure: 4.2. *SEM images of the silver nanoparticles synthesized at different concentrations of DNA (A, B, C represent 0. 05 wt%, 0. 1 wt%, 0.15 wt% of DNA respectively).*

Fig. 4.2 illustrates the SEM images of silver nanoparticles at different concentrations of DNA template. Number of silver nanoparticles formed is less at higher concentration of DNA. It is clear from pictures that the particle separation is high as concentration of DNA increases implying less aggregation.

4.5. OPEN APERTURE Z-SCAN

One of the important applications of silver nano colloid is in the field of photonic materials due to its large third order nonlinearity. Fig. 4.3 is the plot of open aperture Z-scan measurement which shows the nonlinear absorption of silver nano colloid in three different concentrations of DNA template at a typical fluence of 50 MW/cm^2 for an irradiation wavelength of 532 nm. The data are analyzed by using the procedure described by Bahae *et al* [20], which is described in chapter 2. Z-scan results can be analyzed using two photon absorption processes. The obtained values of the nonlinear absorption coefficient and imaginary part of the susceptibility (Im χ^3) at an intensity of 50 MW/cm^2 are shown in Table 4.1. In this fluence these values are found to be useful for practical applications [14-17]. Also we have observed that as concentration of DNA is increased the nonlinear absorption decreases. This is due to the effect of DNA on silver nano sol. As concentration of DNA increases the number of silver nanoparticles formed is less, which is clear from absorption spectra and SEM images. In effect the nonlinear optical property of the silver nanosol decreases.

Nonlinear optical properties of nanoparticles are strongly influenced by the surface plasmon resonance (SPR) absorption. It is observed that a laser pulse can cause inter band or intra band electron transition in the metal nanoparticle system depending on the excitation wavelength and intensity. The excited electrons are free carriers and lead to transient absorption. This also leads to strong nonlinear absorption. Nonlinear scattering of nanoparticle also contribute

to nonlinear absorption. From table 4.1.and absorption spectra, it is clear that the nonlinear absorption decreases by approximately 30% when going from C1 to C3 while the height of surface plasmon absorption changes by 10% only. This discrepancy may be attributed to nonlinear scattering. As concentration of DNA increases number of silver nanoparticle in solution is decreased so that nonlinear scattering is also decreased. Here enhanced absorption of the silver nanoparticles may be due to the interaction between the nanoparticles with DNA matrix which support them. The surface plasmon resonance associated with collective oscillations of electrons in the nanoparticles is strongly influenced by the host dielectric function. Optical response of the nanoparticles may vary when dielectric function of the surface layer of the nanoparticles changes with stabilizing agent [14]. Here DNA acts as a good stabilizing agent for the nanoparticles.

Fig. 4.4 shows the open aperture Z-scan curves of the same sample at higher fluence of 175 MW/cm^2[2]. The obtained values of the nonlinear absorption coefficient β and Im χ^3 at an intensity of 175 MW/cm^2 are given in Table 4.2. At high pump power the value of the β is found to be decreased compared to low pump power even though it shows high optical nonlinearity. The increase in the laser intensity induces bleaching in the ground state absorption, which results in a transmittance increase (SA process). This may be the reason for the decreased nonlinearity at high pump power. It is clear from the Fig. 4.4 and table 4.2 that at high pump power the nonlinearity of the prepared samples do not depend on the concentration of the DNA. This is due to the effect of DNA on nonlinear optical properties of silver nano particles. At high pump power DNA shows third order optical nonlinearity [21-23]. So at high pump power as concentration of the DNA increases, the number of silver nanoparticles formed are less, at the same time nonlinearity of the DNA increases with concentration. These two

effects compensate each other. In effect at high pump power the concentration of DNA does not effect the nonlinearity of silver nano sol.
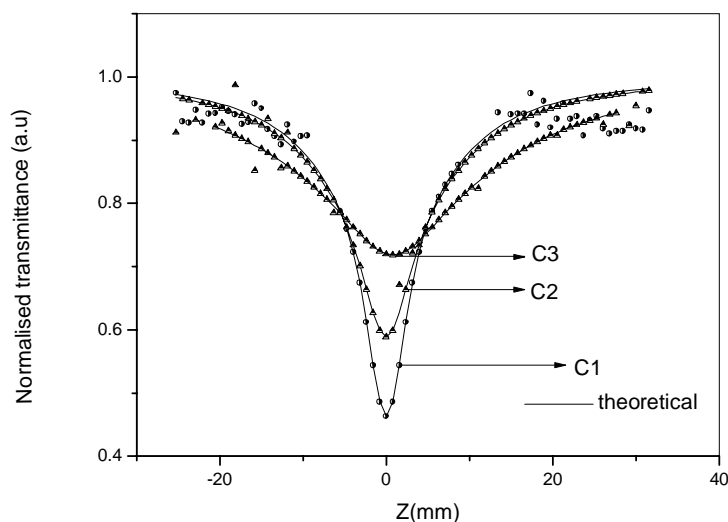
Figure: 4.3. *Open aperture Z-scan curves of silver nanoparticles in aqueous solution at different concentration of DNA at a typical fluence of 50 MW/cm^2. (where C1, C2 ,C3 represents 0.05 wt%, 0.1 wt%, 0.15 wt% of DNA respectively)*

Table: 4.1. **Measured value of nonlinear absorption coefficient β and imaginary part of third order susceptibility Im[$\chi^{(3)}$] for silver nanoparticles in aqueous solution at different concentration of DNA at a typical fluence of 50 MW/cm^2**

Concentration of DNA	β cmGW^{-1}	Im[$\chi^{(3)}$] x10^{-7} esu
0.05wt%	295.634	5.048
0.1wt%	265.467	4.537
0.15wt%	212.173	3.626
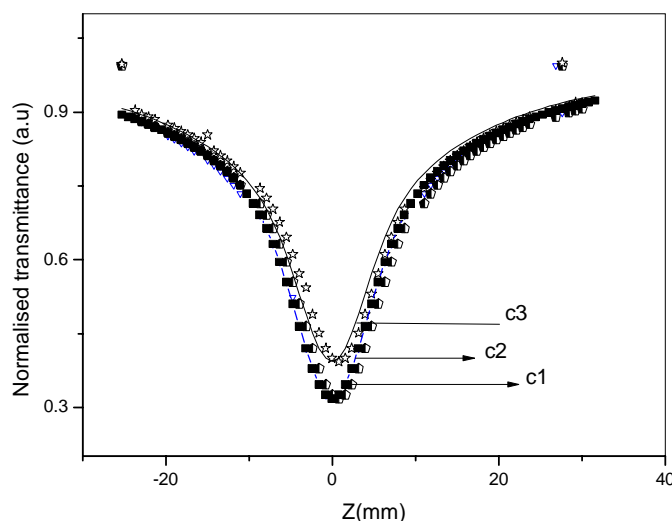
Figure: 4.4. *Open aperture Z-scan curves of siver nanoparticles in aqueous solution at different concentration of DNA at a typical fluence of 175 MW/cm^{2}. (where C1, C2, C3 represents 0.05 wt%, 0.1 wt%, 0.15 wt% of DNA respectively)*

Table: 4.2. Measured value of nonlinear absorption coefficient β and imaginary part of third order susceptibility Im[χ^3] for silver nanoparticles in aqueous solution at different concentration of DNA at a typical fluence of 175 MW/cm^2

Concentration of DNA	β **cmGW**$^{-1}$	**Im[** $\chi^{(3)}$ **] x10**$^{-7}$ **esu**
0.05wt%	91.619	1.448
0.1wt%	92.09	1.456
0.15wt%	89.058	1.418

To estimate the role of DNA on nonlinear optical property of silver nanoparticles we also performed open aperture Z-scan measurements on DNA (0. 05wt %) in water at laser intensity of 50 MW/cm^2 and 175 MW/cm^2. As

shown in Fig. 4.5 no obvious nonlinear absorption effect was found at 50 MW/cm^2 but DNA shows strong nonlinear absorption at 175 MW/cm^2 (β = 12 cm/GW). Marek Samoc et al. reported that DNA shows moderate nonlinear absoption at 532 nm [23]. Nonlinear optical property of the DNA depends on the polymerisation of DNA, molecular weight, host material etc.
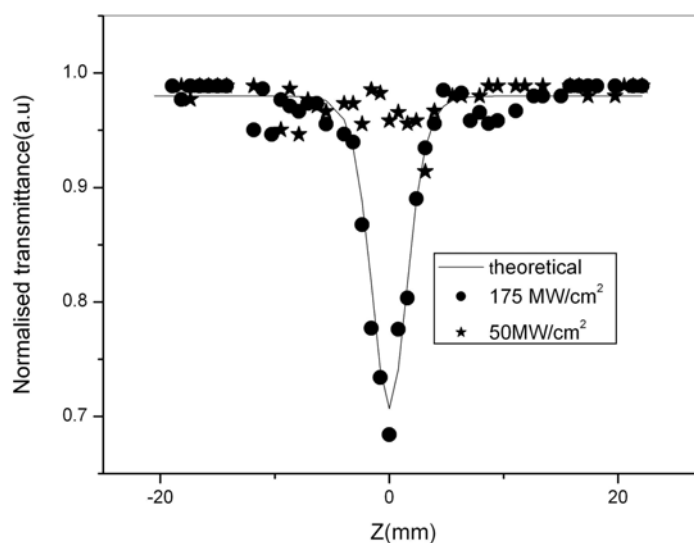
Figure: 4.5. *Open aperture Z-scan curves of aqueous solution of DNA (0.05 wt%) at a typical fluence of 50 MW/cm^2 and 175 MW/cm^2*

To examine the optical limiting property of the silver nanopartcles in DNA matrix the nonlinear transmission of the silver nano sol is studied as a function of input fluence (Fig. 4.6). The fluence level for optical limiting at 532 nm for different concentration of DNA is found to be 88 MW/cm^2. An important term in the optical limiting measurement is the limiting threshold. It is obvious that the lower the optical limiting threshold, the better the optical limiting material. Optical limiters are devices that transmit light at low input fluences or intensities, but become opaque at high inputs. The optical limiting property occurs mostly due to mechanisms like excited state absorption, two-photon absorption and nonlinear scattering as well. [24].
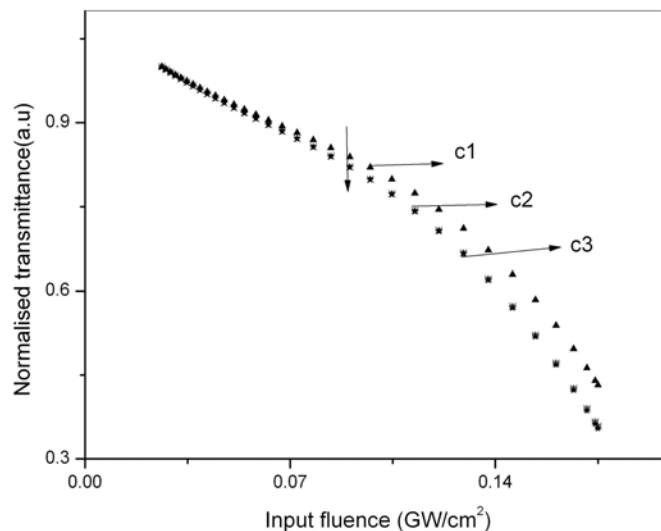
Figure: 4.6. *Optical limiting performance of siver nanoparticles in aqueous solution with different concentration of DNA. (Where C1, C2, C3 represents 0.05wt%, 0.1wt%, 0.15wt% of DNA respectively)*

4.6. FLUORESCENCE EMISSION

Fluorescence spectra of silver nanoparticles are recorded using spectrofluorimeter (Cary Eclipse). Figure 4.7 shows the fluorescence emission spectra for silver nanoparticles at different concentrations of DNA(C1- 0.05 wt%, C2-0.1 wt%, C3-0.15 wt% of DNA). The excitation wavelength was fixed at 250nm and emission spectra were recorded. Silver nano particle showed fluorescence peak at 530 nm at less concentration of DNA and fluorescence peak get blue shifted by 100 nm by increasing the concentration of DNA from 0.05 wt% to 0.15 wt%. The emission in the region 400-600 nm is in good agreement with the previous report [16-19]. The luminescence of silver metal is generally attributed to electronic transitions between the upper d band and conduction sp band [16-19]. It is clear from the Fig. 4.7 that fluorescence signal has been enhanced seven times as concentration of DNA changes from 0.05wt% to 0.15 wt%.

Reduction in aggregation will show fluorescence emission related to lower concentration which will cause, apart from fluorescence enhancement, blue shift in fluorescence peak with enhanced DNA concentration. Nanoparticles, as described above, can be situated inside the double helix structure or at some grooves beside the main chains. Because of the intercalation or groove binding of nanoparticles in the DNA strand, particles get isolated from each other, thereby reducing the fluorescence quenching caused by aggregation. This may be one of the reasons for fluorescence enhancement in the case of silver nanoparticles also. Similar enhancement in fluorescent emission is observed in the case of dyes in DNA matrix [25-28]. The SEM image shows that silver nano particles stay apart as concentration of DNA increases. At higher concentration of DNA, the longer polymer chain introduces large spatial block for the aggregation of the nano particles. It decreases quenching of the fluorescence of silver nanoparticles. This may lead to enhancement in the fluorescence intensity at higher concentration of DNA.
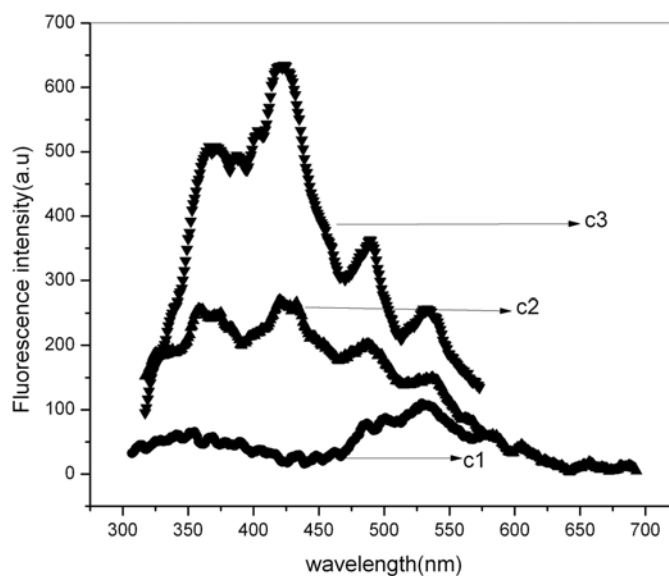
Figure: 4.7. *Photoluminescence spectra of the silver nanoparticles stabilised by DNA excited at 250nm(c1, c2, c3 represents 0.05 wt%, 0.1 wt%, 0.15 wt% of DNA respectively)*

Fig. 4.8 shows the fluorescence emission spectra for silver nanoparticles at different concentration of DNA (C1-0.05wt%, C2-0.1wt%, C3-0.15 wt% of DNA) at excitation wavelength 350 nm. Here also silver nanoparticles show fluorescence peak at 530 nm at less concentration of DNA and fluorescence peak get blue shifted by 100nm by increasing the concentration of DNA from 0.05 wt% to 0.15 wt%. This figure clearly shows fluorescence enhancement as concentration of DNA changes from 0.05 wt% to 0.15 wt%.
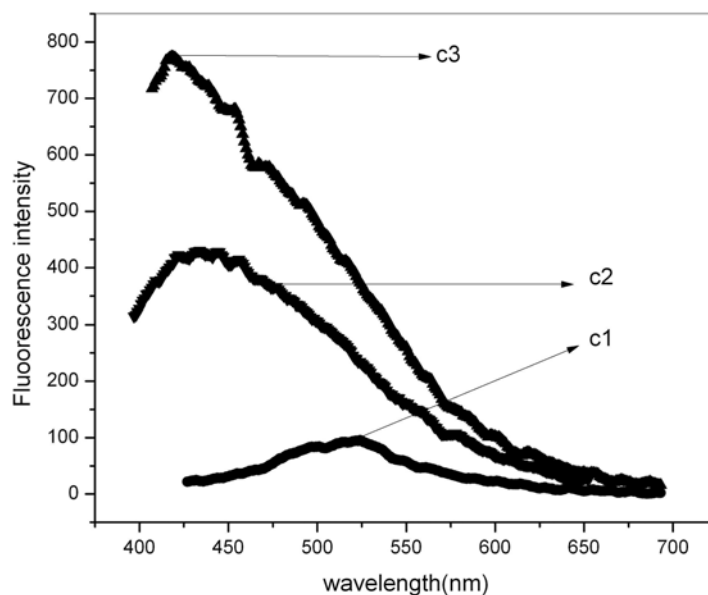
Figure: 4.8. *Photoluminescence spectra of the silver nanoparticles stabilised by DNA excited at 350nm (c1, c2, c3 represents 0.05 wt%, 0.1 wt%, 0.15 wt% of DNA respectively*

Fig. 4.9 shows the emission spectra of silver nanoparticles with different concentration of DNA at excitation wavelength of 420 nm (SPR peak). Here also we observed the same nature of fluorescence enhancement as concentration of DNA increases.
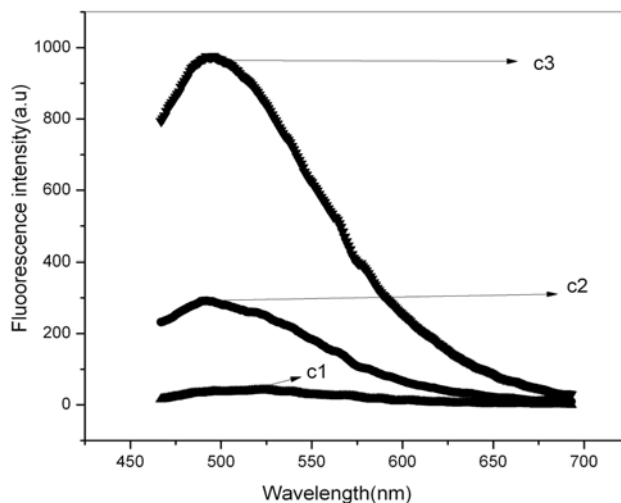
Figure: 4.9. *Photoluminescence spectra of the silver nano particles stabilised by DNA excited at 420nm (c1, c2, c3 represents 0.05 wt%, 0.1 wt%, 0.15 wt% of DNA respectively*
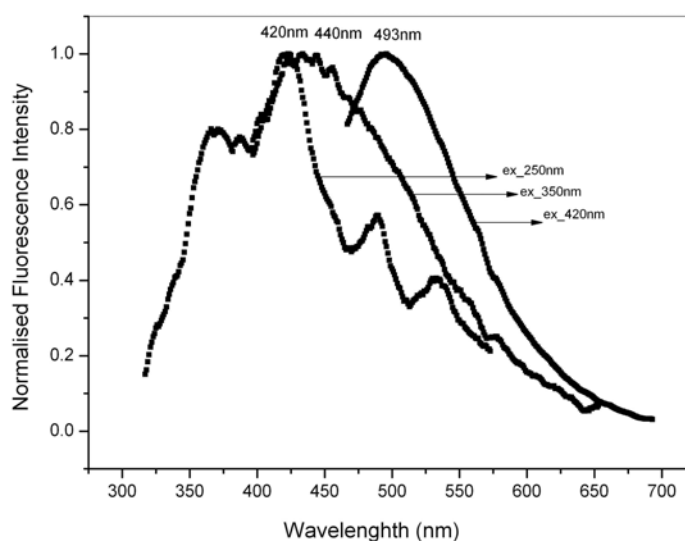
Figure: 4.10. *Photoluminescence spectra of the silver nano particles stabilized by DNA (0. 15 wt %) excited at different wavelength*

The excitation wavelength dependence on the fluorescence emission of silver nanoparticles is studied. Significant excitation wavelength dependence

on emission spectra of silver nano particles is observed at higher concentration of DNA. Excitation wavelength dependence of silver nano particles prepared in DNA of concentration 0.15 wt% is displayed in Fig. 4.10. The fluorescence maximum shifts towards red as the excitation wavelength is increased. The red shift in fluorescence emission as a function of excitation wavelength may be due to size distribution of the silver nano particles in medium.

4.7. CONCLUSIONS

In conclusion, we synthesized highly stable silver nano particles in aqueous solution at room temperature by standard reduction method using DNA. The linear and nonlinear optical properties of silver nanoparticles at three concentration (0.05 wt%, 0.1 wt%, 0.15 wt %) of DNA is studied. Absorption spectra shows the Ag plasmon resonance lies around 410nm and silver nano-particles formed at higher concentration are less. The nonlinear absorption coefficient β and imaginary part of third order susceptibility depend on the concentration of DNA at low pump power of 50MW/cm^2. It is observed that at high pump power of 175 MW/cm^2 the nonlinear absorption coefficient (β) and imaginary part of third order susceptibility do not depend on the concentration of the DNA. The imaginary parts of third order nonlinear optical susceptibility measured by Z-scan technique revealed that silver nano particle synthesized in aqueous solution of DNA have good nonlinear optical response and could be chosen as ideal candidate with potential applications for nonlinear optics. We have studied photo luminescence of silver nanoparticles at different concentration of DNA. It is observed that the emission of silver nanoparticles is getting enhanced as concentration of DNA increases. The fluorescence maximum shifts towards red as the excitation wavelength is increased for silver nanoparticles prepared at higher concentration of DNA, which can be attributed to the size distribution of particles in the media.

REFERENCES

1.   Braun E, Eichen Y, Sivan U, Ben-Yoseph G; *"DNA-templated assembly and electrode attachment of a conducting silver wire",* Nature, **391**, 775(1998)

2.   Zhiguo Liu, Yuangang Zu , Yujie Fu, Yuliang Zhang, Huili Liang; *"Growth of the oxidized nickel nanoparticles on a DNA template in aqueous solution"*, Mater. Lett. **62,** 2315(2008)

3.   Yong Yao, Yonghai Song , Li Wang; *"Synthesis of CdS nanoparticles based on DNA network templates",* Nanotechnology **19,** 405601(2008)

4.   Gang Wei, Li Wang, Zhiguo Liu, Yonghai Song, Lanlan Sun, Tao, Yang, and Zhuang Liz; *"DNA-Network-Templated Self Assembly of Silver Nanoparticles and their application in Surface enhanced Raman scattering"* , J. Phys. Chem. B. **109,** 23941 (2005)

5.   Zhu, Xuehong Liao, Hong-Yuan Chen Junji; *"Electrochemical preparation of silver dendrited in the presence of DNA",* Material Research Bulletin **36**, 1687(2001)

6.   S. Forster, M.Antonietti; *"Amphiphilic Block Copolymers in Structure-Controlled Nanomaterial Hybrids"*, Adv. Mater. **10**, 195(1998)

7.   M. Moffit, A. Eisenberg; *"Size Control of Nanoparticles in Semiconductor-Polymer Composites.1.Control via Multiplet Aggregation Numbers in Styrene-Based Random Ionomers",* Chem. Mater. **7**, 1178 (1995)

8.   R. P. Andres, J. D. Bielefeld, J. I. Henderson, D. B. Janes, R. Kolagunta, C. P. Kubuiak, W. J. Mahoney, R. J. Osifchin*; "Self-Assembly of a Two-Dimensional Superlattice of Molecularly Linked Metal Cluster"*, Science **273**, 1690(1996)

9.   C. Petit, P. Lixon, M. P. Pileni; "*In Situ synthesis of silver nanocluster in AOT reverse micelles*", J. Phys. Chem.**97** ,12974(1993)

10. R. A. Ganeev, M. Baba, A. I. Ryasnyanskii, M. Suzuki, and H. Kuroda; "*Laser Ablation of Silver in Different Liquids: Optical and Nonlinear Optical Properties of Silver Nanoparticles*", Opt. Spectosc. **99**, 694(2005)

11. C. Wang, Y. Fu, Z.Zhou, Y. Cheng, and Z. Xu; "*Femtosecond filamentation and supercontinuum generation in silver-nanoparticle-doped water*", Appl. Phys. Lett.**90**, 181119(2007)

12. D. Rativa, R. E. de Araujo, and A. S. L. Gomes; "*One photon nonresonant high-order nonlinear optical properties of silver nanoparticles in aqueous solution*", Opt. Express. **16**, 19244(2008)

13. R. A. Ganeev, A. I. Ryasnyansky; "*Nonlinear optical characteristics of nanoparticles in suspensions and solid matrices*", Appl. Phys. B **84**, 295 (2006)

14. Luis A. Gomez, Cid B. de Araujo, A. M. Brito Silva, and Andre Galembeck; "*Influance of stabilizing agents on the nonlinear susceptibility of silver nanoparticles*" , J. Opt. Soc. Am. B **24**, 2136(2007)

15. L. A. Gomez, C. B de Araujo, A. M. Brito-Silva, A.*Galembeck; "Solvent effect on the linear and nonlinear optical response of Silver nanoparticles*", Appl. Phys. B **92**, 61(2008)

16. Junpeng Gao, Jun Fu, Cuikun Lin, Jun Lin, Yanchun Han, Xiang Yu, and Caiyuan Pan; "*Formation and Photoluminescence of Silver Nanoparticles Stabilized by a Two-Armed Polymer with a Crown Ether Core*", Langmuir **20**, 9775(2004)

17. Jian Xu, Xia Han, Honglai Liu, Ying Hu; "*Synthesis and optical properties of silver nanoparticles stabilized by gemini surfactant*", Colloids and Surfaces A: Physicochem. Eng. Aspects **273** 179(2006)

18. Oleg A. Yeshchenko, Igor M. Dmitruk,Alexandr A. Alexeenko, Mykhaylo Yu. Losytskyy, Andriy V. Kotko,and Anatoliy O. Pinchuk; *"Size-dependent surface plasmon-enhanced photoluminescence from silver nanoparticles embedded in silica"*, Physical review B **79**, 235438 (2009)

19. Alqudami Abdullah and S Annapoorn; " *Fluorescent silver nanoparticles via exploding wire technique"* , *Pramana J. Phys.* **65**, 815 (2005)

20. M. Sheik Bahae, A. A. Said, T.Wei, D. J. Hagan, E. W. Van Stryland ; "*Sensitive measurements optical nonlinearities using a single beam",* IEEE **26**, 760 (1990)

21. James G. Grote et.al; "*DNA-based materials for electro-optic applications: current status"*, Proc. SPIE. **5934**, 593406 (2005);

22. G. Zhang, H. Takahashi, L. Wang, J. Yoshida, S. Kobayathi, S. Horinouchi, and N.Ogata; *"Nonlinear optical materials derived from Biopolymer DNA –surfactant –Azo Dye Complex*", Proc. SPIE. **4905**, 375(2002**)**

23. Marek Samoc, Anna Samoc James G Grote; *"Complex nonlinear refractive index of DNA",* Chem. Phy. Lett. **431,**132(2006)

24. Zhengle Mao, Lingling Qiao, Fei He, Yang Liao, Chen Wang, Ya Cheng; "*Thermal-induced nonlinear optical characteristics of ethanol solution doped with silver nanoparticles*", Chinese Opt. Lett. **7**, 949 (2009)

25. Y. Kawabe, L. Wang, S. Horinouchi, and N. Ogata; "*Amplified spontaneous emission from fluorescent-dye-doped DNAsurfactant complex films"*, Adv. Mater. **12**, 1281 (2000).

26. Z. Yu, W. Li, J. A. Hagen, Y. Zhou, D. Klotzkin, J. G. Grote, and A. J. Steckl; *"Photoluminescence and lasing from deoxyribonucleic acid*

(DNA) thin films doped with sulforhodamine", Appl. Opt. **46**, 1507 (2007).

27. Y. Kawabe, L. Wang, T. Nakamura, and N. Ogata; *"Thin-filmlasers based on dye–deoxyribonucleic acid–lipid complexes*", Appl. Phys. Lett. **81**, 1372(2002).

28. G. S. He, Q. Zheng, P. N. Prasad, J. Grote, and F. K. Hopkins; *"Infrared two-photon-excited visible lasing from a DNA–surfactant–chromophore complex*", Opt. Lett. **31**, 359(2006).

...........ॐ..........

Chapter 5
Linear and nonlinear optical properties of silver nanoparticles stabilized by bovine serum albumin

Abstract

We have synthesized highly stable silver nanoparticles in aqueous solution at room temperature by standard reduction method using bovine serum albumin (BSA) as a stabilizing agent. The nonlinear optical properties of nanoparticles are investigated using Z-scan technique at 532 nm. The obtained nonlinear absorption coefficient and negative nonlinear refractive index are found to be 88.36 cm/GW and -5.1×10^{-7} esu respectively. The real and imaginary part of third order susceptibility of silver nanoparticles are found to be 1.553×10^{-7} esu and 0.7×10^{-7} esu respectively. The silver nanoparticles in BSA template show good optical limiting property.

5.1. INTRODUCTION

There is a keen interest in the different preparation technique for obtaining materials at the nanometer level, and today it constitute a major area of research due to its potential application in biology, catalysis, optical, magnetic and electronic devices [1-4]. One of the challenges in nanomaterial synthesis is developing methodologies with biological molecules as templates for nano material synthesis. Nano scale biocompatible materials are currently receiving considerable attention in biological applications [5-8]. Many preparation techniques have already been reported to produce Ag nanoparticles however, relatively few methods produce silver nanoparticles stabilized with biomolecules.

Bovine serum albumin (also known as BSA) is a serum albumin protein that has numerous biochemical applications can be used as good stabilising agent in nanoparticle synthesis. Biological macromolecules are capable of controlling nucleation and growth to a remarkable degree through biomineralization. A simple and convenient method for the synthesis of gold, silver and their alloy nanoparticles in a foam matrix using the protein bovine serum albumin (BSA) is reported [8]. There are many reports in literature where polypeptides/ proteins have been used to assemble nanoparticles or the nanoparticle surfaces have been modified by protein/polymer coatings. Studies on nanoparticle synthesis using DNA were the subject matter of chapter 4. In this chapter we describe the work related to the synthesis of silver nano particles using BSA biopolymer.

5.2. EXPERIMENTAL METHODS

Silver nano particle is synthesized in aqueous solution of BSA (SRL) by standard reduction technique. A 20 mL solution with a concentration of

0.25 mM AgNO$_3$ and bovine serum albumin at preferred concentration in water are prepared. While stirring vigorously 0.6 ml of 10 mM NaBH4 was added at once. Stirring was stopped after 30 seconds. The solution became deep yellow in colour and is stable for several weeks. The silver nanoparticles are characterized by UV-VIS absorption spectroscopy and scanning electron microscopy method. The photoluminescence of silver nanosol in BSA is studied using spectro fluorimrter. Z-scan study is performed at 532 nm on Ag nano sol.

5.3. RESULTS AND DISCUSSIONS

5.3.1. Characterization of Nanoparticles

Silver nanosol is synthesized successfully in aqueous solution of BSA by standard reduction technique using AgNO$_3$ and NaBH4. Before carrying out the characterization of the optical nonlinearities, the linear absorption spectra of silver nano sol in BSA matrix was obtained. Optical absorption measurement is an initial step to observe the nanosol behaviour. Absorption spectra of silver nanosol at different concentration of BSA is shown in Fig. 5.1. A strong absorption peak at approximately 410 nm originating from the surface plasmon resonance (SPR) is observed at all concentration of of BSA. BSA possesses a zwitterionic character at the iso electric point with exposed ionic groups (C and N terminus) at the side chains of the globular protein, which are present in solution and are promising sites for binding cationic and anionic groups. Molecular interactions between the functional groups on the protein surface and the Ag+ ions in solution determines particle formation and arrangement. The affinity of the Ag+ ion to proteins generally depends on the interaction of Ag+ with the amino acid side chains [8]. The good symmetric absorption peak implies that the size distribution of the nanoparticles is narrow.

Fig. 5.2 shows SEM picture of the silver nanoparticles formed on BSA template. SEM image shows aggregation of small particles into big size, which may be due to the evaporation of solvent during film formation.
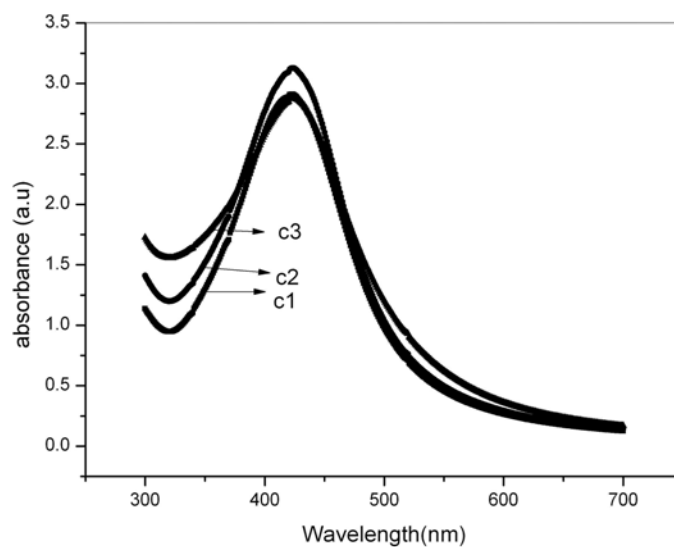
Figure: 5.1. *Absorption spectra of silver nanoparticles in aqueous solution of BSA (where c1, c2, c3 represents BSA concentration 0.05, 0.1, 0.15wt% respectively)*
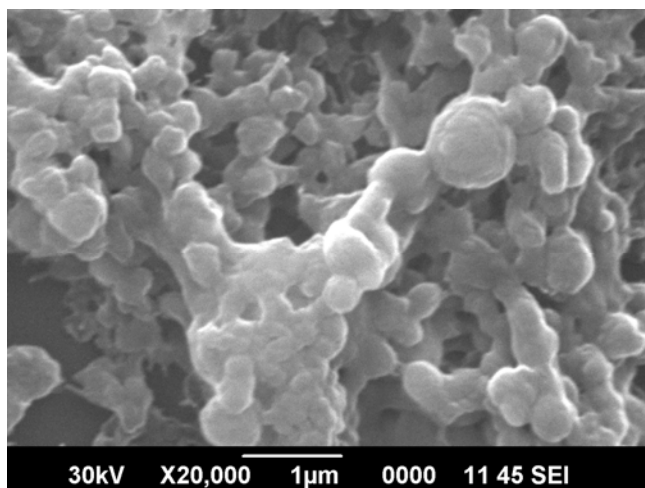
Figure: 5.2. *SEM image of of silver nanoparticles in BSA template.*

5.3.2. Optical Properties of silver nanoparticles stabilized by the protein bovine serum albumin

The luminescence spectrum of the silver particles stabilized by the BSA in aqueous solutions shows an emission peak at 340 nm and 538 nm upon photo excitation at 250 nm (Fig. 5.3). To estimate the role of BSA on photoluminescence of silver nanoparticles, we have taken photoluminescence of aqueous solution of BSA alone. BSA shows strong fluorescence at 348 nm (Fig. 5.4). This indicates that the peak at 340 nm is the fluorescence peak of the BSA. The peak at 538 nm shows the presence of silver nanoparticles. The luminescence of silver metal and that of noble metals is generally attributed to electronic transitions between the upper d band and conduction sp band. The emission in the region 400 – 600 nm is in good agreement with the previous report [9-12].
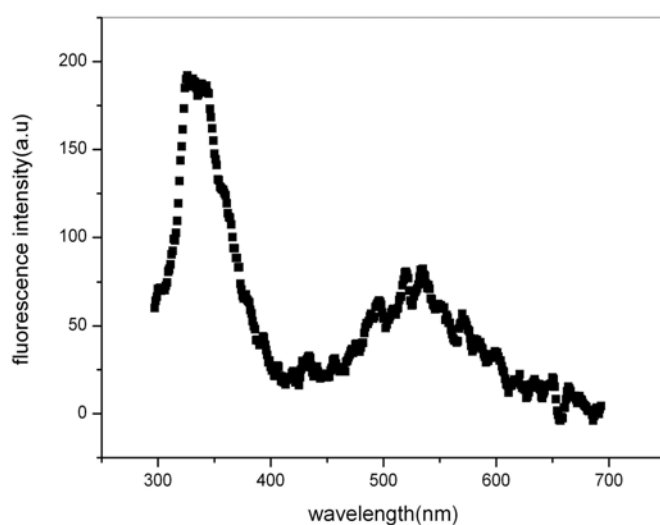
Figure: 5.3. *Photoluminescence from silver nanoparticles in BSA template*
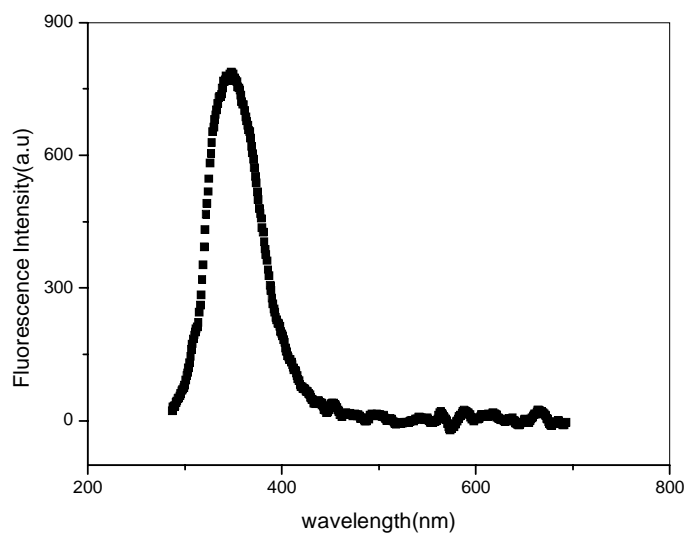
Figure: 5.4. *Photoluminescence from aqueous solution of BSA*

Fig. 5.5 is the plot of open aperture Z-scan measurement which shows (curve b) the nonlinear absorption of silver nano sol in BSA matrix at a typical light intensity of 175 MW/cm^2 for an irradiation wavelength of 532 nm. The data are analyzed by using the procedure described by Bahae *et. al* [13]. The obtained values of the nonlinear absorption coefficient β and imaginary part of the susceptibility (Imχ^3) at an intensity of 175 MW/cm^2 are 88.36 cm/GW, 1.448 x 10^{-7} respectively. In this intensity level these values are found to be good while comparing the results of other investigations reported in literature [14-19]. In Fig. 5.5 Z-scan curve 'a' corresponds to aqueous solution of BSA alone, exhibiting low value of nonlinear optical coefficient (β is 73.6 cm/GW). Here the presence of silver nanoparticles enhances the NLO effect by excitation of SPR of silver nanoparticles through energy transfer between BSA molecules and silver nanoparticles.
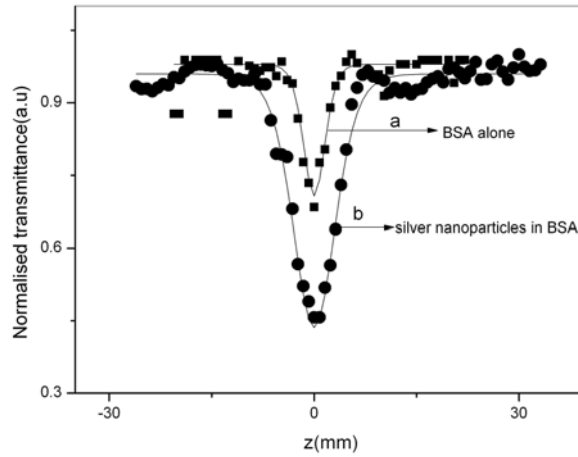
Figure: 5.5. *Open aperture Z-scan curve at 175 MW/cm^2 of (solid line shows theoretical fit)*

a. BSA alone
b. silver nanoparticles in aqueous solution of BSA

To examine the optical limiting property of the silver nanopartcles in BSA matrix the nonlinear transmission of the silver nano sol is studied as a function of input intensity (Fig. 5.6). The light intensity level for optical limiting at 532nm is found to be 34 MW/cm^2. The mechanism producing nonlinear absorption is the reverse saturable absorption (RSA) or excited state absorption or two photon absorption [19].
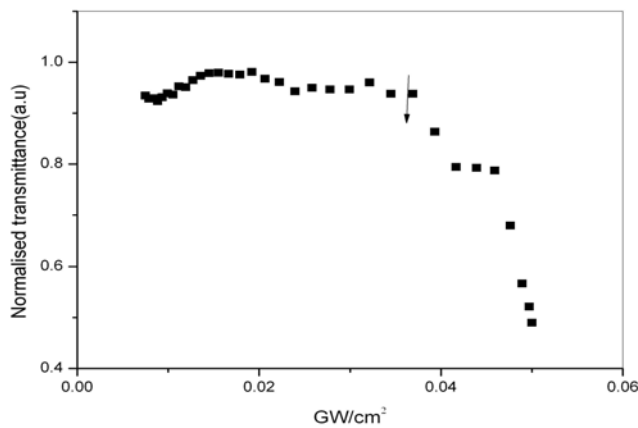
Figure: 5.6. *Optical limiting performance of silver nanoparticles in aqueous solution BSA*
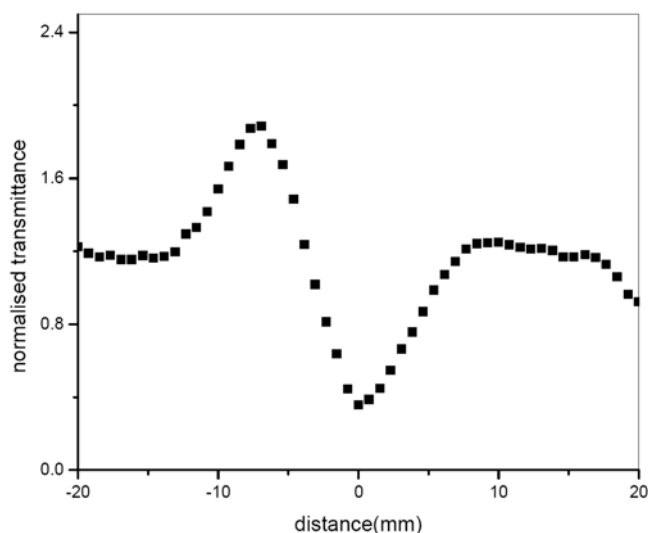
Figure: 5.7. *Experimental result for closed aperture Z-scan of silver nanoparticles in aqueous solution of BSA.*

Typical closed-aperture z scan traces of silver nano sol in BSA template is shown in Fig. 5.7 at an intensity of 175 MW/cm^2. The closed-aperture curve exhibits a peak-valley shape, indicating a negative value of the nonlinear refractive index n_2. For samples with sizable refractive and absorptive nonlinearities, closed-aperture measurements contain contributions from both the intensity - dependent changes in the transmission and in the refractive index. By dividing the normalized closed-aperture transmittance by the corresponding normalized open-aperture data, we can retrieve the phase distortion created due to the change in the refractive index. The value of the difference between the normalized peak and valley transmittance Tp-v can be calculated from the closed aperture Z-scan plot. The nonlinear refractive index n_2 and the real part of the nonlinear susceptibility [Reχ^3] are given, respectively, by Eq 5.1 and 5.2.

$$n_2(esu) = \frac{Cn_0}{40\pi^2} \frac{\lambda\Delta T_{p-v}}{.812(1-S)^{.25} L_{eff} I_0} \qquad ....(5.1)$$

$$\text{Re } \chi^{(3)}(esu) = \frac{n_0 n_2(esu)}{3\pi} \qquad ....(5.2)$$

The negative nonlinear refractive index n_2 and the real part of χ^3 evaluated using the above equations are -5.1 x 10^{-7} esu and 0.7 x 10^{-7} esu respectively. The observed peak-valley structure is the sign of negative nonlinearity which is either electronic or thermal in origin. Therefore the value of nonlinear refraction coefficient is due to the combined effect of these two mechanisms.

5.4. CONCLUSIONS

Highly stable silver nanoparticles in aqueous solution at room temperature is synthesized by standard reduction method using bovine serum albumin (BSA) as a stabilizing agent. Prepared solution shows strong absorption peak at 416 nm originating from the surface plasmon absorption of nanosized silver particles in aqueous solution of BSA. The photo luminescence spectra shows emission peak at 538nm at excitation wavelength of 250 nm.The nonlinear optical properties were investigated by a single beam Z-scan setup. The nanosol show an excellent nonlinear optical property. The obtained nonlinear absorption coefficient and negative nonlinear refractive index are found to be 88.36 cm/GW and -5.1x10^{-7} esu respectively. The real and imaginary part of third order susceptibility of silver nanoparticles is found to be 1.553x10^{-7} esu and 0.7x10^{-7} esu. The silver nanoparticles in BSA template show good optical limiting property with a threshold of 34 MW/cm^2. Silver nanoparticles in BSA template are potential candidate for optoelctronic device application.

REFERENCES

1. S. Forster, M. Antonietti; "*Amphiphilic Block Copolymers in Structure-Controlled Nanomaterial Hybrids*", Adv. Mater. **10,** 195(1998)

2. M. Moffit, A. Eisenberg; "*Size Control of Nanoparticles in Semiconductor-Polymer Composites. 1. Control via Multiplet Aggregation Numbers in Styrene-Based Random Ionomers*", Chem.Mater. **7**, 1178 (1995)

3. R. P. Andres, J. D. Bielefeld, J.I. Henderson, D. B. Janes, R. Kolagunta, C. P. Kubuiak, W. J. Mahoney, R.J. Osifchin; "*Self-Assembly of a Two-Dimensional Superlattice of Molecularly Linked Metal Cluster*", Science **273**,1690 (1996)

4. C. Petit, P. Lixon, M.P.Pileni; "*In Situ synthesis of silver nanocluster in AOT reverse micelles*", J. Phys. Chem. **97**, 12974(1993)

5. Braun E, Eichen Y,Sivan U, Ben-Yoseph,G; "*DNA-templated assembly and electrode attachment of a conducting silver wir*e", Nature **391**,775(1998)

6. Zhiguo Liu, Yuangang Zu , Yujie Fu, Yuliang Zhang, Huili Liang; "*Growth of the oxidized nickel nanoparticles on a DNA template in aqueous solution*" , Mater. Lett. **62**, 2315(2008)

7. Yong Yao, Yonghai Song and Li Wang; "*Synthesis of CdS nanoparticles based on DNA network templates*", Nanotechnology **19,** 405601(2008)

8. Ajay V. Singh, Bapurao M. Bandgar, Manasi Kasture, B. L. V. Prasad and Murali Sastry; "*Synthesis of gold, silver and their alloy nanoparticles using bovine serum albumin as foaming and stabilizing agent*", J. Mater. Chem. **15**, 5115(2005)

9.   Junpeng Gao, Jun Fu, Cuikun Lin, Jun Lin, Yanchun Han, Xiang Yu,§ and Caiyuan Pan; *"Formation and Photoluminescence of Silver Nanoparticles Stabilized by a Two-Armed Polymer with a Crown Ether Core"*, Langmuir **20**, 9775(2004)

10.   Jian Xu, Xia Han, Honglai Liu, Ying Hu; *"Synthesis and optical properties of silver nanoparticles stabilized by gemini surfactant",* Colloids and Surfaces A: Physicochem. Eng. Aspects **273** 179(2006)

11.   Oleg A. Yeshchenko, Igor M. Dmitruk,Alexandr A. Alexeenko, Mykhaylo Yu. Losytskyy, Andriy V. Kotko, and Anatoliy O. Pinchuk; *"Size-dependent surface plasmon-enhanced photoluminescence from silver nanoparticles embedded in silica",* Phys. rev. B **79**, 235438 (2009)

12.   Alqudami Abdullah and S Annapoorn; *"Fluorescent silver nanoparticles via exploding wire technique", Pramana J. Phys.,* **65**,(2005)

13.   Mansoor Sheik Bahae et al; *"Sensitive Measurement of Optical Nonlinearities Using a Single Beam"*, IEEE J. Quantum electronics. **26**,760

14.   Luis A. Gomez, Cid B. de Araujo, A. M. Brito Silva, and Andre Galembeck; *"Influance of stabilizing agents on the nonlinear susceptibility of silver nanoparticles"* , J. Opt. Soc. Am. B **24**, 2136(2007)

15.   Marek Samoc, Anna Samoc, James G Grote; *"Complex nonlinear refractive index of DNA",* Chem. Phys. Lett. **43**, 1132(2006)

16.   S. R. Mishra, H. S. Rawat, M. P. Joshi, S. C. Mehendale; *"The role of non-linear scattering in optical limiting in C_{60} solutions"*, Appl. Phys. B **27**, L 157(1994)

17.   Xin Chen, Gang Zou, Yan Deng , Qijin Zhang; *"Synthesis and nonlinear optical properties of nanometer-size silver-coated polydiacetylene composite vesicles",* Nanotechnology **19** ,195703(2008)

18. L. A. Gomez, C. B De Araujo, A. M. Brito-Silva, A.Galembeck; "*Solvent effect on the linear and nonlinear optical response of Silver nanoparticles*" , Appl. Phys. B **92**,61(2008)

19. Zhengle Mao, Lingling Qiao, Fei He, Yang Liao, Chen Wang, Ya Cheng; "*Thermal-induced nonlinear optical characteristics of ethanol solution doped with silver nanoparticles*", Chinese Opt. Lett. *7, 949 (2009)*

...........ॐ..........

Chapter 6
Studies on CdS nanoparticles prepared in DNA and BSA based biotemplates

Abstract

This chapter discusses band gap tunability of CdS nanoparticles in biotemplates deoxyribonucleic acid (DNA) and bovine serum albumin (BSA). DNA is more efficient in controlling the size of the nanoparticles compared to BSA. Since nanoparticles are capped with biomaterials, they are very useful for biolabeling. The photo luminescence spectrum of CdS nanoparticles in DNA template shows sharp emission peak at 490 nm with shoulders at 430 nm and 530 nm while that of CdS in BSA template has emission peak at 530 nm with shoulders at 477 nm and 410 nm. We also studied excitation wavelength dependence on fluorescence emission of CdS nanoparticles stabilized with DNA and BSA. The excitation wavelength dependent shift of PL peak is found to be between 40 and 50 nm for a change in excitation wavelength from 260 to 420 nm.

6.1. INTRODUCTION

Synthesis of semiconductor nanoparticles having a controlled size distribution has attracted significant interest in research because of their luminescent properties, quantum size effects and other important physical and chemical properties. The broad area of applications include solar energy conversion, optoelectronic devices, molecular and cellular imaging and trace detection. A major feature of semiconductor nano particles is the quantum confinement effect, which leads to spatial enclosure of the electronic charge carriers within the nanocrystal. The spectral properties of these semiconductor nanocrystals can be controlled effectively by tuning the size, composition, surface properties and crystal structure of the nanocrystals. Because of this effect we can tune the light emission from these media throughout the ultraviolet, visible, near-infrared, and mid-infrared spectral ranges. For instance, the band gap emission is tunable over wide wavelengths by adjusting an appropriate size of the particle. The particles prepared from such application viewpoint will be useful as a fluorescent agent for optical and biotechnological applications. In comparison with organic dyes and fluorescent proteins, semiconductor quantum dots represent a new class of fluorescent labels with unique advantages and applications. For example, the fluorescence emission spectra of quantum dots can be continuously tuned by changing the particle size, and a single wavelength can be used for simultaneous excitation of all different sized quantum dots [1-10].

CdS is one of the most important II–VI semiconductor compound having excellent optical properties. It is a direct band gap material of energy band gap 2.42 eV at 300 K. Considerable amount of effort has been devoted to the synthesis and study of optical property of CdS related nanoparticles and quantum dots. Biological applications of CdS quantum dots has increased dramatically because of its unique spectral properties, which enable simultaneous multiplex labelling and detection [11, 12]. Most importantly, highly monodispersed CdS

nanocrystals can be synthesized via size restricting growth modes. Adding surface capping organic materials to the solution is one of the ways to achieve growth restriction. This simple preparation method has opened the way towards tunable light emitting devices and low voltage display devices. One of the highly cited methods for making CdS or CdSe quantum dots is organometallic precursor [13]. Lee and Chang have reported an efficient and non-corrosive polysulphide electrolyte for CdS quantum dot sensitized solar cell application. The efficiency of the CdS-sensitized solar cell was 1.15% [14]. Bulk CdS shows an absorption onset of 2.42 eV and absorbs radiation in the visible region. Semiconductor nanoparticles are known to exhibit unique size dependent optical properties, which make them attractive from the viewpoint of integrated photonic devices. There is significant change in the properties when the dimensions of the nanocrystallites become comparable or less than the Bohr radius of the excitons corresponding to the widening of the energy gap as size decreases. In CdS, quantum size effect is observed for crystallite dimensions below 5 nm which is approximately the Bohr exciton diameter in CdS [15]. Because of the quantum confinement effect, semiconductor nanocrystals exhibit size dependent, molecular like discrete electronic and optical transitions. Nanocrystalline CdS has been prepared by different workers using various techniques such as pulsed laser deposition, chemical bath deposition, spray pyrolysis, successive ionic layer adsorption and reaction, screen printing and sol–gel spin coating method [16-20]. Chemical method is a simple and really cost efeective method.

Among biological molecules deoxyribo nucleic acid (DNA) and bovine serum albumin (BSA) have been used extensively as a biotemplate to grow inorganic quantum confined structure and to organize non biological building blocks into extended hybrid materials because of their physicochemical stability and unique structure [21-24]. The integration of nanotechnology with biology

and medicine is expected to produce major advances in molecular biology, and bioengineering. The development of functional nanoparticles that are covalently linked to biological molecules such as peptides, proteins, and nucleic acids are the recent advances in biotechnonolgy. For example nickel has been successfully synthesized by using DNA network templates [22]. Using biomolecule as a template to synthesis inorganic nano particles is an effective method to fabricate functional materials with well defined structure and controllable dimensions. We adopted the preparation technique reported by Yong Yao et.al. [23] to synthesize CdS nano particles in both DNA and BSA templates. The size and assembly of nano particles can be controlled by changing the amount of biological molecules in medium. In the present chapter we compare the band gap tunability and photoluminescence properties of CdS nano particles in two biological template, DNA and BSA.

6.2. SYNTHESIS

All chemicals and biopolymers used in this work were obtained from commercial sources (SRL, Merck). DNA and BSA capped CdS nanoparticles were synthesized according to published procedures [23]. The concentration of BSA and DNA were varied from 0.05 wt% to 0.2 wt%. Cadmium acetate at 50mM solution and DNA solutions were mixed completely. Thiourea solution was added to the prepared mixture and heated at 70 ^{0} C for 100 min. The yellow reaction product was filtered and dried in a desicater to obtain yellow coloured CdS nano particles. We used aqueous solution of BSA to prepare BSA coated CdS nanoparticles. Concentrations of the both stabilizers needed for effective capping of CdS particle was found to be in the same range.

6.3. CHARACTERIZATIONS

Optical absorption of the samples prepared with various concentrations of capping agent (DNA and BSA) were studied. The UV-visible absorption

spectroscopy has been used to monitor the optical absorption properties of quantum-sized nano particles. The absorption spectra of the nanoparticles of CdS in DNA template are shown in Fig. 6.1, where C1, C2, C3, C4 represent DNA concentration of 0.06, 0.128, 0.16, 0.2 wt% respectively. The spectra exhibit a well - defined absorption edge in the 400-500 region. Blue-shifted absorption edge indicating quantum size effect is clearly seen [25]. Fig. 6.2 shows the absorption spectra of CdS nanoparticles in BSA template. In this case exciton peak appeared around 470 nm which is blue shifted indicating quantum size effect, where C1, C2, C3, C4 represents BSA concentration of 0.06, 0.128, 0.16, 0.2 wt% respectively. Blue shift in the absorption edge increases with increase in stabilizer concentrations for both capping agents. Fig. 6.3 shows absoption spectra of CdS nanoparticles without using DNA and BSA. Here thiourea is used as a sulphur source and capping agent. In this case the absorption edge is found to be around 480 nm. In all cases the absorption band is found to be broad which indicates particle size distribution in samples.
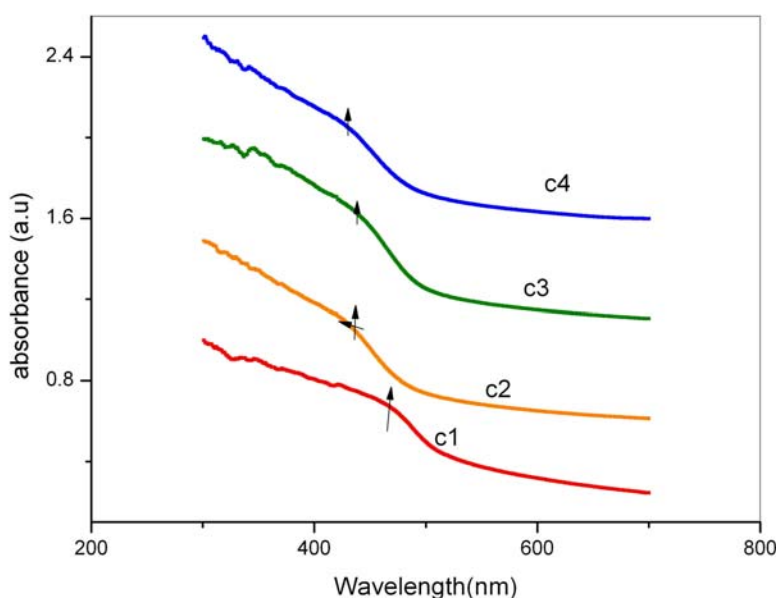

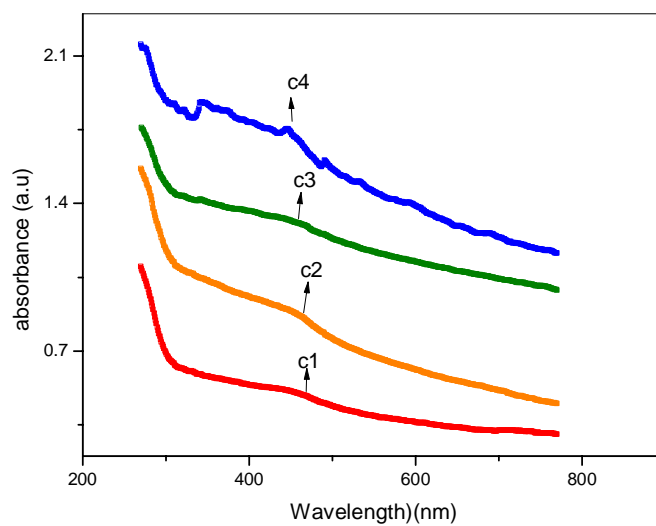**Figure: 6.1.** *Absorption spectra of CdS nanoparticles at different concentration of DNA*

Figure: 6.2. *Absorption spectra of CdS nano particles at different concentration of BSA.*
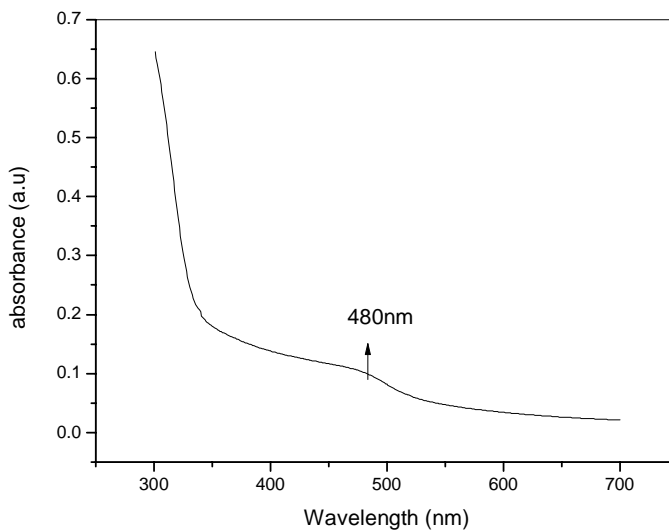
Figure: 6.3. *Absorption spectra of CdS nano particles without adding biopolymers DNA and BSA*

Optical properties of semiconductor nanocrystals depend on the electronic structure of valence and conduction bands. As indicated above one of the most interesting effects of low dimensional semiconductor quantum structures is the size dependent band gap. There are two cases, called the weak confinement and the strong confinement regime depending on the particle size is larger than or smaller than the radius of the electron-hole pair.

A simple model was initially adapted by Efros in 1982 to spherical clusters with infinite potential wells as boundary conditions [26]. These authors assumed an energy dispersion close to the valence band maximum (VBM) and the conduction band minimum (CBM) with effective masses of CBM electron and VBM hole. This model is called the "effective mass approximation" (EMA). A further development of the EMA model has been made by Brus [27, 3]. The latter has introduced the Coloumb interaction. The grain size of CdS nanoparticles can be determined using Brus equation

$$E = Eg + h^2 / 8R^2 \left[1 / m_e^* + 1 / m_h^* \right] - 1.8e^2 / 4\pi\varepsilon_0\varepsilon_\alpha R - 0.124e^4 / \left(h / 2\pi \right)$$
$$\left(4\pi\varepsilon_0\varepsilon_\alpha \right)^2 \left[1 / m_e^* + 1 / m_h^* \right]^{-1}$$

.....(6.1)

where E is the onset of absorption of the sample. Eg is the bulk band gap, R is the radius of the particle, and m_e^*, m_h^* are the reduced masses of the conduction band electron and valence band hole in units of the electron mass, ε_0 is the vacuum permittivity and ε_α is the high-frequency dielectric constant. In semiconductors, the relation connecting the absorption coefficient α, the incident photon energy hν and optical band gap Eg takes the form

αhν = A(hν - Eg)^p ....(6.2)

where A is constant related to the effective masses associated with the bands and p=1/2 for a direct band gap material, 2 for an indirect band gap material and 3/2

for a forbidden direct energy gap. Since better linearity was obtained in the $(\alpha h\nu)^2$ *vs* hν plot, which is shown in Fig.6.4 (CdS in DNA template), the direct band gap values were determined by extrapolating the linear portion of these plots to the energy axis.
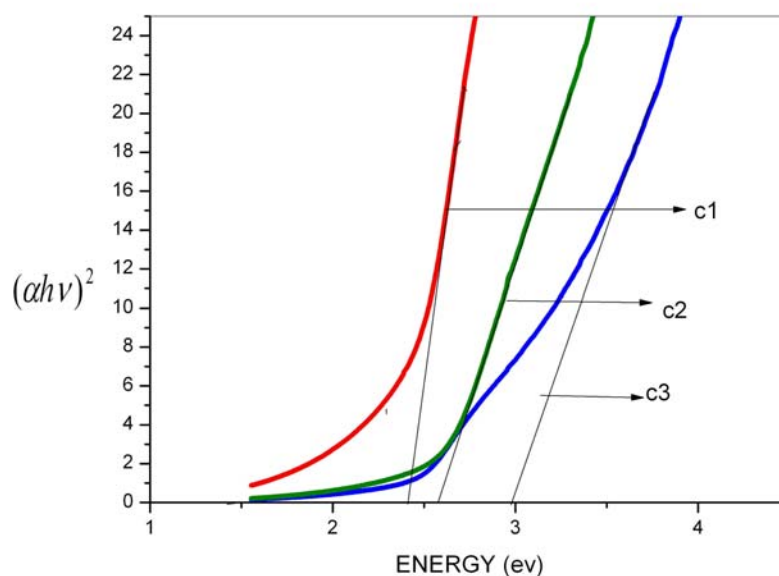
Figure: 6.4. *The $(\alpha h\nu)^2$ vs hν plot of CdS nanoparticles in DNA template*

Value of the band gap obtained from the absorption spectra are given in table 6.1. On increasing the concentration of DNA, the optical band gap was found to increase from 2.58 to 2.92 eV. The reduction in the particle size gives a shift in the optical band gap of the sample since bandgap increases the particle size is reduced. Particles capped with BSA at concentration range 0.06 wt% to 0.2 wt% show band gap tunability from 2.58 eV to 2.73 eV. The wide tunability of band gap is obtained in the case of DNA capped nanoparticles compared to BSA capped.

Table: 6.1. Band gap of semiconductor nanoparticles in DNA and BSA template

Wt% of BSA and DNA	Energy Band Gap of CdS nanoparticle in DNA(ev)	Energy Band Gap of CdS nanoparticle in BSA (ev)
0(Fig. 6.3)	2.58 ± 0.01	2.58 ± 0.01
0.06(C1 in figure)	2.65 ± 0.02	2.64 ± 0.01
0.128(C2 in figure)	2.85 ± 0.01	2.67 ± 0.02
0.16(C3 in figure)	2.89 ± 0.03	2.70 ± 0.02
0.2(C4 in figure)	2.92 ± 0.02	2.73 ± 0.03

X-ray diffraction studies were carried out for DNA and BSA capped CdS samples and a typical pattern for sample C2 is presented in Figs. 6.5 and 6.6.The XRD pattern exhibits prominent, broad peak at value 27^0. The average grain size of the sample is determined using Scherrer's equation [28].

$$D = 0.89\,\lambda\,/\,\beta\cos\theta \qquad ....(6.3)$$

where D is the average diameter of the nano particles, λ is the wavelength of the CuKα line (1.54 Aº), β is the full width half maximum of the diffraction peak in radian and θ is the diffraction angle. The average nano particle diameter calculated from Brus equation and Scherrer formula is shown in table 6.2.

Table: 6.2. Particle size of nanoparticles in DNA and BSA template obtained from X- ray diffraction and optical absorption studies

Wt % of DNA and BSA	Particle size of CdS in DNA template (nm)	Particle size of CdS in BSA template (nm)	Particle size of CdS in DNA template from XRD (nm)	Particle size of CdS in BSA template from XRD (nm)
0	4.71 ± 0.01	4.71 ± 0.01	4.69	4.71
0.06	4.19 ± 0.03	4.23 ± 0.03	4.09	4.11
0.128	3.14 ± 0.02	4.02 ± 0.04	3.28	3.30
0.16	3.03 ± 0.04	3.99 ± 0.05	3.13	3.98
0.2	2.92 ± 0.03	3.68 ± 0.04	2.86	3.58
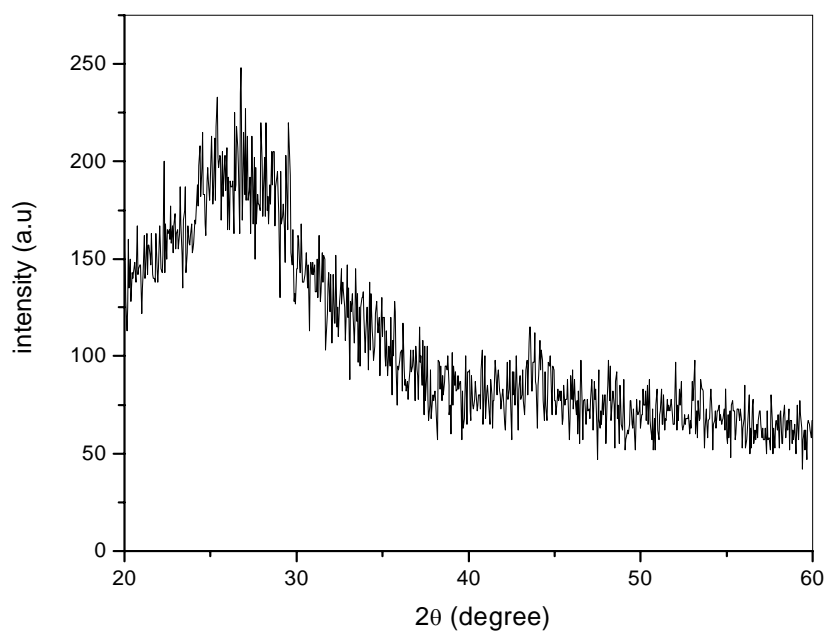
Figure: 6.5. *XRD pattern of CdS nanoparticles in DNA(C3) matrix*

As the particle size obtained from X- ray diffraction and optical absorption studies is smaller than Bohr radius of CdS, the strong confinement

effect can be assumed to be present in the CdS nanoparticles.
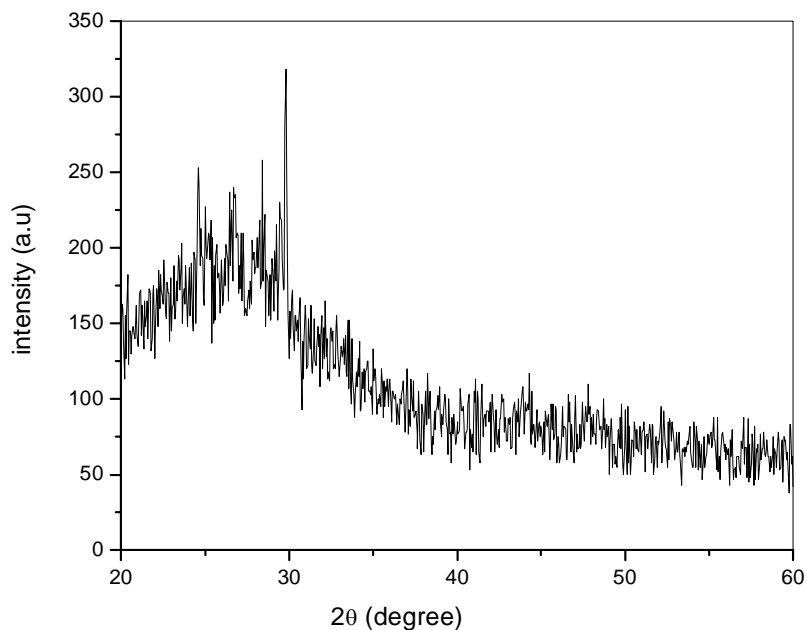
Figure: 6.6. *X RD pattern of CdS nanoparticles in BSA(C3) matrix*

6.4. PHOTOLUMINESCENCE STUDIES

Figure 6.7 shows the photoluminescence (PL) spectra of CdS nanoparticles in DNA template at different concentrations of DNA at excitation wavelength 260 nm. The PL spectrum shows sharp emission peak at 490 nm with shoulders at 430 nm and 530 nm. Luminescence spectra is very broad. As concentration of the DNA increases, PL peak is shifted to blue region indicating quantum confinement effect. PL behaviour of semiconductor nanoparticles gives information on the energies and dynamics of photogenerated charge carriers as well as on the nature of the emitting states. PL occurs when an electron, undergoes radiative recombination either at valence band (band edge luminescence) or at traps/surface states within the forbidden gap [28-30]. Here

emission at 490 nm is the band edge emission due to recombination of the exciton in the mostly delocalized states in nanoparticles and it determines crystalline nature of nanoparticles. Prepared samples shows strong PL which indicates that the surface states remain very shallow, as it is reported that quantum yields of band edge will decrease exponentially with increasing depth of surface state energy levels. PL spectrum at 535 nm is usually attributed to trap state emission arising from surface defect sites. In CdS, defects consist of cadmium vacancies, sulphur vacancies, interstitial sulphur and cadmium atoms adsorbed on the surface. Side lobes in the higher energy side of PL spectra is due to the recombination of charge carriers in deep traps of surface localized states [28, 31-33]. Fig. 6.8 shows the photoluminescence spectra of CdS nanoparticles in BSA template at different concentration of DNA at excitation wavelength 260nm. The PL spectrum shows sharp emission peak at 530 nm with shoulders at 477 nm and 410 nm. The emission band present at 530 nm is known as green emission band of CdS. Emission at 477 nm comes from band edge emission.

CdS nanoparticles with PL peaks at 509, 535, 569 and 585 nm correspond to particle size of 1.6, 2.2, 3.1 and 3.4 nm respectively as reported in literature [28]. In both case, (CdS in DNA and BSA templates) PL spectra consist of many emission peaks indicating particle size distribution in samples. In this case an appropriate excitation energy can excite several nanocrystals simultaneously producing a PL spectrum which contains more than one peak. The present sample may not be strictly mono dispersed and the structure on the high energy side of the green emission may be attributed to selectively excited photoluminescence.
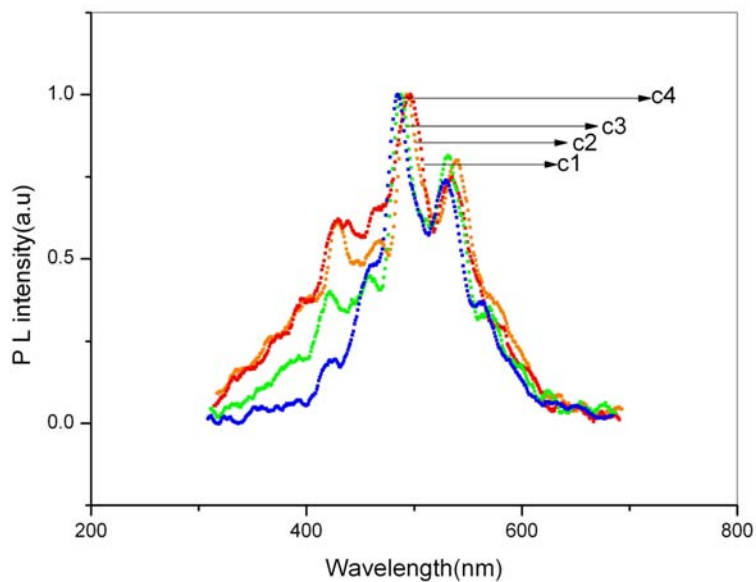
Figure: 6.7. *PL spectrum of DNA capped CdS nanoparticles (where C1,C2,C3,C4 represent DNA concentrations 0.06, 0.128, 0.16, 0.2 wt% respectively)*
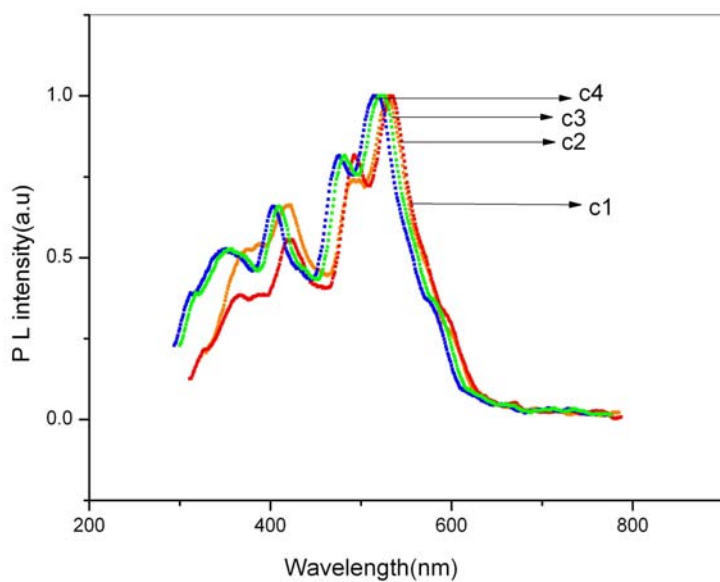
Figure: 6.8. *PL spectrum of BSA capped CdS nanoparticles (where C1,C2,C3,C4 represent BSA concentrations 0.06, 0.128, 0.16, 0.2 wt% respectively)*

Figs. 6.9 and 6.10 show the excitation wavelength dependence of CdS nanoparticle in DNA and BSA templates respectively. In both cases when excitation wavelength changes from 260 nm to 420 nm peak fluorescence shifts towards red side. The shift in the fluorescence maximum is approximately 50 nm in the case of CdS in DNA matrix. A 40 nm shift in fluorescence peak is observed when excitation wavelength changes from 260 nm to 420 nm for CdS in BSA template. The emission maxima is different for both case. Excitation wavelength dependence may be due to the broad particle size distribution in the samples. Different particles may get excited for different excitation wavelength. The emission maxima is different for nanoparticles prepared in DNA and BSA templates. The absorption and emission band positions are dependent on the interaction between the capping agent and nanoparticles.
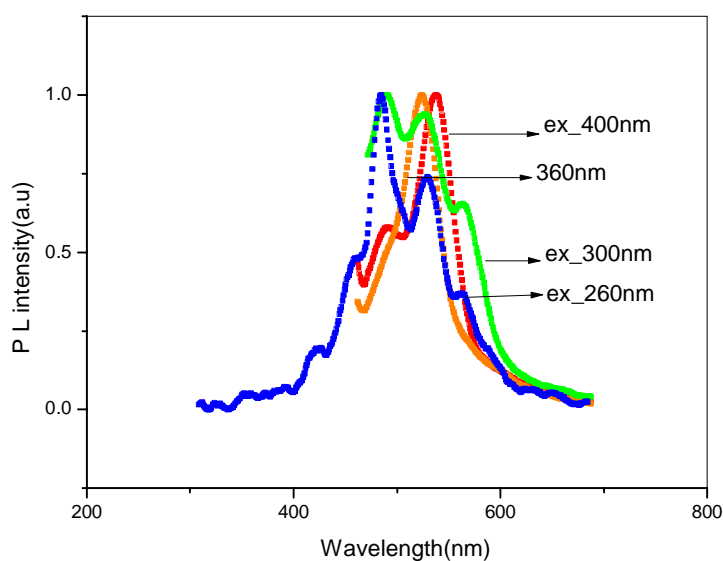
Figure: 6.9. *Normalized fluorescence spectra of DNA capped CdS nanoparticles as a function of excitation wavelength.*
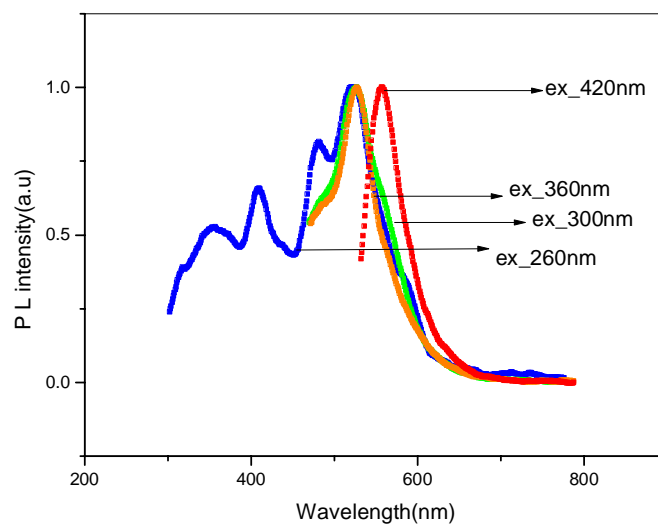
Figure: 6.10. *Normalized fluorescence spectra of BSA capped CdS nanoparticles as a function of excitation wavelength.*

6.5. CONCLUSIONS

The band gap tunability of CdS nanoparticles in biotemplates de-oxyribonucleic acid (DNA) and bovine serum albumin (BSA) is studied. The band gap of these semiconductor nano particles can be controlled effectively by changing the concentration of biopolymers DNA and BSA. DNA is more efficient in controlling the size of the nanoparticles compared to BSA. Since nanoparticles are capped with biomaterials, they are found to be useful for biolabeling. The PL spectrum of CdS nanoparticles in DNA template shows sharp emission peak at 490 nm with shoulders at 430 nm and 530 nm. The PL spectra of CdS in BSA template shows sharp emission peak at 530nm with shoulders at 477 nm and 410 nm. The emission band present at 530 nm is known as green emission band of CdS. Emission at 477 nm and 490 nm come from band edge emission. Studies on excitation wavelength dependence of PL spectra shows, shift of peak emission towards red side when excitation wavelength

changes from 260 nm to 420 nm. The fluorescence emission spectra of nanoparticles can be continuously tuned by changing the concentration of BSA or DNA and excitation wavelength. The particles prepared from such viewpoint should be useful as a fluorescence agent for optical and biotechnological applications

REFERENCES

1. A. P. Alivisatos; "*Semiconductor Clusters, Nanocrystals, and Quantum Dots*" , Science **271,** 933(1996)

2. M. Bruchez, M. Moronne, P. Gin, S. Weiss, A. P. Alivisatos; "*Semiconductor Nanocrystals as Fluorescent Biological Labels*" , Science **281**, 2013(1998)

3. N. Heron, J. C. Calabrese, W. F. Farneth, Y. Wang; "*Crystal Structure and Optical Properties of $Cd_{32}S_{14}(SC_6H_5)_{36}$. DMF_4, a Cluster with a 15 Angstrom CdS Core*", Science **259**, 1426 (1993).

4. L. Brus; "*Quantum Crystallites and Nonlinear Optics*", Appl. Phy. A **53**, 2283 (1991).

5. A. Henglein; "*Small-particle research: physicochemical properties of extremely small colloidal metal and semiconductor particles*", Chem. Rev. **89**, 1861 (1989).

6. Ron Gill, Ronit Freeman, Jian-Ping Xu, Itamar Willner, Shira Winograd, Itzik Shweky,Uri Banin; "*Probing Biocatalytic Transformations with CdSe−ZnS QDs*", J. Am. Chem. Soc.*,* **128** , 15376(2006)

7. V. L. Colvin, M. C. Schlamp , "A. P. Alivisatos; *Light-emitting diodes made from cadmium selenide nanocrystals and a semiconducting polymers*", Nature, **370**, 354 (1994)

8.   K K Caswell, Rahina Mahtab, Catherine J Murphy; *"Optical detection of thymine dinucleoside monophosphate and its cis-syn photodimer by inorganic nanoparticles"*, J. Fluorescence **14**, 407(2004)

9.   P. P. Favero, M. de Souza-Parise; J. L. R. Fernandez; R. Miotto; A. C. Ferraz; *"Surface properties of CdS nanoparticles"*, *Braz. J. Phy.* **36,** 1032(2006)

10.   B. O. Dabbousi, M. G. Bawendi, O. Onitsuka, and M. F. Rubner; *"Electroluminescence from CdSe quantum dot/polymer composites"*, Braz. J. Appl. Phys. Lett. **66**, 1316 (1995)

11.   Zhou M, Ghosh I; "*Quantum Dots and Peptides: A Bright Future Together"* , Biopolymers, **88**, 325(**2007)**

12.   Kobayashi H, Hama Y, Koyama Y, Barrett T, Regino CA, Urano Y, Choyke PL; *"Simultaneous multicolor imaging of five different lymphatic basins using quantum dots"*, Nano Lett. **7,** 1711(2007)

13.   V. Nogriya J. K. Dongre M. Ramrakhiani, B. P. Chandra; *"Electro and photo luminescence studies of CdS nanocrystals prepared by orgenometalic precursor"*, Chalcogenide Lett. **5**, 365 (2008)

14.   Yuh Lang Lee, Chi Hsiu Chang; *"Efficient polysulfide electrolyte for CdS quantum dot-sensitized solar cells",* J. Power Sources, **185**, 584(2008)

15.   Petrov D, Santos BS, Pereira GAL, De Mello Donega C ; *"Size and Band-Gap Dependences of the First Hyperpolarizability of CdxZn1-xS Nanocrystals",* J. Phys. Chem. B **106**, 5325(2002)

16.   K.R. Murali, S. Kumaresan and J. Joseph Prince; *"Properties of brush plated CdS films", J*. Mater. Sci. Mater. Electron **18**, 487(2007)

17.   D Patidar, R Sharma, N Jain, T P Sharma and N S Saxena; *"Optical properties of CdS sintered film"*, Bull. Mater. Sci., **29**, 21(2004)

18. P. Raji, C. Sanjeeviraja, K. Ramachandran; *"Thermal and structural properties of spray pyrolysed CdS thin film",* Bull. Mater. Sci. **28**, 233 (2005).

19. Basudev Pradhan, Ashwani K.Sharma, Asim K. Ray; *"Conduction studies on chemical bath-deposited nanocrystalline CdS thin films",* J. Cryst. Growth **304**, 388 (2007)

20. M. Thambidurai, N. Murugan, N. Muthukumarasamy, S. Vasantha, R Balasundaraprbhu, S. Agilan; *"Preparation and characterization of nanocrystalline CdS thin films"* ,Chalcogenide Lett. **6,** 171 (2009)

21. Braun E, Eichen Y, Sivan U, Ben-Yoseph,G; *"DNA-templated assembly and electrode attachment of a conducting silver wire"*, Nature **391**,775(1998)

22. Zhiguo Liu, Yuangang Zu , Yujie Fu, Yuliang Zhang, Huili Liang; *"Growth of the oxidized nickel nanoparticles on a DNA template in aqueous solution"*, Mater. Lett. **62,** 2315(2008)

23. Yong Yao, Yonghai Song and Li Wang; *"Synthesis of CdS nanoparticles based on DNA network templates"* , Nanotechnology **19,** 405601(2008)

24. Ajay V. Singh, Bapurao M. Bandgar, Manasi Kasture, B. L. V. Prasad and Murali Sastry; *"Synthesis of gold, silver and their alloy nanoparticles using bovine serum albumin as foaming and stabilizing agent"*, J. Materials Chemistry **15,** 5115(2005)

25. D. K. Dwivedi, Dayashankara, Maheswar Dubey; *"Synthesis,structural and optical characterization of CdS nanoparticles"*, J. Ovonic **6**, 57(2010)

26. A. D. Yoffe; *"Low-dimensional systems: Quantum size effects ad electronic properties of semiconductor microcrystallites (zero dimensional systems) and some quasi-two-dimensional systems"* Advances in Physics **51,** 799 (2002)

27. L. E. Brus; "*Electron–electron and electron‑hole interactions in small semiconductor crystallites: The size dependence of the lowest excited electronic state*" , J. Chem. Phys. **80**, 4403 (1984)

28. M. Thambidurai, N. Muthukumarasamy, S. Agilan, N. Murugan, S. Vasantha, R. Balasundaraprabhu and T. S. Senthil; **"***Strong quantum confinement effect in nanocrystalline CdS*", J. Mater. Sci. **45**,3254(2010)

29. Skinner DE, Colombo DP, Caveleri JJ, Bowman RM; "*Femtosecond Investigation of Electron Trapping in Semiconductor nanoclusters*", J. Phys. Chem. **99**,7853(1995)

30. Roberti T.W, Cherepy N.J, Zhang J.Z; "*Nature of the power-dependent ultrafast relaxation process of photoexcited charge carriers in II-VI semiconductor quantum dots: Effects of particle size, surface, and electronic structure*", J. Phys. Chem. A **108** ,2143(1998)

31. Lin Y, Zhang J, Sargent E.H, Kumacheva E; "*Photonic Pseudo-Gap-Based Modification of Photoluminescence from CdS Nanocrystal Satellites around Polymer Microspheres in a Photonic Crystal*", Appl. Phys. Lett. **81**, 3134(2002)

32. Qi L, Colfen H, Antonietti M; "*Synthesis and Characterization of CdS Nanoparticles Stabilized by Double-Hydrophilic Block Copolymers*", Nano Lett. *1, 61(2001)*

33. J. R. Heath and J. J. Shiang; "*Covalency in Semiconductor Quantum Dots*", Chem. Soc. Rev. **27**, 65 (1998)

...........ॐ..........

Chapter 7
Studies on bacterial colony growth dynamics by laser induced fluorescence

Abstract

The growth kinetics of an aerial bacterial colony on solid agar media is studied using laser induced fluorescence technique. Fluorescence quenching of Rhodamine B by the bacterial colony is utilized for the study. The lag phase, log phase, and stationary phase of growth curve of bacterial colony are identified by measuring peak fluorescence intensity of dye doped bacterial colony.

7.1. INTRODUCTION

Microbial growth can be defined as an increase in cellular components. It leads to an increase in cell number when microorganisms reproduce by processes like budding or binary fission. Growth also results when cells simply become longer or larger [1]. Investigating colonial growth of micro organism is of considerable importance both in theoretical as well as applied research. There are many ways to measure microbial growth. The most obvious way to determine microbial number is through direct counting using different techniques such as microscopic counts, membrane filter technique, plate count etc. Microbial growth can also be determined by measuring cell mass. The most direct approach for measuring cell mass is the determination of microbial dry weight. However, no single technique is always the best; the most appropriate approach will depend on the experimental situation [1].

The present chapter deals with Laser induced fluorescence (LIF) technique to study the growth kinetics of an aerial bacterial colony in a closed system. Laser Induced Fluorescence has proven to be a versatile tool for a myriad of applications [2-9]. It is a powerful technique for studying molecular interactions in analytical chemistry, biochemistry, cell biology, physiology, nephrology, cardiology, photochemistry, and environmental science. The first gastrointestinal laser-Induced fluorescence spectroscopy (LIFS) study was performed by Kapadia et al. in 1990 [2]. In an ex vivo study the authors were able to discriminate 16 colon adenomas from hyper plastic polyps with a sensitivity and specificity of 100% and 94% respectively [3]. Rex et al. [4] utilized laser induced fluorescence to determine NADH in experimental neuroscience using an optical fiber probe. Giorgadze et al. [5] measured degree of abnormality of tissue with the help of LIF. Shomacker [6] confirmed the ability of LIFS to differentiate between neoplastic and non-neoplastic tissue with a sensitivity and specificity of 80 and 92%. There are many examples in

biological applications where LIF technique is applied. In bacteriological studies, the LIF has been shown to be a very sensitive analytical tool to distinguish between the two species of bacteria [7].

Study on growth kinetics of bacterial colony using LIF was carried out by doping Rhodamine B dye in culture medium. Rhodamine B is an appropriate dye for doping because of its high fluorescence quantum efficiency [10, 11]. It was found that the concentration of Rhodamine B at 0.3×10^{-4} M was appropriate to give sufficient fluorescence intensity. Higher concentration of the dye effects bacterial growth negatively.

7.2. EXPERIMENTAL DETAILS

Nutrient agar medium containing 0.3×10^{-4} M Rhodamine B dye was used for the study. The nutrient agar was exposed to air for a short duration and then incubated at 25^{0}C at room temperature. In general terms, bacterial colonies grown from single cells on nutrient-poor media show ramified structures, whilst on nutrient-rich media the compact colonies have an overall circular shape with a rough edge. The colonies developed on the surface were observed and a circular colony with regular margin was selected for studying the growth kinetics. Fig.7.1 shows digital photographic images of the dye doped aerial bacterial colony formed on agar plate.

Figure: 7.1. *Aerial bacterial colony formed on dye doped nutrient agar medium*

The selected pure culture was streaked on to fresh nutrient agar plate containing Rhodamine B and the intensity of fluorescent emission was measured. Diode pumped solid state laser of 532 nm (5 mW) with a spot size of 3 mm was used as an excitation source. The power of the laser source was reduced using neutral density filters. The laser was irradiated on to the colony in such a way that it excites the entire colony. A multimode plastic fiber having a core diameter of 980 μm was used to collect the fluorescent emission, which was placed at an angle of 42 ^{0} with excitation source. The other end of the fiber was coupled to the slit of 0.25 m monochromator-PMT (Mc Pherson) assembly [Fig.7.2]. The size variation of the growing colonies were measured with the help of an eyepiece micrometer of a binocular magnifier.
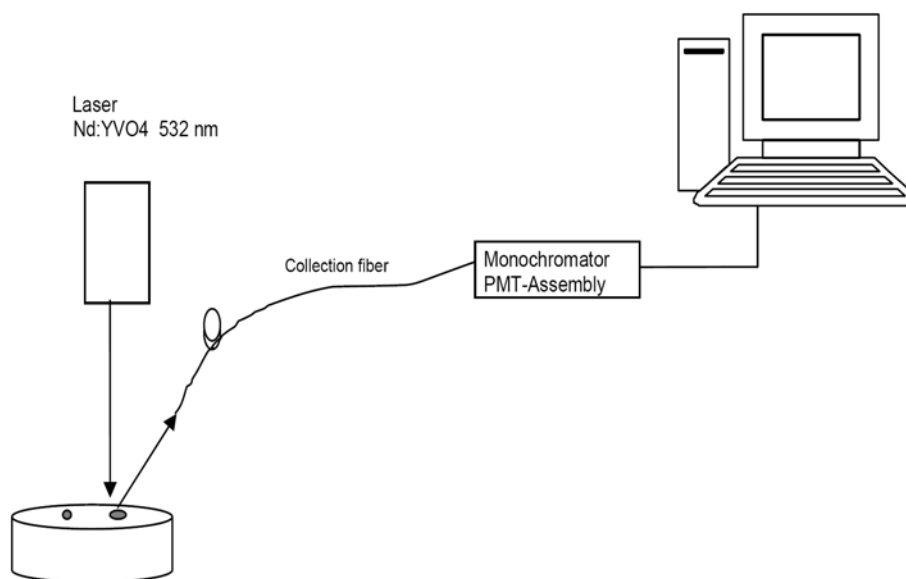

Figure: 7.2. *Experimental setup to study the growth kinetics of bacterial colony by using Laser Induced Fluorescence technique*

7.3. RESULTS AND DISCUSSIONS

7.3.1. Effect of Growth of Bacterial Colony on Fluorescence.

The fluorescence spectra of bacterial colony sample marked by Rhodamine B was studied at different days (Fig.7.3). As seen in this figure the intensity of emission was reduced with number of days due to fluorescence quenching by bacterial colony. So it is clear that fluorescence of dye is strongly quenched by bacterial colony. This indicates that the cultured bacterium was a gram positive bacterium and it was confirmed with gram staining method. The quenching effect of dye by gram positive bacterium is due to its thick cell wall. It consists of a thick layer of peptidoglycan embedded with techoic acids. The peptidoglycan is the binding site of dye and the thick layer blocks the dye from further penetrating into the cell. The quenching effect of the dye is due to the effect of techoic acid [7, 12-14].
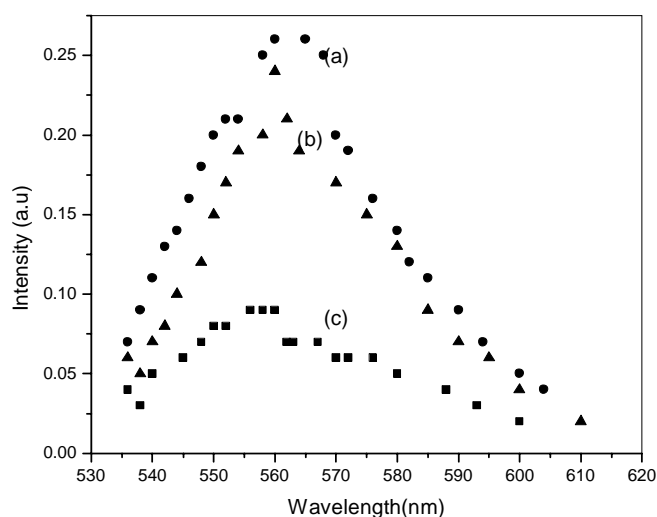

Figure: 7.3. *Fluorescence spectra of bacterial colony marked by RhodaminB showing Quenching Effect. (a,b,c represent fluorescence spectra corresponding 4th,5th ,6th day)*

7.3.2. Growth Kinetics of bacterial colony as inferred from fluorescent emission intensity

7.3.2.1. Radial growth of bacterial colony as a function of time.

To study the growth dynamics of bacterial colony, radius of the colony vs time is plotted (Fig.7.4). Radius measurement started after 12 hrs of incubation. From Fig.7.4, it is clear that after 25 hrs of growth, the colony radius R appeared to increase linearly with time. Radial growth rate of the colony (μ_r) is found to be 0.083 mm/hr. The value of μ_r remains constant as long as the growth condition in the peripheral zone do not change. A plot of area of bacterial colony against time is shown in Fig. 7.5. Here area increases exponentially after 25hrs of growth. Rate of exponential growth is calculated to be 0.039 mm^2/hr by theoretical fit. This indicates the exponential growth of bacterial population associated during this period to exponential phase of colony growth. After 85 hrs, the growth was terminated. At initial stage also the value of μ_r is found to be very small. The shape of the bacterial growth curves depends on medium composition and inoculums density [15].
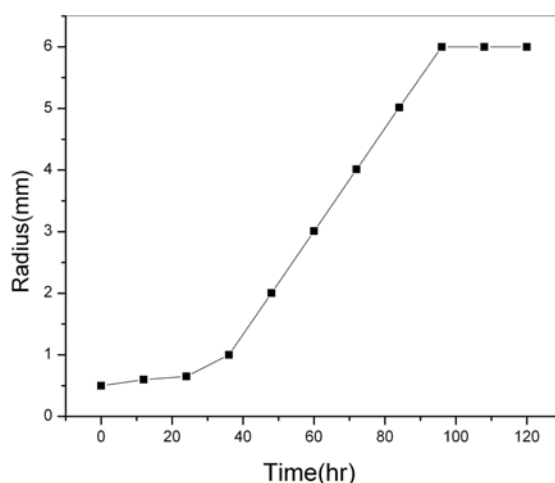

Figure: 7.4. *Radial growth of Bacterial Colony Vs Time*
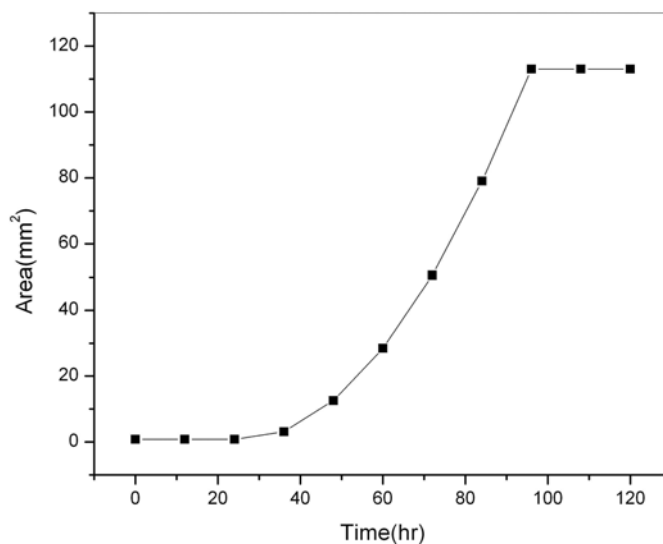
Figure: 7.5. *Area of the Bacterial Colony Vs Time*

Fig. 7.6 shows the typical growth curve of microbes grown in a batch culture or closed system. Here the growth of microorganism is plotted as the logarithm of the number of viable cells versus the incubation time. Since the area of the bacterial colony is proportional to the number of cells in colony it is possible to compare Fig.7.6 and Fig.7.5. By comparing these two plots it is clear that the lag phase represents initial points in Fig. 7.5. During the period of 25 to 85 hrs of growth, the area increases exponentially representing exponential or log phase of growth curve. It is clear from Figs. 7.5 and 7.6 that bacterial colony enters into stationary phase after 85 hrs of growth.

7.3.2.2. Peak fluorescence intensity *vs* time plot

Fig. 7.7 shows peak fluorescence intensity *vs* time plot of growth of growing bacterial colony. From the figure it is clear that the fluorescence intensity decreases as bacteria grows. The rate of reduction in fluorescence intensity was negligible at initial stage (up to 25hr). By comparing with Figs. 7.5

and 7.6 it is clear that, this stage represents lag phase of bacterial growth curve. Although cell division does not take place right away and there is no net increase in mass, the cell is synthesizing new components. The lag phase varies considerably in length with the condition of the micro organism and the nature of the medium. After 25 hrs of growth the fluorescence intensity decreases exponentially. The rate of decay of fluorescence is found to be 0.034 V/hr by theoretical fit. During this period area of the colony increases exponentially with a rate of 0.039 mm^2/ hr. It is clear that quenching of the fluorescence of dye by bacterial colony is proportional to the increase in growth rate of the bacterial colony. This can be identified as the log phase or exponential phase of growth curve. In this phase micro organisms are growing and dividing at the maximal rate. That is microorganism are dividing and doubling in number at regular intervals and their rate of growth is constant. The intensity of the fluorescence is constant after 85 hrs of growth. This stage represents the stationary phase of growth curve. Bacterial cells enter into stationary phase mainly because of nutrient depletion and accumulation of toxic waste products. The reason for quenching of fluorescence is due to thick layer of bacterial cell wall as mentioned earlier. Quenching effect of dye is a measure of growth of gram positive bacterial cells.
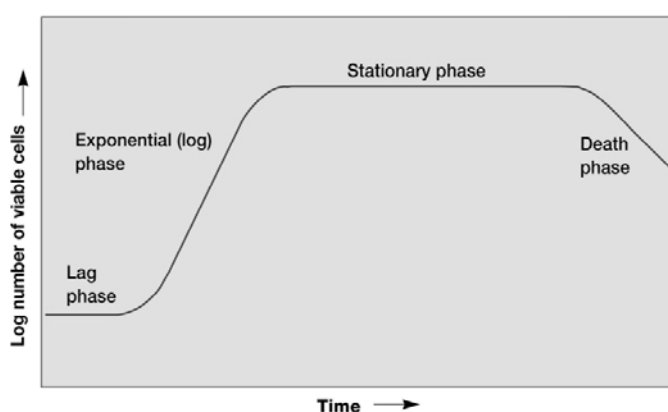
Figure: 7.6. *Microbial growth curve in a closed system*
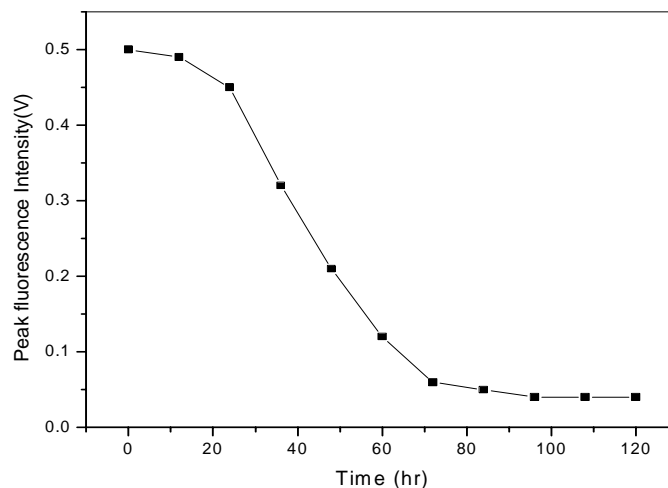
Figure: 7.7. *Peak fluorescence intensity vs time plot of growth of growing bacterial colony.*

7.4. THEORY OF GROWTH KINETICS OF BACTERIAL COLONY

The cultivation of bacteria on the surface of a solid nutrient agar medium is a general experimental technique. But no satisfactory quantitative theory was so far proposed to describe the development of bacterial colonies. The growth of bacterial colonies on the surface of a solid medium is a common process and by appropriate variation of the environmental conditions a wide variety of colony morphologies can be observed. To study the growth dynamics of bacteria, it is necessary to know the rate of development of microbial growth and size of the colony. A few workers have described simplified model profiles for particular bacterial species [16-20]. Pirt (1975) developed a model that describes the growth of a bacterial colony on solid homogeneous surface [16,21] In a pioneering study of the growth kinetics of surface colonies of bacteria, a virtual constant rate of radial growth for colonies of *Escherichia coli,* Klebsiella

aerogenes and Streptococcus faecalis is observed [17]. Julian W et. al described simple method for measuring the profile of bacterial colonies[18].

In the present study, the growth dynamics of the bacterial colony was determined by analyzing fluorescence intensity of dye which is doped in culture medium. From the study it is found that quenching of the fluorescence is in exponential manner in log phase.

Let I be the intensity of fluorescence of dye doped bacterial colony at time t. By assuming that the specific growth rate **μ** remains constant, growth equation can be written as

$$\frac{dI}{dt} = -\mu I \qquad \qquad ....(7.1)$$

which gives fluorescence intensity at given time t, which describes growth dynamics of bacterial colony during exponential phase.

7.5. CONCLUSIONS

Growth dynamics of an aerial gram positive bacterial colony on nutrient agar medium was studied using laser induced fluorescence technique. This technique has been shown to be a useful technique for obtaining information about the different growth phase of the bacterial colony. Quenching effect of dye by bacterial colony can be effectively used to analyze growth kinetics of bacterial colony. Quenching effect of fluorescence indicates that cultured bacteria were gram positive. The rate of quenching of fluorescence of dye from bacterial colony was proportional to the rate of increase in area of the bacterial colony which in turn indicates that the rate of quenching of the fluorescence was proportional to rate of growth of bacteria.

REFERENCES

1. J. Willey, L. Sherwood, and C. J. Woolverton, *Prescott, Harley, Klein's Microbiology,7th ed*, McGraw-Hill, New York, (2007)

2. Kapadia CR, Cutruzzola FW, Brien KM, Stetz M, Enriquez R, Deckelbaum L; *"Laser-induced fluorescence spectroscopy of human colonic mucosa. Detection of adenomatous transformation"*. Gastroenterology **99**, 150(1990)

3. Cothren RM, Richards-Kortum R, Sivak MV, van Dam J, Petras RE, Fitzmaurice M, et al*; "Gastrointestinal tissue diagnosis by laser induced fluorescence spectroscopy at endoscopy"*, Gastrointest. Endosc. **36**, 105 (1990)

4. A. Rex and F. Fink; *"Applications of laser-induced fluorescence spectroscopy for the determination of NADH in experimental neuroscience",* Laser Phys. Lett. **3**, 452 (2006).

5. G. K. Giorgadze, Z. V. Jaliashvili, K. M. Mardaleishvili,T. D. Medoize, and Z. G. Melikishvili; *"Measurement of the abnormality degree in the biological tissue by the laser induced fluorescence",* Laser Phys. Lett.**3**, 89 (2006).

6. Shomacker KT, Frisoli JK, Compton CC, Flotte TJ; "Ultraviolet *laser-induced fluorescence of colonic tissue:basic biology and diagnostic potential",* Lasers Surg. Med. **12**, 63(1992)

7. P. M. Sandeep, S. W. B. Rajeev, M. Sheeba, S. G. Bhat, and V. P. N. Nampoori; *"Laser induced fluorescence based optical fiber probe for analyzing bacteria"* Laser Phys. Lett. **1**, 5 (2007)

8. N D Gómez, V M Freytes, J Codnia, F A Manzano and M L Azcárate; *"Implementation of laser induced fluorescence technique to study the*

kinetics of radicals generated in the IR multiphoton dissociation of chloroform", J. Phys. Conf. Ser. ***274*** *012097(2011)*

9. C. Neal Stewart Jr et.al; *"Laser-Induced Fluorescence Imaging and Spectroscopy of GFP Transgenic Plants",* J. Fluorescence **15***, 697(2005)*

10. V. Romano, A. D. Zweig, M. Frenz, and H. P. Weber; *"Time-resolved thermal microscopy with fluorescent films"*, Appl. Phys. B **49**, 527 (1989).

11. J. R. Lakowicz, G. Piszczek, and J. S. Kang; *"On the Possibility of Long-Wavelength Long-Lifetime High-Quantum-Yield Luminophores"*, Anal. Biochem. **288**, 62 (2001).

12. J. Baddiley; *"Mechanism and control of cell wall synthesis in bacteria"*, Pure Appl. Chem. **42**, 417(1975)

13. J Baddiley, *"Teichoic acids in cell walls and membranes of bacteria",* Essays in Biochemistry **8**, 35 (1972).

14. D. W. Tempest, J. W. Dicks and D. C. Eliwood; *"Influence of growth condition on the concentration of potassium in Bacillus subtilis var. niger and its possible relationship to cellular ribonucleic acid, teichoic acid and teichuronic acid"* , Biochem. J. **106**, 237(1968).

15. N. S. Panikov, S. E. Belova, and A. G. Dorofeev; *"Nonlinearity in the Growth of Bacterial Colonies: Conditions and Causes"*, Microbiology **71**, 59 (2002).

16. S. J. Pirt, *"Principles of Microbe and Cell Cultivation",* Blackwell Sci., Oxford, (1975)

17. M J Grimson and G C Barker; *"A continuum model for the growth of bacterial colonies on a surface"*, J. *Phys. A: Math. Gen.* **26** 5645(1993)

18. Coopera L, Dean A. C. R, Hinshel Wood C; "*Factors affecting the growth of bacterial colonies on agar plates*", Proceedings of the Royal Society **B171**, 175 (1968),

19. Palumbso A, Johnsonm G, Rieck V. T, Witter L. D; "*Growth measurements on surface colonies of bacteria*", Journal of General Microbiology **66**, 137(1971).

20. Wimpenny J W.T and Lewis M .W.A; "*The growth and respiration of bacterial colonies*", *J. General Microbiology* **103**, 9 (1977).

21. S. J.Pirt, "*A kinetic study of the mode of growth of surface colonies of bacteria and fungi*", J. General Microbiology **47**, 181(1967).

...........ೞ..........

Chapter **8**

Conclusions and Future Prospects

8.1. GENERAL CONCLUSIONS

Photonics will continue to evolve and play an increasingly significant role in the technological revolution. The next frontier in organic and photonic devices is the use of biomaterials, either naturally occurring or artificially produced based on biological methods. The unique properties of these biomaterials are not easily replicated in conventional organic or inorganic materials, which provide another degree of freedom in terms of device design and produce enhancement in device performance.

In the present investigations, various types of biomaterials suitable for photonics applications have been described. The results which have emerged out of these studies are also presented. We used Poly vinyl alcohol (PVA) for dissolving DNA and dye for carrying out some of the experiments. Since DNA and PVA are water soluble, it is very easy to make thin film of DNA-PVA system by allowing it to get dry. Polyvinyl alcohol (PVA) has excellent film forming, emulsifying and adhesive properties. The absorption spectra and Z-scan studies in solution showed that DNA-PVA matrix is very sensitive to temperature and gets denatured with increase in temperature. It was found that the two photon absorption coefficient of DNA-PVA matrix decreases from 0.5 cm/GW to 0.02 cm/GW as temperature increases from $30\,^{0}$C to $55\,^{0}$C.

DNA plays good role in modifying optical behaviour of Rhodamine 6G-PVA system. Our Z-scan experiments have revealed interesting features of the nonlinear absorption properties of DNA doped rhodamine 6G-PVA solution. At 532nm excitation saturable absorption behaviour was observed for Rhodamine 6G –PVA solution. On doping DNA at 2 wt%   in Rhodamine 6G –PVA solution we got RSA behavior near focus and SA behavior away from focus. In thin film of dye –PVA matrix we observed direct switch over from SA to RSA as the concentration of DNA is increased. The simultaneous occurrence of several nonlinear processes in dye-DNA- PVA system can be made use of in developing various photonic devices.

DNA-PVA matrix has been found to be an excellent host material for the laser dye Rhodamine 6G. The intensity of amplified spontaneous emission was found to get enhanced with the addition of DNA. The threshold value of ASE and full width half maxima of ASE spectrum is found to be less while comparing with the system without DNA. We also observed multimode laser emission from transversely pumped dye-doped DNA-PVA thin film. For pump energy of 6 mJ/pulse an intense line with FWHM of 0.2 nm was observed due to energy transfer from other modes. This value was found to be very small when compared with other dye doped DNA matrix. These results establish the occurrence of lasing action in dye doped DNA-PVA system and could be of considerable application in the design of different optical elements.

We have discussed optical properties of silver nanoparticles in DNA and BSA matrix. Both biopolymers act as a good stabilising agent for nanoparticle synthesis. The nonlinear absorption coefficient β measured by Z-scan technique revealed that silver nano particles synthesized in aqueous solution of DNA and BSA show good nonlinear optical response and could be chosen as ideal candidate with potential applications for nonlinear optics. The observed β

value is higher for the silver nanoparticles in DNA matrix compared to those in BSA matrix. However optical limiting response of silver nanoparticles in BSA matrix is found to be greater than that of nanoparticles in DNA matrix.

Enhancement in photo luminescence of silver nanoparticles was observed while increasing the concentration of DNA. The fluorescence maximum got shifted towards red as the excitation wavelength was increased in the case of silver nanoparticles prepared at higher concentration of DNA, which can be attributed to the size distribution of particles in the media. Nanoparticles in BSA matrix do not show such enhancement in PL intensity while increasing concentration of BSA.

The band gap tunability of CdS nanoparticles in biotemplates de-oxyribonucleic acid (DNA) and bovine serum albumin (BSA) were studied. The band gap of these semiconductor nano particles can be controlled effectively by changing the concentration of bio polymers DNA and BSA. DNA is more efficient in controlling the size of the nanoparticles compared to BSA. Since nanoparticles are capped with biomaterials, they are very useful for biolabeling. The PL spectrum of CdS nanoparticles in DNA template shows sharp emission peak at 490 nm with shoulders at 430 nm and 530 nm. The PL spectrum of CdS in BSA template has sharp emission peak at 530 nm with shoulders at 477 nm and 410 nm. The fluorescence emission spectra of nanoparticles can be continuously tuned by changing the concentration of biopolymers and excitation wavelength. The particles prepared from such angle will be useful as a fluorescence agent for optical and biotechnological applications

Growth dynamics of an aerial gram positive bacterial colony on nutrient Agar medium was investigated using laser induced fluorescence technique. This technique has been shown to be a useful for obtaining information about the different growth phase of the bacterial colony. Quenching effect of fluorescence

indicates that cultured bacteria belonged to the class of gram positive. The rate of quenching of fluorescence of dye from bacterial colony was found to be proportional to rate of increase in area of the bacterial colony indicating that the rate of quenching of the fluorescence was proportional to rate of growth of bacteria.

8.2. FUTUTRE PROSPECTS

From results of the studies reported in the present thesis, it is clear that the unique structure of DNA has optical properties which are interesting with respect to photonic applications. It requires further research to understand the mechanism of DNA based photonic devices completely. The significant enhancement in optical gain and nonlinear optical properties observed in Rhodamine6G doped DNA-PVA matrix can be explored in detail. This could be of considerable application in the design of active optical integrated circuits. Different dye mixtures can be used instead of single dye in DNA-PVA matrix. This may lead to wide range of tunability in emission and excitation wavelength. Much research on the basic electroluminescence properties of dye doped DNA-PVA matrix and demonstrating their full potential in display devices will be a potential field of future research.

Use of a biological template in nanoparticle synthesis provides a true opportunity for making different nano structures like nano rods and wires etc. The optical properties of such nano particles can be investigated with respect to device applications. Another useful advantage is that biomaterials can lend themselves for incorporating both inorganic and organic blocks to produce hybrid structures. In the case of DNA, one can intercalate or incorporate different active nano blocks within its duplex structure or attach them on the outer perimeter, which will lead to the development of new multi domain nanocomposites. The structural properties and specificity of interactions

exhibited by biopolymers helps to incorporate a different photonic active group in the bulk of a biomaterial where each domain performs a specific photonic function.

Laser induced fluorescence (LIF) is one of the best techniques for analysing microbial activity in different media. LIF technique can be extended to study mutual interaction of the different microbes in the medium. Fluorescence techniques coupled with rigorous mathematical treatment may be required for analysing growth kinetics of different microbes.

...........ᘓଃଈ..........